Sustainable mobility with bi-modal public transport

Dissertation

for the award of the degree
"Doctor rerum naturalium"
at the Georg-August-Universität Göttingen

within the doctoral degree programme

of the Georg-August University School of Sciences (GAUSS)

submitted by

Puneet Sharma
from Dangarh, India

Göttingen, October 26, 2023

Thesis advisory committee

Prof. Dr. Stephan Herminghaus

Dynamics of Complex Fluids
Max Planck Institute for Dynamics and Self-Organization

Prof. Dr. Stefan Klumpp

Institut für Dynamik komplexer Systeme
Georg-August-Universität Göttingen

Prof. Dr. Peter Sollich

Physikalisches Institut
Georg-August-Universität Göttingen

Members of the examination board:

Referee:
Prof. Dr. Stephan Herminghaus

Dynamics of Complex Fluids
Max Planck Institute for Dynamics and Self-Organization

Co-referee:
Prof. Dr. Stefan Klumpp

Institut für Dynamik komplexer Systeme
Georg-August-Universität Göttingen

Prof. Dr. Peter Sollich

Physikalisches Institut
Georg-August-Universität Göttingen

Dr. David Zwicker

Theory of biological fluids
Max Planck Institute for Dynamics and Self-Organization

Dr. Knut Heidemann

Dynamics of Complex Fluids
Max Planck Institute for Dynamics and Self-Organization

Prof. Dr. Alexander Ecker

Institute for Computer Science
Georg-August-Universität Göttingen

Date of the oral examination: December 5, 2023

Acknowledgments

My Ph.D. journey has been full of learning. While some lessons were learned through others' wisdom, some had to be learned the hard way. I am grateful to Prof. Stephan Herminghaus for imparting the following lessons:

- Go where it hurts - to not shy away from doing essential but less enjoyable tasks.
- Focus on one variable at a time.
- The essence of scientific writing - non-repetitive, simple, and direct communication.
- Value of a scientific contribution - "What do we know now that we did not know earlier and why is the world a better place now?"

I am grateful to Dr. Knut M. Heidemann for contributing to my scientific writing and his support in this journey. I am very grateful to Prof. Stefan Klumpp and Prof. Peter Sollich for their kind support and advice whenever needed.

I have had some very enjoyable discussions with Prakhar Godara about the quality and trends in science, to which I am very grateful. I would like to extend my gratitude to Monika Teuteberg for supporting me through all administrative matters, Dr. Kristian Hantke (superman of MPIDS), Thomas Eggers, and Yorck-Fabian Beensen for all technical support. I am thankful to Riccardo Carlucci for the interesting discussions.

A heartfelt thanks to Sheelendra Sharma and Mamta Sharma for their unrestricted love, infallible support, and enthusiasm, and especially for their patience during the time that I could not be with them. Thank you for tolerating all my chaos.

Table of Contents

List of Figures

Abstract

The escalating problems of pollution, traffic congestion, resource consumption, and environmental degradation are becoming increasingly significant due to the growing demand for urban mobility. This mounting crisis is largely attributed to the dominant use of private cars as the primary mode of transportation. While other alternatives like public transport offer a promising solution, they are often perceived as inconvenient and less attractive. In this Ph.D. thesis, we propose an alternative hybrid mode of transportation, bi-modal transportation, that combines a fixed rail service with on-demand shuttles. Line services, characterized by fixed routes and schedules, facilitate high vehicle occupancy and faster service. Meanwhile, shuttles offer seamless on-demand transportation to and from line service stops. In a first approach, we consider an idealized model geometry with a square grid of railways (line service) on which transport occurs via trains. We identify the conflicting objectives for optimization, i.e., user convenience and energy consumption, and evaluate the system's performance in terms of Pareto fronts. By means of simulation and analytical theory, we find that energy consumption can be significantly reduced as compared to private cars, at line service densities typically found in real settings. We then study the impact of rail stop density on system performance, revealing that, within realistic technical parameters, more stops can slow down trains without substantial improvements in overall performance. Consequently, we propose reducing the number of stops in existing railway systems and integrating bi-modal transit as a complementary solution. Finally, we study the feasibility of bi-modal transportation in Berlin and Brandenburg. We find that the existing network of rails with shuttles can be used to deploy a bi-modal public transit system that can reduce energy consumption while providing a service quality superior to customary public transit systems. With this work, we provide a possible answer to the pressing question of designing sustainable future mobility solutions.

Transportation is a vital function of human society, just as blood is essential to human life. Both blood and transportation move essential materials.

Damian J. Kush [1]

1 Introduction

The invention of the wheel marked a pivotal moment in human history, propelling us from nomadic hunter-gatherer societies into the realm of civilization. It revolutionized the movement of goods, opening up pathways for flourishing trade and the exchange of ideas. With efficient transportation at their disposal, explorers embarked on voyages, uncovering new continents and expanding the boundaries of human knowledge. Without these advances in mobility, humans might have remained confined to nomadic ways of life, and the very idea of setting foot on the moon would have been inconceivable. The ever-expanding capabilities of transportation have not only facilitated physical movement but have also been instrumental in fostering social, cultural, and economic activities on all scales. They played a pivotal role in propelling the Industrial Revolution. In essence, the progress of civilization is deeply intertwined with the evolution of transportation systems.

During the Industrial Revolution, several innovations reshaped transportation forever: the invention of the railroad, the advent of the internal combustion engine (ICE), and the introduction of the assembly-line method. The latter two gave birth to motorized individual vehicles (MIVs), commonly known as cars, which revolutionized the way people traveled, making longer journeys for both work and leisure more comfortable and accessible. It is no surprise that, to this day, MIVs maintain their dominant position in the transportation market [2, 3], primarily due to their unmatched convenience.

Empowered by the technological shift that characterized the Industrial Revolution, human influence on Earth underwent a profound and far-reaching expansion. This era

marked an extraordinary departure from traditional agrarian civilization. As technological innovations swept across industries, previously labor-intensive tasks became mechanized and more efficient. This, in turn, fueled an unprecedented surge in productivity, economic growth, and global interconnectedness.

The impact of anthropogenic activities on Earth has been so profound that it might mark the onset of a new geological epoch known as the Anthropocene [4, 5]. The transition from the Holocene to the Anthropocene might be a perilous moment in Earth's history, signifying a shift from a relatively stable and favorable environment for human civilization to a more uncertain and challenging era. The Holocene, which began around 11,700 years ago, provided the stable climatic conditions that allowed agriculture to flourish, giving rise to settled societies and the foundations of modern civilization.

In 2009, Johan Rockström and his colleagues proposed the concept of "safe operating space for humanity" in their influential paper titled "A Safe Operating Space for Humanity" [6]. In order to maintain the Holocene epoch, they proposed nine boundaries that define the safe operating space for humanity with respect to the Earth system that are associated with the planet's biophysical subsystems or processes. Three of the boundaries, those concerning biodiversity, biogeochemistry (nitrogen cycle), and climate have already been exceeded. In this thesis, we will focus on mitigating the effect of anthropogenic activities, particularly those associated with transportation activities, on climate change.

1.1 Climate crisis

In the annals of human history, the current epoch stands at a crossroads, a pivotal moment where the very sustenance of our species hangs in the balance. The challenges that loom large on our collective horizon are complex and inextricably intertwined. At the forefront of these challenges lies the climate crisis, an existential threat that transcends borders, ideologies, and generations.

1.1.1 Historical roots

The seeds of the climate crisis were sown during the late 18^{th} century with the advent of the Industrial Revolution [7]. This transformative period saw the widespread adoption of fossil fuels, such as coal and later oil, to power factories and machinery. While this marked a remarkable leap in technological progress and economic growth, it also initiated the mass release of greenhouse gases into the atmosphere.

Throughout the 19^{th} and 20^{th} centuries, industrialization and urbanization intensified, leading to even greater emissions of carbon dioxide and other greenhouse gases. The consequences of these emissions became evident in the 20^{th} century, as global temperatures began to rise, glaciers started to melt, and extreme weather events became more frequent

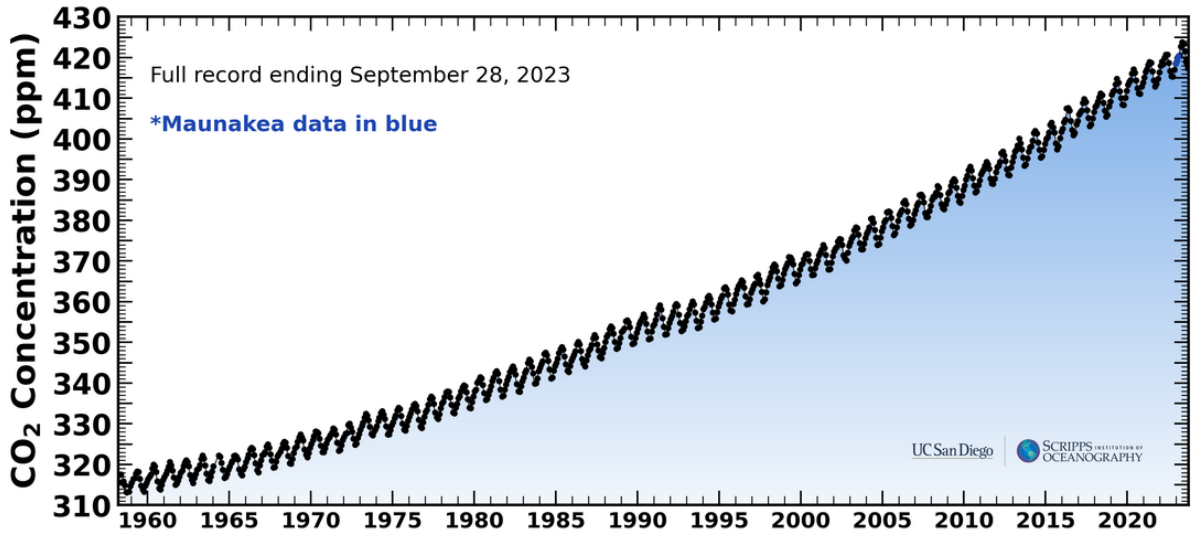

Figure 1.1: **Keeling Curve:** CO_2 in ppm at Mauna Loa observatory [8]. The oscillating black curve tracks the monthly average of measured atmospheric CO_2 over time.

and severe.

1.1.2 Milestones in climate awareness

The 20th century also witnessed significant milestones in climate awareness and research. In 1958, Charles David Keeling began recording atmospheric CO_2 concentrations at Mauna Loa Observatory, revealing an alarming upward trend, now known as the Keeling Curve (see Fig. 1.1). This empirical evidence linked human activities to rising CO_2 levels, global warming, and climate change.

Alarmed by climate change concerns, the First World Climate Conference (FWCC or WCC-1) was sponsored by the World Meteorological Organization (WMO) in 1979 [9] and the United Nations established the Intergovernmental Panel on Climate Change (IPCC) in 1988 to assess scientific information related to climate change. The IPCC's reports have been instrumental in shaping global climate policy.

1.1.3 Contemporary climate crisis

In 21st century, the climate crisis has intensified. The Earth's average temperature continues to rise, leading to more frequent and severe heatwaves, hurricanes, floods, and wildfires. Melting ice caps and rising sea levels threaten coastal communities, and ecosystems are under duress.

The effects of the climate crisis can be felt by a global average surface temperature which has increased by 1^{o}C since the pre-industrial era [10], furthermore, there is a growing convergence towards an increase by 2^{o}C [6]. When considering the heat capacity of oceans, a temperature rise as small as 1 degree Celsius requires immense heat, and

most of this heat is stored in oceans. The direct impact of global temperature rise on climate is felt by reduced snow cover [11], rising sea levels and intensified rain, causing floods [12, 13]. This is alarming because the world's most populous cities like Mumbai, and Kolkata (India), Miami and New York (USA), Amsterdam (Netherlands), etc. are located close to the sea. Global CO_2 emissions are the leading cause of climate change [6] and current level of CO_2 concentration exceeds the threshold of 350ppm [6]. This increases the risk of irreversible climate change, such as the loss of ice sheets, accelerated sea-level rise, etc. [6].

1.2 Impact of transportation on climate crisis

The energy-intensive nature of transportation, largely reliant on fossil fuels, has triggered a concerning surge in greenhouse gas (GHG) emissions. In regions like the USA and Europe, where road transportation is deeply ingrained in daily life, this sector is a major contributor, accounting for more than a quarter of total GHG emissions stemming from anthropogenic activities [14].

The very force that propelled humanity toward civilization, transportation, now stands as a looming threat to our sustainability. It is a stark reminder that the systems that once ushered us into an era of progress now demands our immediate attention and transformation. Addressing this alarming rise in emissions from transportation is not just a matter of environmental stewardship, but it is a critical step toward preserving the planet for future generations. The intertwining of transportation with our daily lives makes it a challenge we can no longer ignore. The climate crisis compels us to rethink our approach to mobility, embrace sustainable alternatives, and innovate for a cleaner, greener future.

The system of transportation is not coherent; it is not treated as integral. Roads compete with railroads and airlines in a chaotic fashion and at immense cost to the nation.

Anthony Stafford Beer

2

Pathways of mobility: unveiling transportation modes

This chapter examines contemporary modes of transportation. We discuss the limitations and challenges of the modes and present a novel approach to address these challenges.

2.1 Traditional modes of transportation

Traditional transportation modes have an enduring legacy in urban life. For generations, the private automobile has symbolized personal freedom and mobility, while public transit systems have formed the arteries of cities, connecting people and places. Walking and bicycling, often overshadowed by their motorized counterparts, remain elemental modes of human movement. Let us unravel the significance, challenges, and the evolving landscapes they have shaped.

2.1.1 Private automobiles

Private automobiles, primarily Motorized Individual Vehicles (MIVs), commonly known as private cars, offer elevated comfort, unmatched flexibility, and unparalleled convenience. As eloquently stated,

> "rarely...has technology provided a more successful satisfier of basic human needs and motives than the car, and it is unlikely that the feat will ever be

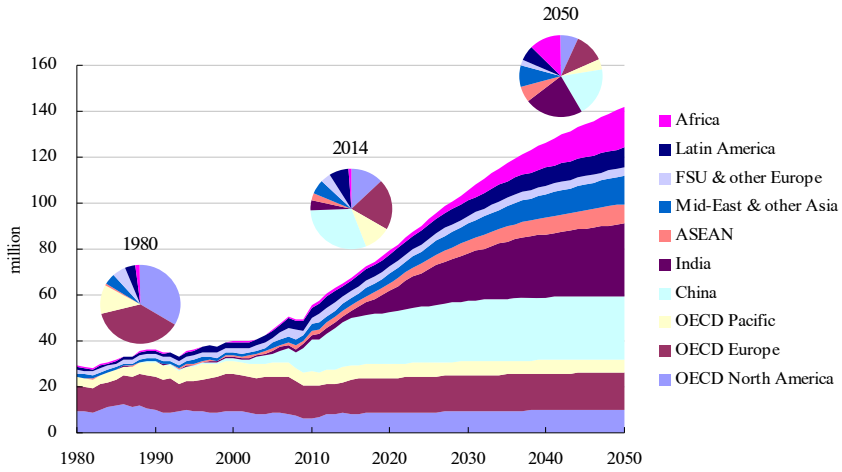

Figure 2.1: Global and regional car sales 1980-2050 [27]

repeated [15]."

However, the utilization of MIVs for passenger transportation is notably inefficient because for the following reasons:

- **Wastefulness:** It necessitates the movement of a ton of material to transport just one person. [16, 17]. Also, on average, a car spends 95% of its lifetime parked. This wastefulness causes air pollution [18, 19] and other environmental impact [20, 21].
- **Traffic congestion:** The proliferation of private vehicles has led to severe traffic congestion [22, 23, 24, 25] in many cities, resulting in time and productivity losses.
- **Urban sprawl:** The prevalence of private automobiles necessitates the development of extensive infrastructure like roads and parking facilities, consuming valuable land resources and contributing to urban sprawl.

Despite these concerns, the continued dominance of MIVs in the market persists, primarily owing to their undeniable convenience [26]. Globally, car sales have almost doubled between 1980 and 2014 (see Fig. 2.1). These challenges underscore the urgent need for more sustainable and efficient transportation solutions. As we continue to rely heavily on MIVs, their environmental impact has become increasingly evident. The emissions from these vehicles contribute significantly to air pollution and greenhouse gases, exacerbating climate change and posing severe health risks.

2.1.2 Public transit

Public transit is a system of shared vehicles and infrastructure designed to transport large numbers of people within urban and suburban areas. It is a service provided by

governments or private entities to help residents move around in a more efficient, cost-effective, and environmentally friendly way compared to using private cars.

Public transit systems typically include buses, trams, subways (metros or undergrounds), commuter trains, light rail, and other forms of shared transportation. These systems operate on scheduled routes, have designated stops or stations, and charge passengers a fare for their services. Public transit is a highly efficient mode of transportation for the following reasons:

- **Mass mobility:** Public transit systems provide efficient mass transportation, reducing the number of private vehicles on the road [28].
- **Support Urban Planning:** Public transit can influence urban development by encouraging higher-density, mixed-use developments near transit hubs, reducing the need for extensive suburban sprawl.

Therefore, many large cities (e.g., Tokyo) rely heavily on transportation by line services [29, 30, 31]. They come, however, with a serious downside when compared to MIV. With the latter, users can freely choose the starting time, location, and destination. This is not possible for line services, which must follow fixed schedules and fixed routes [32]. Users thus may have to walk significant distances to and from stations and need to know the schedules of the involved lines. This severely limits the utilization of public transit to its full potential.

2.1.3 Walking and bicycling

Active transportation modes, such as walking and bicycling, are typically used for commuting shorter distances within urban and suburban areas. While they offer numerous advantages, including health benefits and reduced environmental impact, they are less frequently employed for long-distance travel primarily due to practical limitations related to time and physical exertion.

2.1.4 Taxi

Taxis, a ubiquitous presence in urban transportation systems, play a vital role in providing convenient, on-demand mobility services to passengers. These vehicles for hire offer flexible point-to-point travel options, allowing individuals to reach their destinations swiftly and comfortably. However, the convenience offered by taxis often comes at a price beyond the fare, they contribute significantly to urban traffic congestion and environmental challenges. The high density of taxis in metropolitan areas can exacerbate traffic woes, leading to increased travel times and reduced overall road efficiency. Furthermore, due to the reliance on internal combustion engines, these vehicles contribute to air pollution and greenhouse gas emissions, posing environmental concerns.

2.2 Emerging trends in urban transportation

As urban landscapes continue to evolve, so do the methods by which we navigate them. A new era of urban mobility has dawned, marked by the emergence of innovative transportation trends. Ride-pooling and on-demand services have disrupted the traditional taxi paradigm, electric vehicles are redefining the automotive industry, and micro-mobility options offer nimble solutions for the short urban journey.

2.2.1 Demand responsive ride pooling

Demand-responsive ride-pooling (DRRP) [33] deploys many shuttles that pick up and drop off users at the desired locations. This service relies on a centralized facility that collects travel requests and employs powerful algorithms that combine these requests to formulate optimized shuttle routes [34], thus providing door-to-door transport, similar to MIVs and taxis and better pooling. However, in order to pool people, these services necessitate detour [33, 35] when compared to the direct routes feasible via individually owned vehicles (MIVs) and taxis. This trade-off [36] inevitably caps the achievable pooling efficiency, often restricting it to well below ten passengers per vehicle [37]. It's noteworthy that DRRP systems, in their pursuit of convenience, may inadvertently contribute to urban traffic congestion, thus presenting a trade-off in terms of traffic management. Furthermore, they often find themselves in competition with traditional public transportation systems, which possess superior pooling efficiency through their fixed routes and schedules.

2.2.2 Micromobility

Micromobility options, including electric scooters and e-bikes, are gaining prominence in urban environments, serving as practical solutions, especially for short-distance travel needs. They excel in addressing the crucial first and last-mile connectivity puzzle within urban transportation systems. However, their suitability diminishes when considering longer journeys due to limitations in range and speed compared to conventional vehicles.

It is imperative to highlight that the effective deployment of micromobility solutions hinges on the presence of dedicated infrastructure. This infrastructure often includes designated lanes, akin to those designated for bicycles, ensuring safe and efficient mobility for these options within the urban landscape.

2.3 Challenges

The world of urban transportation is a multifaceted system, and as our cities grow and transform, they bring forth a new set of challenges. These challenges revolve around finding a balance between mitigating traffic issues and environmental harm while preserving the convenience of transportation.

Personal vehicles, like cars, offer exceptional convenience, yet they pose significant environmental threats. On the other hand, public transportation, such as light rail with fixed routes, has the potential to transport many passengers, thus conserving resources efficiently. However, it often sacrifices convenience due to fixed routes and schedules.

The door-to-door shuttle services like demand responsive ride-pooling (DRRP) provide exceptional convenience by picking passengers up at their doorstep, but they struggle to pool passengers efficiently because they often need to take detours in order to pool people. This detouring becomes more pronounced as more passengers share the shuttle. These services also pose a competition to the more efficient public transport service.

Our objective within this intricate urban transportation realm is to harmonize vital urban convenience with strategies that alleviate traffic challenges and environmental impacts.

2.4 Our approach

Combining line services with a fleet of shared shuttles in an integrated so-called bi-modal system may provide on-demand door-to-door service at a service level superior to current public transport with significantly less resource consumption than MIV. In chapter 3, we introduce a generic model of bi-modal public transit and characterize its critical parameters of operation. We will gradually increase the complexity of our model in subsequent chapters, aligning our model more closely with real-world scenarios. With each step, we gain deeper insights into the operational dynamics that underpin the functionality and efficiency of bi-modal transit systems within the intricate urban landscapes of urban mobility.

In the realm of complex systems, toy models are physicist's conduit to profound understanding.

3

Bi-modal public transit systems

This chapter lays down the foundations for the research conducted in this thesis. First, the system under study and its critical parameters of operations are defined. This is followed by a detailed discussion on demand-responsive ride-pooling (DRRP) and public transit systems. Toward the end, theoretical results for a bi-modal public transit system are presented.

3.1 Definition of the system

3.1.1 Bi-modal transit

A bi-modal public transit system consists of a combination of demand-responsive ride-pooling and public transit modes. A line service, with fixed routes and schedule, shall coexist with a fleet of shuttles that pick up users and bring them either to or from line service stations, or serve shorter-distance requests directly. This provides both door-to-door transport by virtue of the shuttles and a large average pooling efficiency due to the involvement of line service vehicles.

3.1.2 User environment

For the sake of conciseness and simplicity, we consider a planar area uniformly populated at density E with potential users of the public transit system under study. Users are

city/district	type	E [km^{-2}]	D [km]	v_0 [km/h]	m [km^2]	$\tilde{\ell}$	Λ
New York City	dense urban	$1.1 \cdot 10^4$	4.99	11.3	2.0	0.28	$1.5 \cdot 10^4$
Berlin	urban	$4.1 \cdot 10^3$	5.90	19.8	3.6	0.32	$5.0 \cdot 10^3$
Ruhr (north)	urban	$3.6 \cdot 10^3$	15.7	44.9	94	0.62	$3.6 \cdot 10^4$
Emsland	rural	$1.1 \cdot 10^2$	16.7	58.7	1200	2.1	$1.0 \cdot 10^3$

Table 3.1: **City data.** Typical values of population density E, average traveled distance D, speeds of shuttles v_0, as well as the resulting dimensionless demand $\Lambda = D^3 E\nu/v_0$, and dimensionless mess size $\tilde{\ell}$, for a few selected areas. $\tilde{\ell} = \sqrt{m}/D$, where m is the average area enclosed by surrounding rail services. We assume $\nu = 2/17h^{-1}$, i.e., two trips per day per user given time of service of 17 h per day. Road vehicle velocities for Ruhr (north) and Emsland have been obtained by averaging Google navigator data over many relations randomly chosen within the respective area.

assumed to place transit requests in an uncorrelated fashion, each consisting of a desired pick-up ($\mathcal{P}$) and drop-off ($\mathcal{D}$) location, at an average rate ν per passenger. Requested travel distances $d = \overline{\mathcal{P}\mathcal{D}}$ are assumed to follow a certain distribution, $p(d)$, with mean D [33].

For a transparent discussion, it is useful to introduce dimensionless parameters characterizing the system under study. By combining the intrinsic length scale D with a characteristic road vehicle velocity, v_0, we obtain an intrinsic time scale, $t_0 = D/v_0$. This is the average time a travel request would need to be completed by MIV. The demand of transport within the system can then be characterized by the dimensionless parameter $\Lambda = E\nu D^3/v_0$[1], which can reach well beyond 10^4 in a densely populated area. Tab. 3.1 provides a few typical parameters encountered in real systems for reference. Note that $\tilde{\ell} = \ell/D = \sqrt{m}/D$, where m is the average area enclosed by surrounding rail (line) services, and $\tilde{\ell}$ is the spacing of line service routes (see Fig.3.1a)

3.1.3 Model system geometry

For an overarching systematic study, it is useful to consider an idealized model geometry (see Fig. 3.1). We assume that transport occurs via the DRRP shuttle service, combined with a square grid of railways on which transport occurs via trains. The connection points (train stations) between the two subsystems lie at all railway intersections and are spaced with a lattice constant ℓ (see Fig. 3.1). The transit system is further characterized by a shuttle density B in the plane and a train frequency μ at all train stations, with trains having a seating capacity k. Shuttles and trains move with velocities v_0 and v_{train}, respectively. They require energy e_{shuttle} and e_{train}, respectively, per unit distance of travel.

[1] Average number of incoming requests in an area D^2 in time t_0.

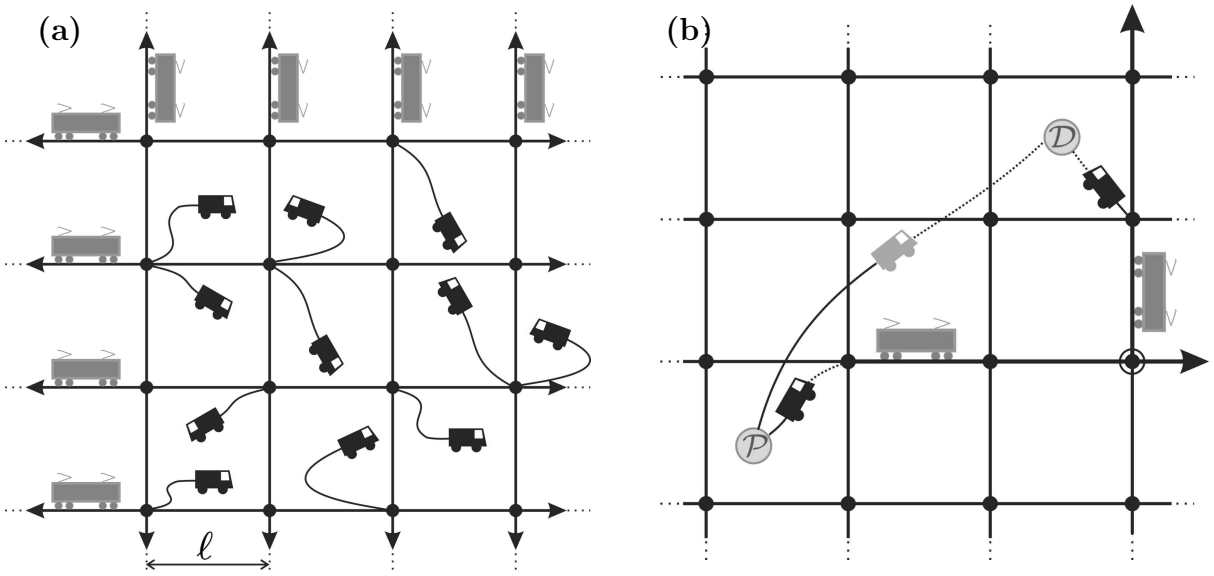

Figure 3.1: **Bi-modal transport network on a square grid. (a)** A bi-modal network with trains (grey vehicles) operating along the solid lines. Shuttles (black vehicles) are used as a feeder service to carry people to and from the train stations (black dots at intersection points) separated by distance ℓ. Trains operate periodically at a frequency μ, with vehicle seating capacity k. **(b)** Two alternative ways to serve a transport request from $\mathcal{P}$ (pick-up) to $\mathcal{D}$ (drop-off). Bi-modal transport involves a shuttle ride from $\mathcal{P}$ to the train station, transport by train (arrows, here with one change (circle)), and another shuttle ride from the train station to $\mathcal{D}$. Uni-modal transport service is a direct shuttle (grey) ride from $\mathcal{P}$ to $\mathcal{D}$. A major task of the system is to appropriately decide which of these two types of transport services to choose.

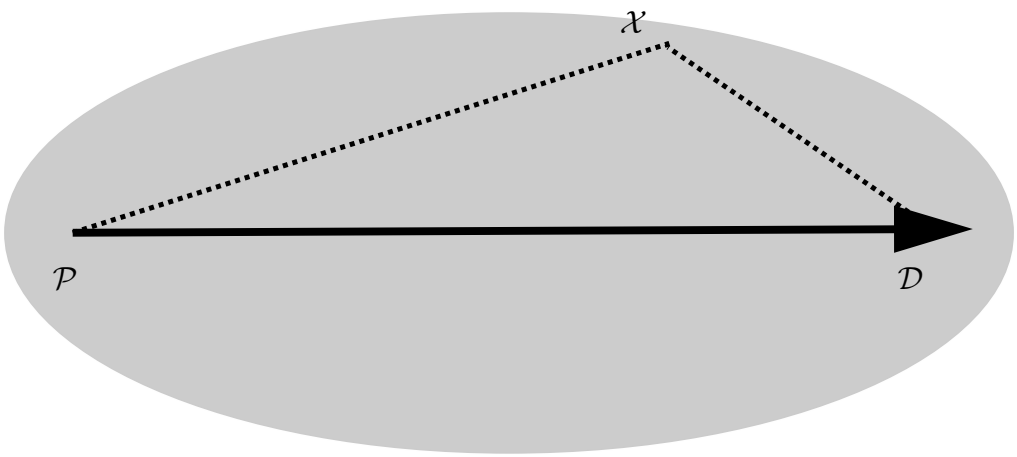

Figure 3.2: **Ellipse criterion:** An elliptical area of acceptance. The dotted line with length l represents the detour incurred due to the extra stop at $\mathcal{X}$. The latter is within the ellipse, meaning that the detour incurred is less than the maximum allowed detour.

The main goal of the bi-modal system under consideration is to provide high-quality (i.e., rapid) door-to-door transportation service at minimal energy consumption, thereby minimal carbon emission. To reach this goal, the provider of bi-modal transit may vary certain parameters of operation, which we discuss in Sec. 3.3.

3.2 Components

This section discusses the two essential components of the bi-modal transit system.

3.2.1 Demand responsive ride pooling (DRRP)

It is an essential component of our bi-modal transit system, where it acts as a feeder service that brings people to and from the train station. The main challenge here is assigning routes to vehicles in real-time under the constraints set by previous requests. We discuss the critical parameters and constraints of DRRP.

Occupancy

It is paramount for DRRP service to maintain a high vehicle occupancy, b. To do so, the vehicles must deviate from their direct path to accommodate more passengers in the same trip.

Detour

When serving i^{th} request going from $\mathcal{P}$ to $\mathcal{D}$, the vehicle may not be able to follow the shortest path $\overline{\mathcal{PD}}$ of length D_i, because there may be other requests to serve. We define

the detour, δ, as the ratio between the actual path taken and the direct path, i.e.,

$$\delta_i = \frac{l_i}{D_i} = \frac{\overline{\mathcal{PX}} + \overline{\mathcal{XD}}}{\overline{\mathcal{PD}}}. \tag{3.1}$$

A new request can share the ride with an existing passenger if $\delta \leq \delta_{\max}$, where $\delta_{\max}$ is the detour parameter. Note that this criterion defines an ellipse with the foci on $\mathcal{P}$ and $\mathcal{D}$ as shown in Fig. 3.2. A request arising within the ellipse can be pooled with the existing request. A higher pooling can be achieved for a higher detour parameter.

Pooling efficiency

The trade-off between pooling passengers and detours encountered severely restricts the pooling efficiency. We define the pooling efficiency, η, as the ratio between mean occupancy of the vehicles, b, and mean detour, δ,

$$\eta = \frac{b}{\delta}. \tag{3.2}$$

Pooling efficiency, η, gives an estimate of the ratio of requested direct distance by the users and the driven distance by the shuttle [38]. In simulations of the uni-modal system (shuttles only), it has been observed that η scales with demand Λ roughly in an algebraic manner, $\eta(\Lambda) \propto \Lambda^{\gamma}$, with $\gamma \approx 0.12$ [38].

Waiting time

Unlike private cars, where users can immediately embark on the journey, users have to wait for a certain time to be picked up. For the sake of conciseness and simplicity, we will assume a mean waiting time, τ_w. The mean waiting time is characterized by the system under study. We use simulation results to determine the average waiting time for shuttles, τ_w, and the average detour, δ. In Fig. 3.3, mean detour and mean waiting time are plotted as a function of user demand. Users are assumed to have a maximum accepted waiting time of t_0. We observe that mean waiting time τ_w grows with demand and saturates around 0.65. Similarly the mean detour δ grows with demand and saturates around 1.65.

Speed

The speed at which shuttles move is characteristic of the environment in which the system is deployed. For the sake of simplicity, we assume that the shuttles move at an average speed v_0, which is equal to the average speed of a car.

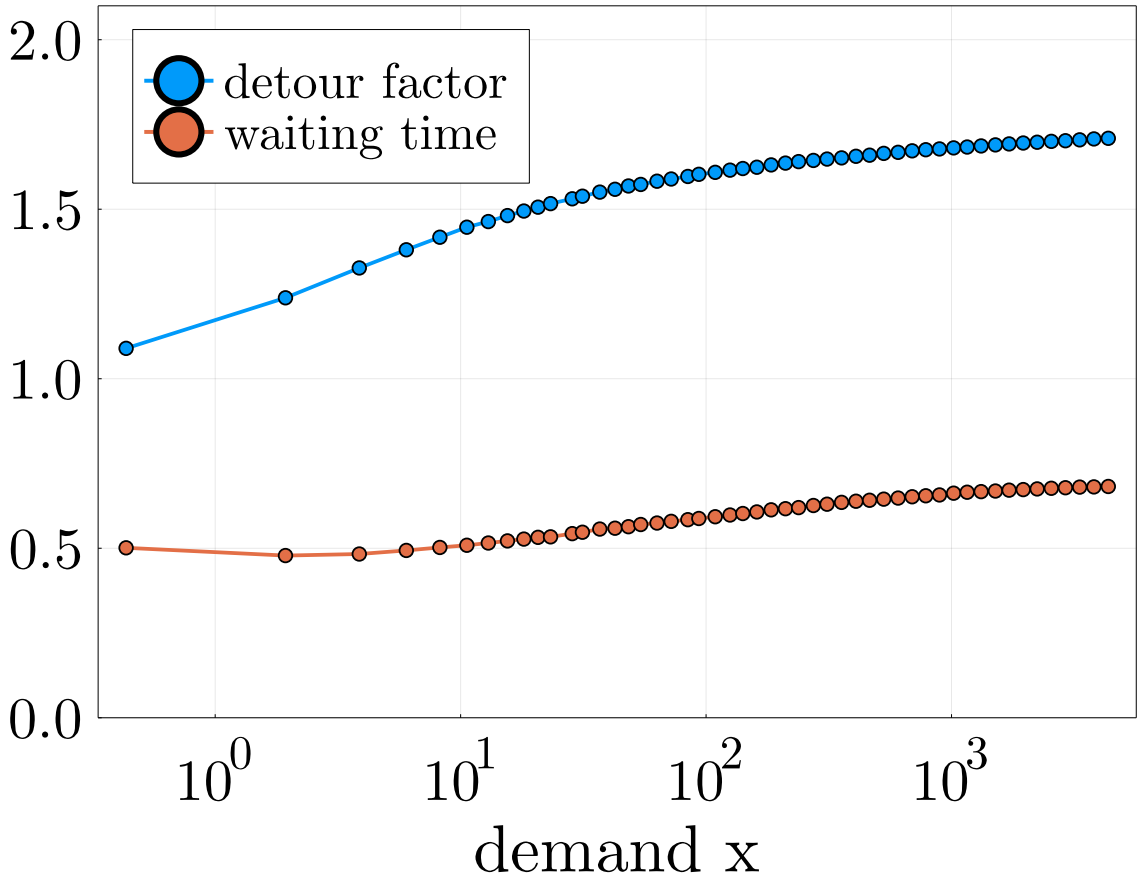

Figure 3.3: Detour factor (δ) and mean waiting time (τ_w) for various demands [39].

Energy consumption

We use the numbers found for frequently used transport vehicles for shuttle services. Specifically, we consider the Mercedes Sprinter (8.8 liters of Diesel per 100km)[40], yielding, $e_{\text{shuttle}} = 3.28\text{kN}$.

3.2.2 Public transit (PT)

Public transit is used as a primary mode of transportation because people can be pooled together. It is used to travel over larger distances. While public transit typically includes buses, trams, subways, light rails, etc., in this chapter, we consider electric light rails for our analysis. Below we discuss the essential ingredients of the public transit system.

Speed

Unlike shuttles, public transit operates on fixed routes and schedules, thus making them a faster and more reliable mode of transit. The effective train speed v_{train}, depends on the inter-station distance ℓ. If trains are assumed to have a maximum operating speed of v_m, acceleration and deceleration time t_a, and a stop time of t_s at every station. The effective average train speed is therefore

$$v_{\text{train}} = \begin{cases} \frac{\ell}{\frac{\ell}{v_m}+t_a+t_s}, & \text{if } \ell \geq v_m \cdot t_a \\ \frac{\ell}{2\sqrt{\frac{\ell t_a}{v_m}}+t_s}, & \text{otherwise} \end{cases} . \tag{3.3}$$

For New York, we use $v_m = 89\,\text{km/h}$ and $v_{\text{train}} = 28\,\text{km/h}$ [41] at $\tilde{\ell} = 0.28$ (see Tab. 3.1). We use Eq. 3.3 to determine t_a and t_s by assuming that $t_a = t_s$. Similarly, for Berlin we use $v_m = 72\,\text{km/h}$ and $v_{\text{train}} = 30.7\,\text{km/h}$ [42] at $\tilde{\ell} = 0.32$. For our analysis, we use New York train speed as a proxy for $\Lambda = 10^4$ and Berlin train speed for $\Lambda = \{10^3, 10^2\}$.

Frequency and capacity

Trains operate at regular intervals, defined by a frequency, μ. Additionally, these trains are assumed to operate at a capacity of $k = 100$ passengers. The choice of the frequency parameter μ is crucial, to optimize the efficient utilization of resources. Detailed discussion on this frequency parameter can be found in Subsec. 3.3.2.

Energy consumption

We consider electric light rails with a maximum seating capacity, $k = 100$, and $e_{\text{train}} = 9.72\text{kN}$[43].

3.3 Parameters of operation

In order to achieve the objective of providing a highly efficient door-to-door transportation service with minimal energy consumption, the providers of bi-modal transit must carefully consider and strategically adjust specific parameters of operation. These critical adjustments play a pivotal role in optimizing the overall performance and sustainability of the transportation system (which we discuss in Sec. 3.4), ultimately benefiting both the service providers and the environment. In this section, we will explore the key parameters that influence the operation of bi-modal transit.

3.3.1 Choosing the type of transport service

Within the framework of our model system, an individual traveler has the option of utilizing either a uni-modal service, which exclusively employs shuttles (referred to as DRRP), or a more versatile bimodal service. The bimodal service involves a sequence of steps, commencing with a shuttle ride from their origin point $\mathcal{P} = (x_p, y_p)$ to the nearest train station. From there, the journey continues with a train ride, and finally, another shuttle journey takes the traveler to their destination at point $\mathcal{D} = (x_d, y_d)$ (see Fig. 3.1b).

In addition to the intricate task of optimizing shuttle routes to maximize pooling efficiency, the dispatching system assumes a central role in the decision-making process. Specifically, it is tasked with the critical responsibility of determining, for each individual travel request, $(\mathcal{P}, \mathcal{D})$, whether the most effective means of providing door-to-door service is through the uni-modal or bi-modal service option. This decision is pivotal in ensuring the efficient and tailored provision of transportation services to meet the diverse needs of travelers within our system.

Convenience

If only user convenience were considered relevant, one would just need to calculate which type of transport service (uni-modal or bi-modal) requires less time for completing the transit, and then to choose that one. This requires knowledge of the parameters v_0, v_{train}, and the frequency of line service, μ. The latter can be assumed to be just sufficient to carry the bi-modal passenger load. Its derivation will be discussed further below (see Subsec. 3.3.2). By sampling random transport requests in the plane, and distances from the probability distribution $p(d)$ of travel distances, we can compile a histogram of relative travel times, t_{bi} and t_{uni}. In Fig. 3.4a, we compare the time it takes to serve a new user request $(\mathcal{P}, \mathcal{D})$ by bi-modal and uni-modal transportation. In order to do so we sample $N = 10^5$ pick-up $(\mathcal{P})$ and drop-off $(\mathcal{D})$ pairs. The trains operate at $\tilde{\mu} = 2$.

The time it takes to serve a randomly sampled user request $(\mathcal{P}, \mathcal{D})$ by bi-modal transportation (t_{bi}) comprises of driving time in two shuttles to the nearest train station,

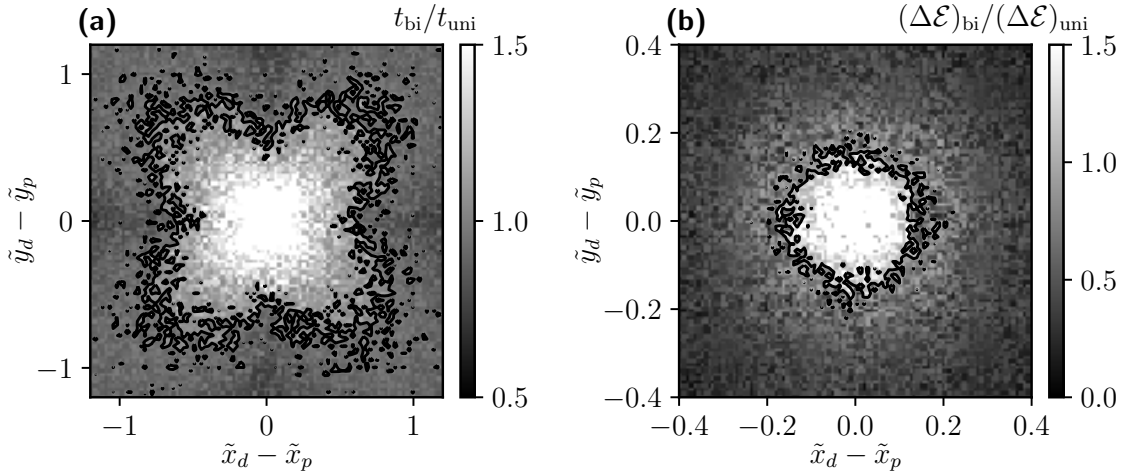

Figure 3.4: **Choosing the type of transport service.** Relative characteristics of either bi-modal (shuttle-train(s)-shuttle) or uni-modal (just shuttle) service, in the plane spanned by the individual trip vector from pick-up $\mathcal{P} = (x_p, y_p)$ to drop-off $\mathcal{D} = (x_d, y_d)$. **(a)** Bi-modal travel time, t_{bi}, divided by uni-modal travel time, t_{uni}. The black curve represents the contour line where both are equal. Requests outside this region are served faster with bi-modal transportation. **(b)** Increment in total energy consumption if a new user is served by bi-modal transportation, $(\Delta\mathcal{E})_{\mathrm{bi}}$ divided by the increment in total energy consumption if the same user is served by uni-modal transportation, $(\Delta\mathcal{E})_{\mathrm{uni}}$. The black curve represents the contour line where both are equal, i.e., from the perspective of energy consumption both types of transport service are equivalent. Requests outside the white region lead to lower energy consumption if served by bi-modal transportation.

driving time in train between the two train stations, waiting time due to shuttles and waiting time at the train station. If $\mathcal{S}_\mathcal{P}$ and $\mathcal{S}_\mathcal{D}$ represent the location of the train station next to $\mathcal{P}$ and $\mathcal{D}$, respectively, then

$$t_{\text{bi}} = \underbrace{2t_w^{\text{shuttle}} + \delta\frac{\overline{\mathcal{P}\mathcal{S}_\mathcal{P}}}{v_0} + \delta\frac{\overline{\mathcal{D}\mathcal{S}_\mathcal{D}}}{v_0}}_{\text{two shuttle trips}} + \underbrace{t_w^{\text{train}} + \frac{\overline{\mathcal{S}_\mathcal{P}\mathcal{S}_\mathcal{D}}}{v_{\text{train}}}}_{\text{train}}, \tag{3.4}$$

where $t_w^{\text{shuttle}}, t_w^{\text{train}}$ are the waiting times incurred due to shuttles and trains and are assumed to take the values $t_0/2$ and $1/2\mu$, respectively.

The time taken to serve the same request by uni-modal transportation (shuttles only) is:

$$t_{\text{uni}} = t_w^{\text{shuttle}} + \delta\frac{\overline{\mathcal{P}\mathcal{D}}}{v_0}. \tag{3.5}$$

The resulting ratio $t_{\text{bi}}/t_{\text{uni}}$ is displayed as a scatter heat map in the plane spanned by the vector $\overline{\mathcal{P}\mathcal{D}}$. Requests corresponding to the area within the black curve (contour curve of $t_{\text{bi}}/t_{\text{uni}} = 1$) would then be served uni-modally by a single shuttle services, while for all others, the dispatcher would offer bi-modal transport service.

Energy

In order to choose, for an incoming request $(\mathcal{P}, \mathcal{D})$, the type of transport service that consumes the least incremental amount of energy, we have to compute the energy increment $(\Delta\mathcal{E})_{\text{bi}}$ needed for bi-modal transport, and compare it to the energy increment $(\Delta\mathcal{E})_{\text{uni}}$ assuming direct transport via a single shuttle. This ratio of energy increments is equal to the ratio of driven distances by the shuttles for each type of service. We assume that a single request does not alter the line service frequency, i.e, the energy consumption of the line service does not change. In analogy to the travel times shown in Fig. 3.4a, we plot the ratio of increment in energy usage for serving a new user request in Fig. 3.4b.

The increment in energy usage when serving a new request by bi-modal transportation comprises of the increment in energy usage by two shuttle trips,

$$(\Delta\mathcal{E})_{\text{bi}} = \eta^{-1} \cdot e_{\text{shuttle}} \cdot (\overline{\mathcal{P}\mathcal{S}_\mathcal{P}} + \overline{\mathcal{D}\mathcal{S}_\mathcal{D}}). \tag{3.6}$$

The increment in energy usage, when served by uni-modal transportation, comprises only a single shuttle trip,

$$(\Delta\mathcal{E})_{\text{uni}} = \eta^{-1} \cdot e_{\text{shuttle}} \cdot \overline{\mathcal{P}\mathcal{D}}. \tag{3.7}$$

The ratio $(\Delta\mathcal{E})_{\text{bi}}/(\Delta\mathcal{E})_{\text{uni}}$, i.e., $\frac{\overline{\mathcal{P}\mathcal{S}_\mathcal{P}}+\overline{\mathcal{D}\mathcal{S}_\mathcal{D}}}{\overline{\mathcal{P}\mathcal{D}}}$, if greater than 1 (less than 1), indicates whether the two trips to/from the train stations are longer (shorter) than a direct trip.

Note that only shuttles contribute to $\Delta\mathcal{E}$ because a single user request is assumed to have no effect on train operations. Again, we see that while for small requested distances

uni-modal service is advisable, bi-modal service should be preferred for larger distances, corresponding to the area outside the black contour curve.

Comparison of Figs. 3.4a and 3.4b reveals that there is a significant range of distances that lie outside the solid curve in Fig. 3.4b, but still well inside the curve depicted in Fig. 3.4a. This shows that we may have to deal with conflicting objectives for quite a number of incoming transport requests. The notion of optimality then depends upon the relative valuation of energy consumption and service quality. As a generally accepted way of dealing with conflicting objectives, we will tackle this problem by means of Pareto fronts [44, 45, 46] further below (see Subsec. 3.5.1).

While the plot in Fig. 3.4b represents a rather isotropic structure, we encounter a shamrock-like shape in Fig. 3.4a. This reflects the orthogonal geometry of our model line service system (Fig. 3.1). In a real situation, the geometry will in general not be this simple. Instead, the directions at which rails are installed will vary from one station to another. We thus expect a structure like the 'shamrock' to be less pronounced in reality, if discernible at all. Hence although a perfectly isotropic structure may not be expected, the anisotropy will certainly be less pronounced. We assume that it will be a reasonable approximation to consider the contour line of service times as 'sufficiently' circular. Therefore we consider henceforth only the requested travel distance, $d = |\overline{\mathcal{PD}}|$, as the discriminating parameter for the choice of type of transport service, irrespective of its direction. The task of the dispatcher will then be to determine a proper cutoff distance, $\boldsymbol{d}_\mathrm{c}$, such that for $d > \boldsymbol{d}_\mathrm{c}$, bi-modal service is offered, while for $d \leq \boldsymbol{d}_\mathrm{c}$, the system will provide uni-modal service, by shuttle only.

Note that the above approximation provides a lower bound of the performance achievable. In a real system, the type of transport service may be decided upon the true expected travel times and energy consumption, for which data will be available with ever-improving quality over time.

3.3.2 Choice of line service frequency

It is clear that the capacity k and frequency μ of the line service must be sufficient to carry the flux of shuttle passengers towards and from the train stations. The total number of requests emanating in unit time in an area of ℓ^2 around a train station is $\nu E \ell^2$. Out of these, only a fraction $F = F(\boldsymbol{d}_\mathrm{c}) = \int_{\boldsymbol{d}_\mathrm{c}}^{\infty} p(d)\, \mathrm{d}d$ is served by bi-modal transportation. However, trains are also occupied by passengers from previous stations. If D_train is the average distance that users travel on trains, then a user travels D_train/ℓ stations on train on average. Therefore, the total number of users to be transported at this station per unit time is

$$\mathcal{J}_\mathrm{in} = \nu E \ell^2 F \frac{D_\mathrm{train}}{\ell}\,. \tag{3.8}$$

We find that $D_{\text{train}} = \frac{4}{\pi}\langle d\rangle_{d>\boldsymbol{d}_c}$[2], with $\langle d\rangle_{d>\boldsymbol{d}_c}$ the mean of requested distances larger than $\boldsymbol{d}_c$.

A similar relation holds for the number of users per unit time that can be transported by trains arriving at one train station (with frequency μ_0 and going into four directions), namely

$$\mathcal{J}_{\text{out}} = 4 \cdot \mu_0 \cdot k\,. \tag{3.9}$$

Balancing $\mathcal{J}_{\text{in}}$ with $\mathcal{J}_{\text{out}}$, we obtain

$$\tilde{\mu}_0 = \frac{\Lambda\tilde{\ell}}{\pi k}\langle\tilde{d}\rangle_{\tilde{d}>\tilde{\boldsymbol{d}}_c} F \tag{3.10}$$

for the minimum frequency required to carry all passengers conveyed by the shuttles. The $\tilde{}$ indicates quantities non-dimensionalized via division by the respective unit, i.e., D or t_0. We refer to Eq. 3.10 as passenger flux balance.

If we allow trains to operate at a frequency $\tilde{\mu}$ larger than the minimum required frequency $\tilde{\mu}_0$, the train occupancy is given by $\boldsymbol{\alpha} = \tilde{\mu}_0/\tilde{\mu} \in [0, 1]$. As this can be adjusted within some range when operating the line service, $\boldsymbol{\alpha}$ provides an additional free variable in system operation.

3.4 Objectives of operation

We identify the conflicting objectives for optimization, i.e., user convenience and energy consumption. Below we discuss these objectives in details and their dependence on the parameters of operation (discussed in Sec. 3.3).

3.4.1 Service quality

We define the service quality as the ratio between average travel time by MIV and by the bi-modal system

$$\mathcal{Q} = \frac{t_0}{(1-F)\cdot t_{\text{uni}} + F \cdot t_{\text{bi}}}\,. \tag{3.11}$$

For assessing the overall quality of service, suitable averaging has to be applied. Transportation by shuttles is always assumed to be delayed with respect to MIV by a waiting time, which we assume (on average) to be of order one half the direct travel time, $t_0/2$ (see Fig. 3.3 for motivation). The average time taken to serve a request in a bi-modal system (i.e., the denominator of $\mathcal{Q}$ in Eq. 3.11) is then

$$t_0\,\mathcal{Q}^{-1} = (1-F)\cdot \underbrace{\left(\frac{t_0}{2} + \frac{\delta\langle d\rangle_{d<\boldsymbol{d}_c}}{v_0}\right)}_{t_{\text{uni}}} + F\cdot \underbrace{\left(t_0 + \frac{2\beta\ell\delta}{v_0} + \frac{1}{\mu} + \frac{4}{\pi}\frac{\langle d\rangle_{d>\boldsymbol{d}_c}}{v_{\text{train}}}\right)}_{t_{\text{bi}}}, \tag{3.12}$$

[2] Averaging the 1-norm $\|\overline{\mathcal{PD}}\|_1$ over distances and orientations.

where $\langle d\rangle_{d<\boldsymbol{d}_c}$ represents the mean of all requested distances less than $\boldsymbol{d}_c$ (i.e., served uni-modally) and δ is the average detour[3] incurred by the shuttles due to the necessity of pooling several different transport requests into one vehicle route. For the second term (t_{bi}), t_0 is the total average waiting time for two shuttle trips (to and from the station), $1/\mu$ is the average waiting time for two train rides (usually there is a change involved), $\beta\ell$ is the average distance of a randomly chosen point from the next train station, with a geometrical constant $\beta \approx 0.383$[4], and $4\pi^{-1}\langle d\rangle_{d>\boldsymbol{d}_c}$ is the average distance traveled on trains. The effective train velocity, v_{train}, depends on the inter-station distance ℓ and is modeled based on train vehicle data (see Subsec. 3.2.2).

If we use D, t_0, and v_0 as units for length, time, and velocity, respectively, we can write:

$$\mathcal{Q}^{-1} = (1-F)\cdot\left(\frac{1}{2}+\delta\langle\tilde{d}\rangle_{\tilde{d}\leq\tilde{\boldsymbol{d}}_c}\right) + F\cdot\left(1+2\beta\tilde{\ell}\delta+\frac{1}{\tilde{\mu}}+\frac{4}{\pi}\frac{\langle\tilde{d}\rangle_{\tilde{d}>\tilde{\boldsymbol{d}}_c}}{\tilde{v}_{train}}\right). \tag{3.13}$$

3.4.2 Energy consumption

In order to assess the efficiency of a transit system in terms of energy consumption, it is essential to consider the total distances over which passengers are being transported in the different vehicles involved (see Eq. 3.14). The bi-modal energy consumption can be written as

$$\mathcal{E} \equiv \frac{\Delta_{shuttle}\cdot e_{shuttle}+\Delta_{train}\cdot e_{train}}{\Delta_{MIV}\cdot e_{MIV}}, \tag{3.14}$$

where $\Delta_\cdot$ denotes the (mode-specific) total distance traveled in a unit cell of size ℓ^2 per unit time, and $e_{shuttle/train}$ is the vehicle-specific energy consumption per unit distance. Note that this expression is already normalized with respect to the MIV energy consumption (denominator), as this is the door-to-door transportation system we intend to compare with. For $\mathcal{E} > 1$ (< 1) energy requirement for bi-modal transportation is more (less) than for private cars serving the same requests.

Shuttles Both uni-modal (shuttle only) and bi-modal trips contribute to the total distance driven by shuttles per unit time due to requests from a unit cell of size ℓ^2, hence

$$\Delta_{shuttle} = \frac{\nu E\ell^2}{\eta}\left(\underbrace{\langle d\rangle_{d<\boldsymbol{d}_c}(1-F)}_{\text{shuttle only}} + \underbrace{2\beta\ell F}_{\text{two shuttle trips}}\right), \tag{3.15}$$

[3] driven distance / direct distance

[4] A simple calculation shows that $\beta = \frac{1}{6}(\sqrt{2}+\log(1+\sqrt{2})) = 0.383$.

where η is the DRRP pooling efficiency, which is the ratio of requested direct distance by the users and the driven distance by the shuttles (for MIV, $\eta = 1$).

In simulations of the uni-modal system (shuttles only), it has been observed that η scales with demand Λ roughly in an algebraic manner, $\eta(\Lambda) \propto \Lambda^{\gamma}$, with $\gamma \approx 0.12$ [38]. In a bi-modal system, however, some of the demand Λ is directed towards trains, therefore, we need to compute an adjusted demand, $\Lambda_{\text{shuttle}} \equiv (E\nu_{\text{shuttle}} D_{\text{shuttle}}^3)/v_0$, considering shuttle trips only; ν_{shuttle} is the effective request frequency for shuttle trips and D_{shuttle} is the average distance of a shuttle trip. Bi-modal trips consist of two shuttle trips (from and to the station), therefore

$$\nu_{\text{shuttle}} = \underbrace{2\nu F}_{\text{two shuttle trips}} + \underbrace{\nu(1-F)}_{\text{shuttles only}} = \nu(1+F)\,. \tag{3.16}$$

Similarly, the average requested distance for shuttle-borne trips involved in bi-modal transport is

$$D_{\text{shuttle}} = \big(\underbrace{2\beta\ell F}_{\text{two shuttle trips}} + \underbrace{\langle d \rangle_{d<\boldsymbol{d}_c}(1-F)}_{\text{shuttles only}} \big)/(1+F)\,, \tag{3.17}$$

where $(1+F)$ is due to normalization. The bi-modal demand for shuttles is thus given by:

$$\begin{aligned} \Lambda_{\text{shuttle}} &= (E\nu_{\text{shuttle}} D_{\text{shuttle}}^3)/v_0 \\ &= \Lambda\,(1+F)^{-2}((1-F)\langle \tilde{d} \rangle_{\tilde{d}\le\tilde{\boldsymbol{d}}_c} + 2\beta\tilde{\ell}F)^3\,. \end{aligned} \tag{3.18}$$

In simulations, we observe a higher efficiency than suggested by $\eta \propto \Lambda_{\text{shuttle}}^{0.12}$ (see Fig. 3.5 for simulation data). We call this the *common stop effect*, meaning that pooling gets more efficient because bi-modal requests are spatially correlated due to shared pick-up and drop-off locations, i.e., the train stations. We account for this effect via an empirical function $h(F)$ ($1 \le h \le 1.35$, see Fig. 3.5). In particular, we set

$$\eta \equiv \Lambda_{\text{shuttle}}^{0.12} \cdot h(F)\,. \tag{3.19}$$

Line Service and MIV Trains are recurrent every $1/\mu$ time units. Therefore, the cumulative distance driven by all trains in a unit cell of side length ℓ per unit time is

$$\Delta_{\text{train}} = 4 \cdot \mu \cdot \ell\,. \tag{3.20}$$

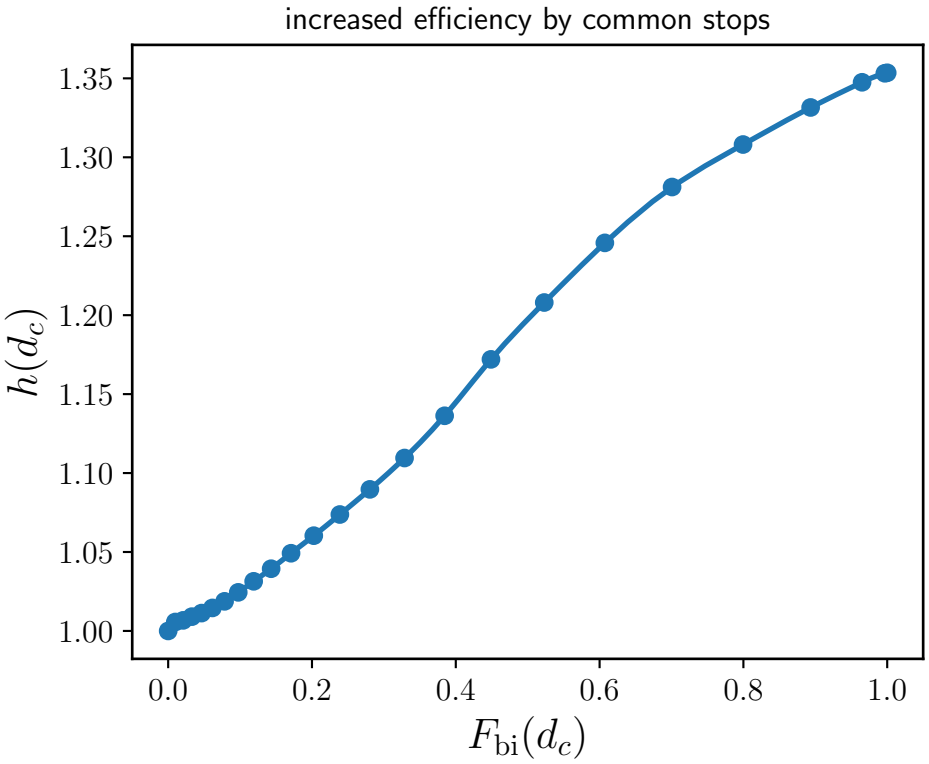

Figure 3.5: $h(F(\boldsymbol{d}_c))$ as a function of $F(\boldsymbol{d}_c)$. The 'common stop effect' is maximal for $F = 1$, this is when all trips are served by bi-modal transport and all trips have either common origin or destination [39].

There is a multiplicative factor of 4 because trains go in four directions at every train station. The total distance driven via MIV for requests from the unit cell amounts to

$$\Delta_{\mathrm{MIV}} = \nu E \ell^2 D. \tag{3.21}$$

Replacing $\Delta_{\mathrm{shuttle}}$, Δ_{train}, and Δ_{MIV} in Eq. 3.14 from Eq. 3.15, 3.20, and 3.21 we obtain the final expression for the energy consumption of bi-modal transit normalized with respect to MIV

$$\mathcal{E} = \underbrace{\eta^{-1}\left(\langle \tilde{d}\rangle_{\tilde{d}\leq \tilde{\boldsymbol{d}}_{\mathrm{c}}}(1-F) + 2\beta\tilde{\ell}F\right)\cdot\frac{e_{\mathrm{shuttle}}}{e_{\mathrm{MIV}}}}_{\text{shuttles}} + \underbrace{\frac{4\tilde{\mu}}{\Lambda\tilde{\ell}}\cdot\frac{e_{\mathrm{train}}}{e_{\mathrm{MIV}}}}_{\text{train}}. \tag{3.22}$$

3.5 Results

We now analyze how the objectives, i.e., energy consumption (Eqs. 3.14, 3.22) and quality (Eqs. 3.11, 3.13), can be optimized by choice of parameters of operation, i.e., cutoff distance $\boldsymbol{d}_{\mathrm{c}}$ and train occupancy $\boldsymbol{\alpha}$, under different 'external' conditions, Λ and $\tilde{\ell}$. Notice that the two control parameters, $\boldsymbol{\alpha}$ and $\boldsymbol{d}_{\mathrm{c}}$, enter the objectives, $\mathcal{Q}$ and $\mathcal{E}$, via $\langle \tilde{d}\rangle_{\tilde{d}\leqslant\tilde{\boldsymbol{d}}_{\mathrm{c}}}$, $F(\boldsymbol{d}_{\mathrm{c}})$, and $\tilde{\mu} = \tilde{\mu}_0(\boldsymbol{d}_{\mathrm{c}})/\boldsymbol{\alpha}$ (Eq. 3.10).

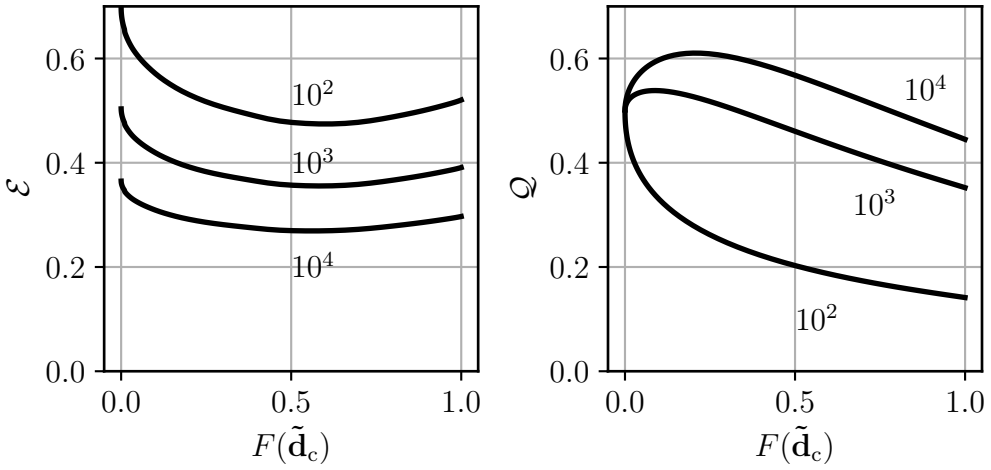

Figure 3.6: **Bi-modal performance characteristics.** Energy consumption $\mathcal{E}$ and service quality $\mathcal{Q}$ for bi-modal transport, normalized with respect to MIV, as a function of the bi-modal fraction $F(\boldsymbol{d}_{\mathrm{c}})$, for three different values of demand $\Lambda = \{10^2, 10^3, 10^4\}$. All data for $\tilde{\ell} = 0.8$ and fully-occupied trains, $\boldsymbol{\alpha} = 1$.

In Fig. 3.6, energy consumption, $\mathcal{E}$, and service quality, $\mathcal{Q}$, for the combined system are shown as a function of the share of bi-modal transport $F(\boldsymbol{d}_{\mathrm{c}})$ at $\tilde{\ell} = 0.8$ for three different values of dimensionless demand, Λ. Trains are operated at full occupancy, i.e., $\boldsymbol{\alpha} = 1$. The general trend of reduction of energy consumption with increasing

demand and involvement of line services is obvious from the data for $\mathcal{E}$. We encounter a minimum of energy consumption at around $F \approx 0.6$ for all values of Λ investigated. Energy consumption can be less than 30% of MIV for sufficiently large (but realistic, see Tab. 3.1) demand. For service quality, we find that typical values are around one half the service quality of MIV, i.e., about twice the travel time. This is customary for public transport systems [47, 48] and generally well accepted by users. Note that our data for service quality represent a safe lower bound, as the (sometimes quite substantial) time required for parking spot search [49, 50] is neglected here in t_0. While for low Λ the involvement of line service seems to generally increase travel times (i.e., reduce service quality), we find an optimum at $F \approx 0.25$ for large Λ. The primary message from Fig. 3.6, however, is that minimizing energy consumption and maximizing service quality cannot be simultaneously achieved.

3.5.1 Pareto fronts in energy consumption and service quality

A tuple of parameter values, in our case $(\mathcal{E}, \mathcal{Q})$, is called Pareto optimal if none of the parameters (or objectives) can be further optimized without compromising on at least one of the others. The set of all such tuples of parameters is called the Pareto front. To illustrate this concept, in Fig. 3.7a, we show all values $\{\mathcal{E}(\boldsymbol{d}_\mathrm{c}, \boldsymbol{\alpha}), \mathcal{Q}(\boldsymbol{d}_\mathrm{c}, \boldsymbol{\alpha})\}$ obtained for different values of $\boldsymbol{d}_\mathrm{c}$ and $\boldsymbol{\alpha}$ as grey dots. The solid black line represents the Pareto-optimal subset, i.e., the Pareto front.

In order to choose the truly optimal point on the Pareto front, one needs to define the relative valuation of the objectives, $\mathcal{E}$ and $\mathcal{Q}$. In other words, the authorities operating the system have to decide how much reduction in service quality they (i.e., the users) would be willing to accept for how much savings in energy. The ratio of these valuations is then expressed in the slope of the dashed line in Fig. 3.7a, which is a tangent to the Pareto front. The point where it touches the front (black dot) represents the optimal set of parameters, under the given valuation.

For our analysis, we fix the train capacity to $k = 100$, and choose a representative set of values for line service mesh size $\tilde{\ell} = \{0.2, 0.4, 0.8\}$ and demand $\Lambda = \{10^2, 10^3, 10^4\}$, corresponding to a typical parameter range encountered in real systems (see Tab. 3.1). Note that fixing k does not reduce the generality of our study, because a different k can be compensated for by properly readjusting μ_0 (see Eq. 3.10).

Fig. 3.7b demonstrates the effect of Λ on the overall performance of the system. Pareto fronts are shown in black. We see that for typical values of Λ, as listed in Tab. 3.1, energy consumption reaches down to well below 40% (even below 20%) of MIV for large values of Λ. At the same time, quality levels are comparable to, mostly even in excess of, what is found in existing public transport in terms of transit time (see Tab. 3.1). Note, however, that our system even provides on-demand door-to-door service, comparable to MIV.

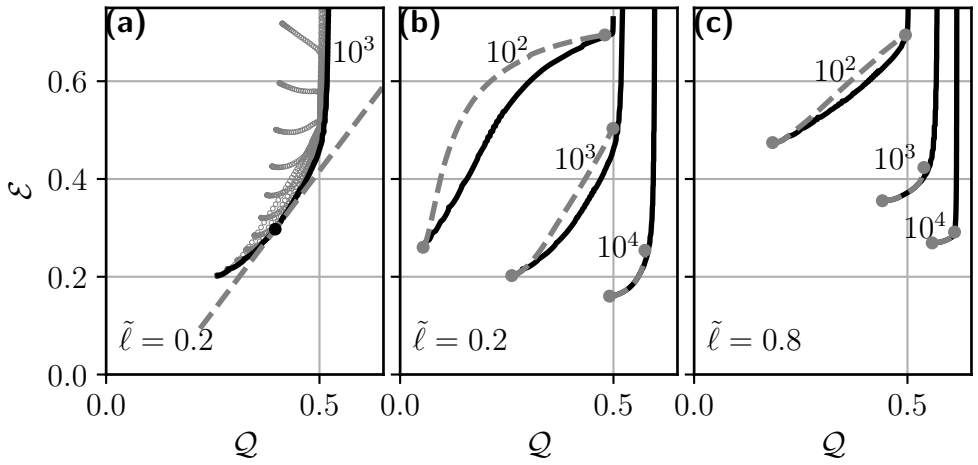

Figure 3.7: **Emergence of Pareto fronts and effects of train occupancy**. **(a)** Grey circles: admissible data for full variation of $\boldsymbol{\alpha}$ and $\boldsymbol{d}_c$, at $\tilde{\ell} = 0.2$ and $\Lambda = 10^3$. Black curve: Pareto front, i.e., the boundary of the full data set towards optimality (low $\mathcal{E}$ and high $\mathcal{Q}$). The slope of the dashed tangent to the Pareto front represents the ratio of valuations (see text). **(b)**. Black curves: Pareto fronts for variable train occupancy $\boldsymbol{\alpha} < 1$ at $\Lambda = \{10^2, 10^3, 10^4\}$ and $\tilde{\ell} = 0.2$. Grey dashed curves: degenerate Pareto fronts obtained at full train occupancy ($\boldsymbol{\alpha} = 1$) at corresponding values of Λ. Grey circles mark the ends of these fronts which are determined by minimum achievable energy consumption and maximum achievable service quality, specific to Λ and $\tilde{\ell}$. **(c)** Same as (b) but for $\tilde{\ell} = 0.8$.

The dashed grey curves indicate the subset of data for train occupancy $\boldsymbol{\alpha} = 1$. We will henceforth call them degenerate Pareto fronts, as they correspond to the variation of only one parameter. They are lying, slightly but consistently, above the Pareto fronts. This indicates that by reducing train occupancy below its maximum ($\boldsymbol{\alpha} < 1$), i.e., operating trains at higher frequency than necessary, one can enhance the overall performance of the system. Service quality increases because the time spent waiting for trains, which is proportional to $1/\mu$, is smaller when trains are operated more frequently. The increase in service quality is found to overcompensate the increase in energy consumption due to higher operation frequency. Since waiting time is inversely proportional to both Λ and $\tilde{\ell}$ (see Eq. 3.10), this effect is more pronounced for small Λ and $\tilde{\ell}$, which is qualitatively corroborated in Fig. 3.7c which shows corresponding data for large mesh size ($\tilde{\ell} = 0.8$). At the resolution of the figure, the Pareto fronts (black) and their degenerate partner (dashed grey) are distinguishable only for smallest values of Λ. Hence for typical values of Λ and $\tilde{\ell}$ it appears sufficient to discuss the degenerate Pareto fronts, which only need one parameter ($\boldsymbol{d}_c$) to be varied. We keep in mind that the true Pareto optimum will still be superior.

Degenerate Pareto fronts are shown in Fig. 3.8 in various presentations. Fig. 3.8a has basically the same information as Fig. 3.7c, but here we show the full data set (grey), where the black curves are the Pareto-optimal subset, i.e., the degenerate Pareto fronts.

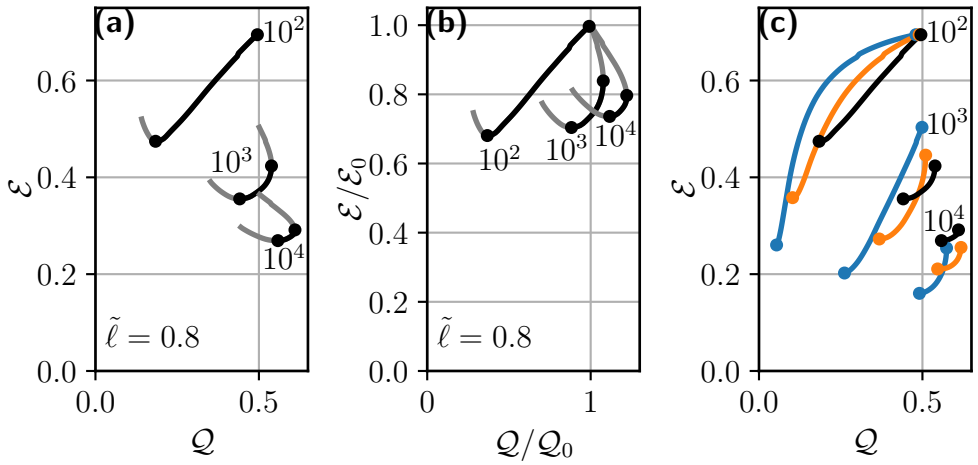

Figure 3.8: **Bi-modal performance with fully-occupied trains.** **(a)** Black curves show degenerate Pareto fronts for fully-occupied trains ($\boldsymbol{\alpha} = 1$) for varying demands $\Lambda = \{10^2, 10^3, 10^4\}$ shown as annotations and $\tilde{\ell} = 0.8$. Black circles mark the end points of the Pareto fronts which are determined by the minimum achievable energy consumption and the maximum achievable service quality. Grey curves show the entire data, i.e., not only the Pareto-optimal set, but all admissible values with $\boldsymbol{d}_c$ as the control parameter. **(b)** Data as in (a), but normalized with respect to the performance, $(\mathcal{Q}_0, \mathcal{E}_0)$, of the uni-modal system (shuttles only). **(c)** Degenerate Pareto fronts as in (a), but for $\tilde{\ell} = \{0.2, 0.4, 0.8\}$ in blue, orange, and black, respectively.

They terminate wherever the tangent becomes either vertical or horizontal (black dots), thus offsetting any tradeoff between the objectives.

Fig. 3.8b shows these data normalized with respect to the performance of a uni-modal (shuttles only) DRRP system, represented by $\mathcal{E}_0$ and $\mathcal{Q}_0$. Clearly in relevant parameter regions the combined bi-modal system outperforms the uni-modal system in both energy consumption ($\mathcal{E} < \mathcal{E}_0$) and service quality ($\mathcal{Q} > \mathcal{Q}_0$).

The effect of inter-station distance (mesh size) on the (degenerate) Pareto fronts is explored in Fig. 3.8c. We see that a dense network of rails (small $\tilde{\ell}$, blue fronts) achieves the best results concerning energy consumption, reaching down to below 20% of MIV, but compromises on achievable service quality. For admissible quality $\mathcal{Q} \approx 0.5$, sparse train networks (black fronts) are Pareto-optimal for low demands. For larger demands, denser train networks (orange and blue fronts) are advantageous.

However, it is remarkable that the overall position of the Pareto fronts in the plane spanned by $\mathcal{Q}$ and $\mathcal{E}$ does not vary dramatically with mesh size, as the position on the front at which the system is operated is largely at the discretion of the operator. This suggests that the density of currently installed rail track systems might already be well suited for deploying a bi-modal on-demand transport systems of the kind we have studied.

3.5.2 Traffic volume

Energy consumption and service quality are not the only possible objectives for optimization of public transport. Road traffic, for example, is a source of noise and local air pollution and occupies significant shares of urban space. Bi-modal ride-pooling reduces traffic by use of shared shuttles, and by directing certain trips towards trains. We quantify this reduction by introducing the relative bi-modal traffic $\tilde{\Delta}_{\text{shuttle}}$ as the ratio of the number of on-road vehicles necessary for bi-modal transportation (i.e., shuttles) to the number of MIV (i.e., cars) needed to serve the same demand.

To derive an expression for road traffic due to shuttles we connect the distance served by busses (left hand side) and the distance traveled by customers (right hand side), with average distance $\langle d \rangle$ traveled on road, for an area of reference A during time $t_0 = D/v_0$, with shuttle speed v_0

$$\underbrace{BA\, v_0 b\, p_{\text{driving}}\, t_0}_{\text{distance served by busses}} = \underbrace{\nu E A\, t_0\, \langle d \rangle \delta\, p_{\text{accept}}}_{\text{distance traveled by customers}} . \tag{3.23}$$

Here B is the shuttle density, b is the average shuttle occupancy, $\nu E A t_0$ is the number of requests in the reference area A during reference time t_0 (with request frequency ν, population density E), δ is the average relative detour of customers (no detour means $\delta = 1$), p_{driving} is the probability of vehicles driving (i.e., not being idle), and p_{accept} is the probability that a user request is accepted. In this study, we assume that all requests can be served ($p_{\text{accept}} = 1$), i.e., no request has to be rejected because certain constraints (like a maximum waiting time) cannot be fulfilled. Substituting $\eta \equiv b/\delta$ (see [38]) in Eq. 3.23, we define the traffic volume, Γ, by the number of driving vehicles, i.e.:

$$\Gamma \equiv BA \cdot p_{\text{driving}} = \frac{\nu E \langle d \rangle A}{\eta v_0} . \tag{3.24}$$

Note that for private cars, $\eta = 1$ and $\langle d \rangle \equiv D$, and for a bi-modal service, $\langle d \rangle = D_{\text{shuttle}}$ and $\nu_{\text{shuttle}} = (1 + F)\nu$ (Eq.3.17, 3.16). Substituting these expressions in Eq. 3.24, we define the normalized traffic volume, $\tilde{\Gamma}$, as the ratio of traffic volume by shuttles in the bi-modal system, Γ_{bi}, and the traffic volume by private cars, Γ_{MIV}, i.e.,

$$\tilde{\Gamma} \equiv \Gamma_{\text{bi}}/\Gamma_{\text{MIV}} = \eta^{-1}(1 + F)\, \tilde{D}_{\text{shuttle}} . \tag{3.25}$$

In Fig. 3.9, $\tilde{\Gamma}$ is plotted against service quality $\mathcal{Q}$ as determined along the degenerate Pareto fronts shown in Fig. 3.8c. For low demand ($\Lambda = 10^2$), uni-modal (shuttles only) transportation allows for about 50% reduction in traffic as compared to MIV (triangle). Bi-modal transportation allows for further reduction in traffic at the cost of service quality. For intermediate and high demand ($\Lambda = \{10^3, 10^4\}$), uni-modal transportation allows for

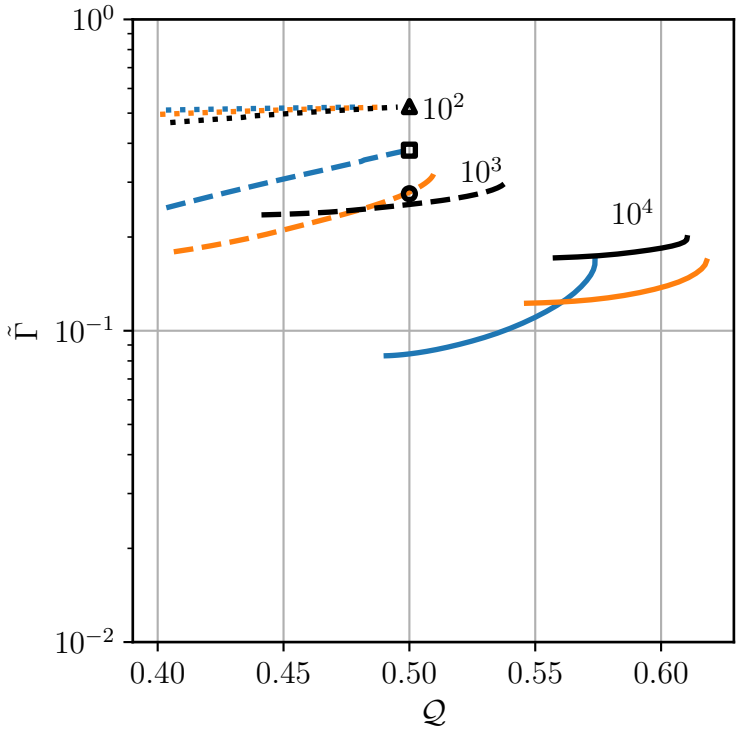

Figure 3.9: **Traffic volume in bi-modal transit.** Relative bi-modal traffic $\tilde{\Gamma}$, as defined in Eq. 3.25, determined along the Pareto fronts in Fig. 3.8c, against corresponding service quality $\mathcal{Q}$. Data are presented for $\Lambda = 10^2$ (triangle, dotted), $\Lambda = 10^3$ (square, dashed), and $\Lambda = 10^4$ (circle, solid). Symbols represent uni-modal traffic volume, $1/\eta$. Color code is as in Fig. 3.8, i.e., $\tilde{\ell} = \{0.2, 0.4, 0.8\}$ in blue, orange, and black, respectively.

about 70% to 80% reduction in traffic as compared to MIV (square, circle). In these cases, bi-modal transportation allows for truly dramatic reductions in traffic ($> 90\%$), at equal or even higher service quality than for uni-modal transport. Combining this finding with typical parameter values in Tab. 3.1, we recognize that even in rural settings, traffic volume is expected to decrease by an order of magnitude, relative to MIV. In urban environments, traffic volume may even be reduced by more than a factor of ten.

3.6 Discussion

In this chapter, our goal was to find whether and under what circumstances bi-modal transport, i.e., on-demand ride-pooling with shared shuttles combined with fixed schedule line services (railway), can be a viable alternative to customary public transportation (line services or DRRP alone) or MIV. For that purpose we introduced a simple model system for bi-modal transport, combined with a mean-field approach, which allowed us to parameterize the user environment (dimensionless demand) as well as the bi-modal service operations (cutoff distance, train occupancy) with few variables, and to write down analytic expressions for key performance characteristics, namely energy consumption and service quality (i.e., transit times), as well as road traffic volume. Our results, in form of Pareto fronts, indicate that bi-modal public transportation systems have the potential to provide on-demand door-to-door service with a quality superior to customary public transportation, while at the same time consuming only a fraction of the energy a corresponding fleet of MIV would require, and with a road traffic volume reduced by an order of magnitude.

In our model, we assume customer demand to be given, more precisely, we assume a spatially uniform demand with constant average request frequency. However, in realistic scenarios, demand will be heterogeneous in space, due to non-homogeneous population density and individual mobility patterns, and fluctuating in time due to phenomena like rush hours or workdays versus weekends. Such spatio-temporal demand patterns can be taken into account by structured railway networks (e.g., more dense in highly-populated areas), spatially varying shuttle densities, and variable service frequencies. In future case studies or real-world applications, these context-specific adjustments can be implemented to provide tailored solutions.

Although demand patterns can be estimated from historical data, there will be fundamental uncertainties in predicting future demand. Such uncertainties will alter the performance of a bi-modal system. Nevertheless, our considerations based on known (average) transportation demand give a valuable estimate of the performance potential of bi-modal transport under various external conditions.

A model should be as simple as possible but not simpler.

Albert Einstein

4

Impact of the density of line service stations

4.1 Introduction

In the previous chapter, we adopted a simplified 'cartesian' network as sketched in Fig. 4.1a, where we assumed line service stations to exist at each crossing. In most cities, however, a line has more stops than crossings with other lines, as sketched in Fig. 4.1b. The impact of these intermediate stops on the overall performance of the system is hitherto not known. On the one hand, intermediate stops increase the user's proximity to transit stations, resulting in shorter shuttle trips to and from train stations. On the other hand, additional stations slow down the trains, potentially impacting the service quality for longer trips. In this chapter, we investigate the impact of intermediate stops on bimodal transit via agent-based simulations. By studying realistic sets of parameters, we aim to provide valuable insights into how the addition of intermediate stops affects factors such as travel time, passenger waiting time, and vehicle occupancy.

In addition, we validate the findings of our study in the previous chapter, which were based on a mean-field approach.

4.2 Methods

For simulating a system of bi-modal transport, with on-demand shuttles and trains operating on lines, we deploy the open-source, multi-agent transport simulation framework, MATSim [51]. In contrast to the mean-field study by in chapter 3, where observables

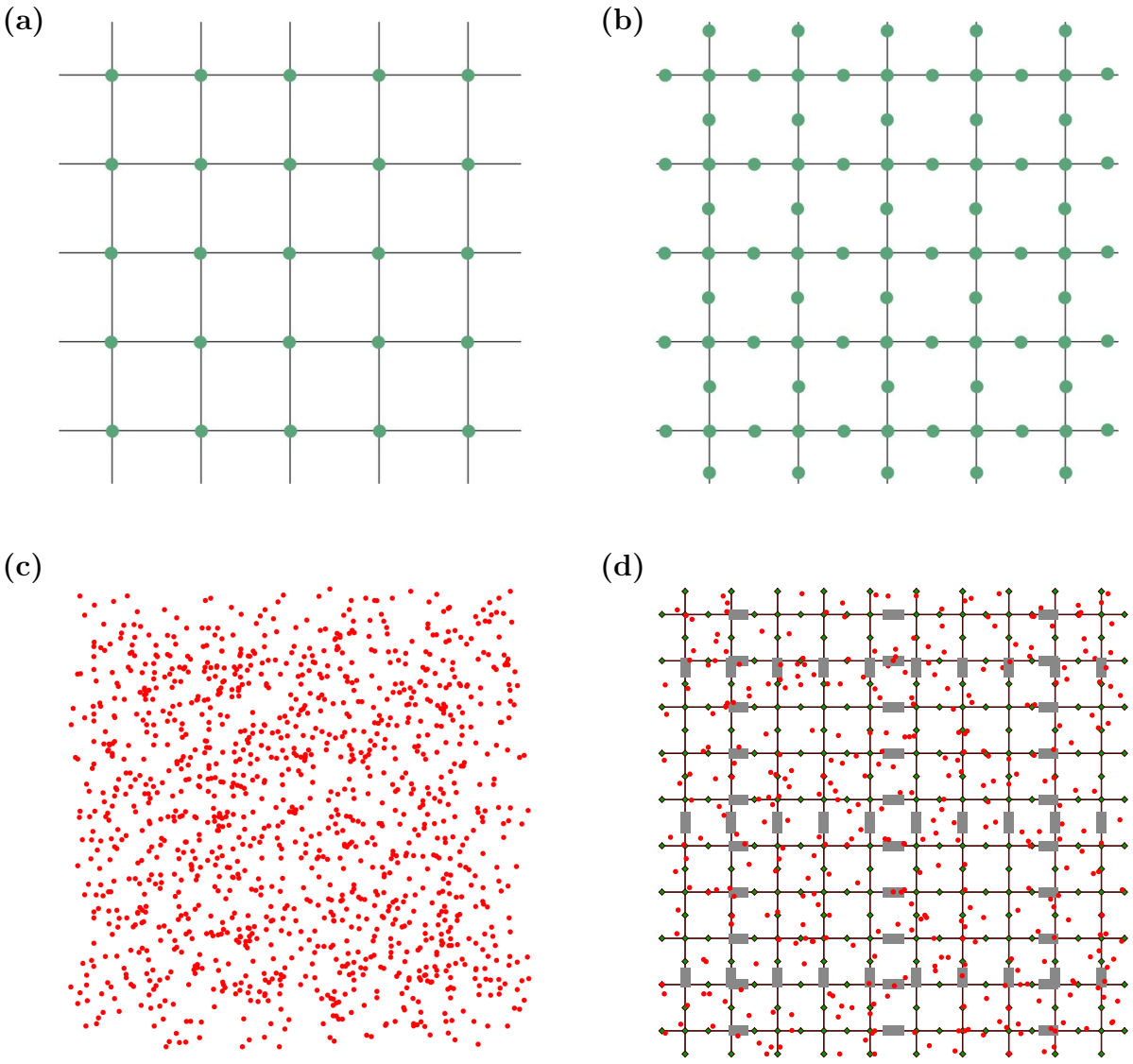

Figure 4.1: **Bi-modal transport network on a square grid. (a)** Idealized line service network. Green nodes at the intersection of railway lines represent the train stations. **(b)** A network as in (a), but with additional (intermediate) stations. **(c)** A snapshot of a simulation where passengers use MIVs (red dots) as the only mode of transportation. **(d)** A snapshot of bi-modal simulations on a network with one intermediate station ($\Theta = 1$). Demand is the same as in (c). Red dots represent shuttles (DRRP), gray rectangles represent trains, and green diamonds represent train stations. The number of required shuttles in a bi-modal system (d) is much lower than the number of MIVS required in (c). See Subsec. 4.3.2 for a quantitative analysis.

like waiting time, vehicle occupancy, or mean detour were estimated by heuristics, in this agent-based framework, transportation requests are served explicitly by individual vehicles (the agents), such that the aforementioned quantities emerge solely based on the user environment and the parameters of operation of the bi-modal transit system. Our methodological contribution lies in the implementation of a bi-modal transit system within an agent-based simulation framework.

4.2.1 Intermediate stops in real cities

We analyzed the subway networks of the cities of Berlin [52] and New York (NYC) [53] with respect to the average number of intermediate stops, Θ, between crossings of disjunct lines. For NYC, we considered Manhattan south of Central Park because in that part of the city, the network is closest to a grid-like structure, as assumed in our study. North of Manhattan, lines are mostly unidirectional (north-south). For Berlin, we took the subway lines inside the "S-Bahn-Ring" (closed loop of the suburban rail system, see Fig. 4.2) from 2016, as a reference. We find on average, $\Theta = 1.08$ for Berlin and $\Theta = 0.983$ for NYC.

4.2.2 Simulation framework

We use an open-source, multi-agent transport simulation framework, MATSim [51]. It can be used for large-scale simulations of microscopic dynamics on (street) networks. The routing is performed using the AStarLandmarks algorithm, which is a modified version of the A* algorithm [54].

MATSim simulation comprises individual users, which are called agents. An initial demand characterizes the trips of the agents. Other inputs for simulations like traffic network, transit schedules for trains and a configuration file that define specific parameters used in the simulations characterize the system under study. Mobility simulations are performed for the specified demand and input parameters. Mobility simulations reported in the chapter paper are queue-based and time-step-based. The links or allowed routes for vehicles are modeled as first-in-first-out (FIFO) queues. Vehicles in the queue leave the link after a time equal to the free flow travel time specific to the link has elapsed. A link is also characterized by the maximum number of vehicles that can be queued. For the purpose of the simulations reported here, we assume that the link capacity is large enough. For the simulations reported here, we consider the uniformly populated planar region of area $\mathcal{A}$ and edges of length $\mathcal{L} = 20\,\mathrm{km}$. The distance ℓ' that separates adjacent transit stations is chosen to be $0.5, 1.0$ and $2.0\,\mathrm{km}$, corresponding to $\Theta = 3, 1,$ and 0, respectively. The distance between major junction stations is fixed to a value of $2\,\mathrm{km}$. For each simulation, $\mathcal{N}$ uncorrelated requests are generated in the region $\mathcal{A}$ over the time $\mathcal{T} = 1\,\mathrm{hr}$.

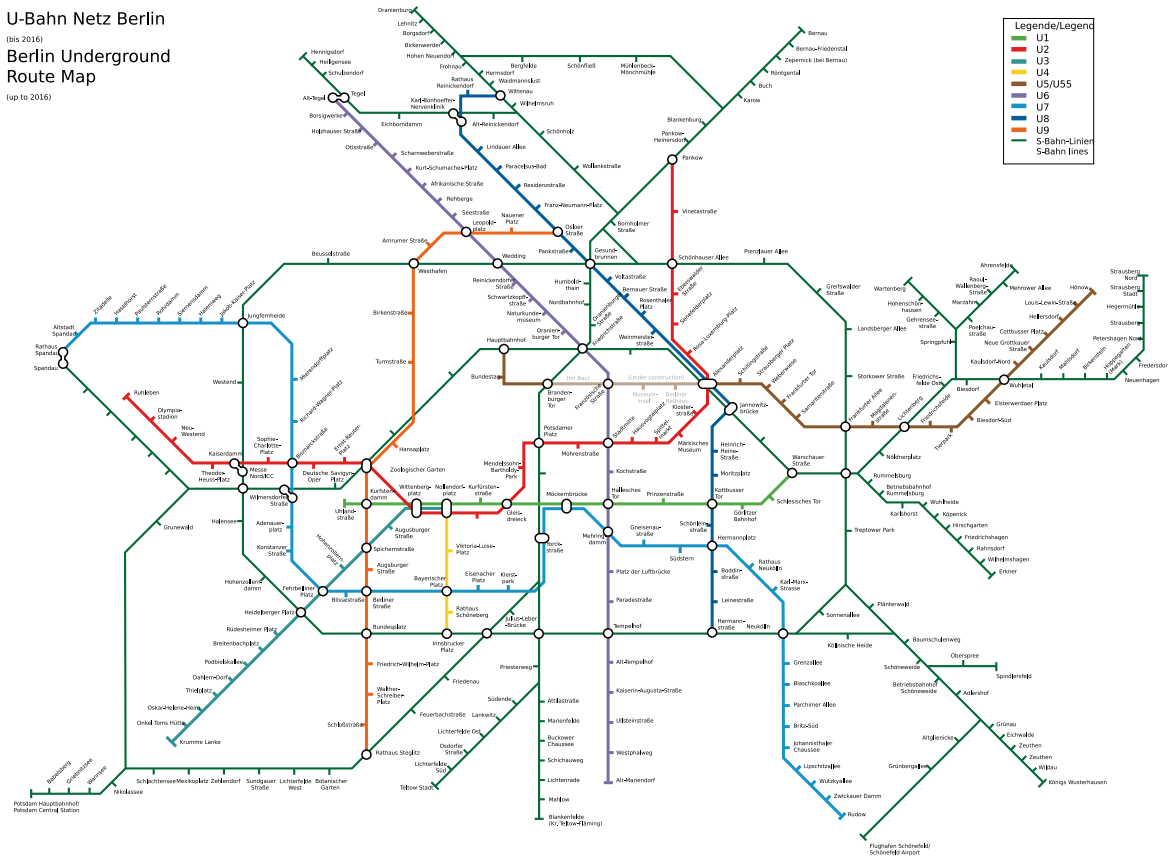

Figure 4.2: Berlin subway and S-Bahn network [52].

4.2.3 User environment

In simulations, we consider a uniformly populated planar region of side length $\mathcal{L} = 20\,\mathrm{km}$, i.e., an area of $\mathcal{A} = 400\,\mathrm{km}^2$, and a total number of transit requests $\mathcal{N}$, uniformly randomly spread over a time $\mathcal{T} = 1\,\mathrm{h}$. Introducing population density E and average request frequency per inhabitant ν, the number of transit requests per time $\mathcal{N}/\mathcal{T} = \nu E\mathcal{A}$. Users are assumed to place transit requests in an uncorrelated fashion, each consisting of a desired pick-up ($\mathcal{P}$) and drop-off ($\mathcal{D}$) location with a requested distance $d = \overline{\mathcal{PD}}$ following a distribution $p(\cdot)$[1]. As average requested distance we choose $D = 5\,\mathrm{km}$ [39] in simulations. We define D as the intrinsic length scale of our system. Shuttles and MIV are assumed to have a characteristic road vehicle velocity, v_0, which we choose to be $30\,\mathrm{km/h}$ [39] in simulations. We can thus obtain the intrinsic time scale[2] $t_0 = D/v_0 = 10\,\mathrm{min}$. This is the average time a travel request would need to be completed by MIV [3]. We denote (non-dimensional) variables measured in these units (D, t_0) with the $\tilde{}$ symbol.

The demand of transport within the system can be characterized by the dimensionless parameter $\Lambda = \frac{\mathcal{N}D^3}{\mathcal{A}\mathcal{T}v_0} = \tilde{\nu}\tilde{E}$, which measures the number of requests for transport in an area of D^2 during time D/v_0 [39]. Typical values range from $\Lambda = 10^2$ to 10^4 for rural up to dense urban transportation scenarios [39].

4.2.4 Bi-modal transit system

We distinguish two types of train stations. Train stations at railway intersections are called junction stations. They are separated by the lattice constant ℓ. Additional train stations are called intermediate stations. The distance between two adjacent train stations along a train line is ℓ'. The number of intermediate stations between two junctions is then $\Theta = \ell/\ell' - 1$. All train stations (intermediate and junction) serve as the connection points between DRRP and line service (see Fig. 4.1b). We restrict our analysis to realistic values of up to three ($\Theta \in \{0, 1, 3\}$) intermediate stations on a grid of length $\ell = 2\,\mathrm{km}$ [39]. This is motivated by what we observe in agglomerations like Berlin and New York, where we find about one intermediate stop on average, and only rarely more than two (see Subsec. 4.2.1). We observed previously in the chapter 3 that the performance of the system is optimal for $\ell/D \approx 0.4$ across an extensive range of user demand [39]. This value is also close to what is found, e.g., for Berlin [39]. Therefore, we fix $\ell/D \approx 0.4$ throughout this study.

The trains operate along orthogonal lines from source to end, the first and the last station of the transit network line in the direction of travel (see Fig. 4.1). The trains

[1] We are using the inverse-gamma distribution as it has been observed in NYC, for example [33].

[2] Introduction of intrinsic length and time scales, D and t_0, as units reduce the number of parameters by two.

[3] $D = 5\,\mathrm{km}$ is at the lower end of typical values for cities/regions and $v_0 = 30\,\mathrm{km/h}$ is at the upper end (see table in [39]), leading to a comparatively short estimate for the average driving time by car.

arrive at stations with a frequency $\mu = 1/10\,\mathrm{min}^{-1}$ and travel at an average speed v_{train}. We assume that trains attain a maximum speed of $3 \cdot v_0$ and the time taken to reach this speed starting from rest is assumed to be $0.05 \cdot t_0$. The trains stop at each connecting station for $0.05 \cdot t_0$. These values are inspired from real data (see [39]). Note that due to these factors, the effective train velocity, v_{train}, depends on the inter-station distance ℓ'. Trains require energy e_{train} per unit distance of travel.

The transit system is further characterized by a number of shuttles, $\mathcal{S}$, in the plane. For the sake of conciseness and simplicity, we assume that the number of shuttles $\mathcal{S}$ is just sufficient to serve all user requests emanating in the system over time $\mathcal{T}$. Shuttles require energy e_{shuttle} per unit distance of travel. User requests served by DRRP/shuttles are subject to the constraint that the maximum accepted detour (traveled distance / direct distance) is $\delta_m = 3$, the maximum waiting time is $\tau_{w,\,\mathrm{max}} = 5\,\mathrm{min} = 0.5 \cdot t_0$ and the maximum travel time is $\alpha \cdot t_{\mathrm{direct}} + \gamma$, where $\alpha = 3$, $\gamma = 10\,\mathrm{min}$ are simulation parameters and t_{direct} is the direct travel time.

We let trains and DRRP operate for a time $2\mathcal{T} = 2\,\mathrm{h}$ in order to ensure that all user requests are served during simulation time.

4.2.5 Average train speed

We assume that trains achieve a maximum speed of $v_m = 3 \cdot v_0$. This value is inspired by data found for New York City subway [55]. The time taken to reach this speed starting from rest is assumed to be $t_a = 0.05 \cdot t_0$. The trains stop at each connecting station for $t_s = 0.05 \cdot t_0$. The average train speed can then be obtained as

$$v_{\mathrm{train}} = \begin{cases} \dfrac{\ell'}{\frac{\ell'}{v_m} + t_a + t_s}, & \text{if } \ell' \geq v_m \cdot t_a \\ \dfrac{\ell'}{2\sqrt{\frac{\ell' t_a}{v_m}} + t_s}, & \text{otherwise} \end{cases}, \tag{4.1}$$

with ℓ' being the inter-station distance. See Fig. 4.3 for explicit values of train speed as a function of inter-station distance.

4.3 Results

We organize our results as follows. First, we present how DRRP performs within a bi-modal system in Subsec. 4.3.1. Then we characterize the overall performance of bi-modal transit systems in terms of energy consumption and service quality in Subsecs. 4.3.2 and 4.3.2. We conclude the results section with an analysis of potential reductions in traffic volume (Subsec. 4.3.2).

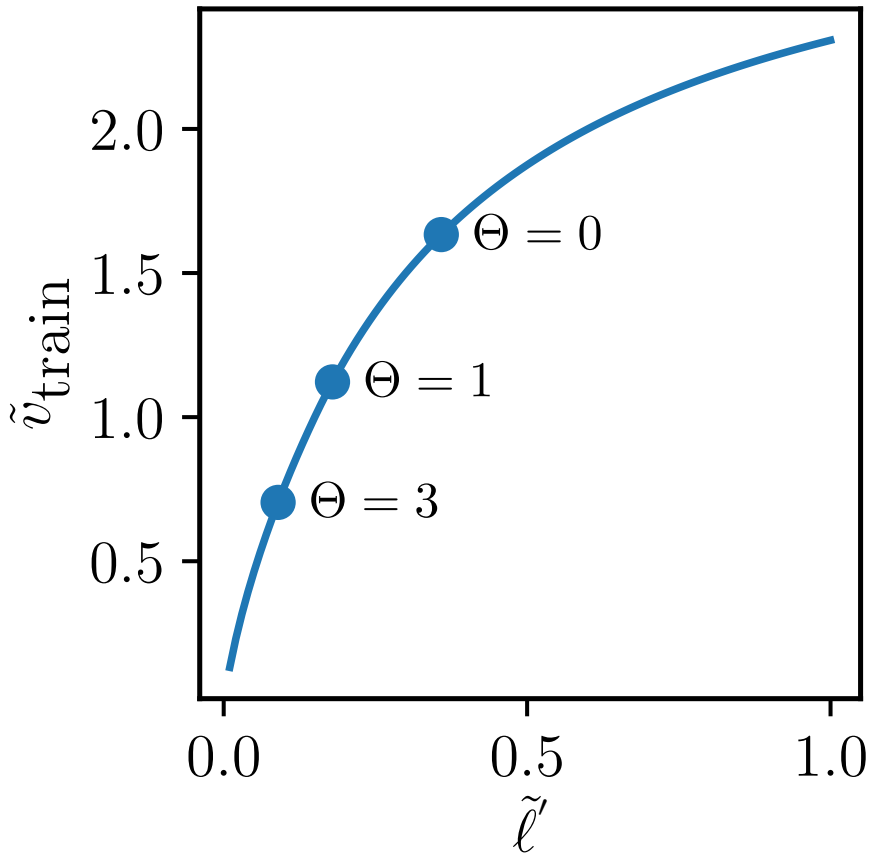

Figure 4.3: **Train speed as a function of station density.** Train speed is plotted as a function of ℓ'. Values of Θ are annotated in the figure. Data for mesh size $\tilde{\ell} = 0.4$.

4.3.1 DRRP performance

Occupancy

Fig. 4.4a shows the mean DRRP occupancy averaged over driving vehicles, namely b, against the bi-modal fraction, F, for various numbers of intermediate stations, Θ, and demands, Λ. We observe that shuttles generally have a higher mean occupancy for large demands because of the greater possibility of pooling. Mean occupancy is observed to decrease with the involvement of trains (increasing F) because trips by shuttles are shortened, resulting in passengers spending less time in shuttles during their transit. We also observe a general trend of decreasing mean occupancy with more intermediate stations, because trips by shuttles for the users assigned to bi-modal transportation become 1) more dispersed and 2) shorter due to the higher number and proximity of train stations, therefore providing less opportunity for pooling.

Detours

From Fig. 4.4b, the general trend of increasing detour with demand is evident. This trend, together with the trend for mean occupancy, b, in Fig. 4.4a, shows the well-known trade-off between detour and pooling for DRRP, i.e., desirable pooling necessitates undesirable detours for passengers [33]. A trend of decreasing detours with increasing involvement of line services (increasing F) can be attributed to a 'common stop effect', that is, passengers are picked up or dropped off at the same train station, thereby reducing detours. We also observe a trend of decreasing detours with more intermediate stations which is due to the lower potential for pooling due to shorter trips, as well as a reduced 'common stop effect'.

Notice that the black dashed curve represents the assumed value of $\delta = 1.5$ for the theoretical analysis in chapter 3. We observe in Sec. 4.3.2, that this assumption does not severely impact the agreement between the theoretical and simulated overall performance of the system.

Pooling efficiency

The ratio between mean occupancy and mean detour, shown in Fig. 4.4c, provides a reasonable estimate for pooling efficiency, η [38], which is defined as the ratio of requested direct distance by the users and driven distance by the shuttles (for MIV, $\eta = 1$). In Fig. 4.4c, we observe a general trend of increasing pooling efficiency, η, with demand, which suggests that deploying shuttles in a region with high demand is favorable. Involvement of line services decreases the DRRP pooling efficiency because user requests are diverted toward the lines, thus shortening the average distance a passenger travels on

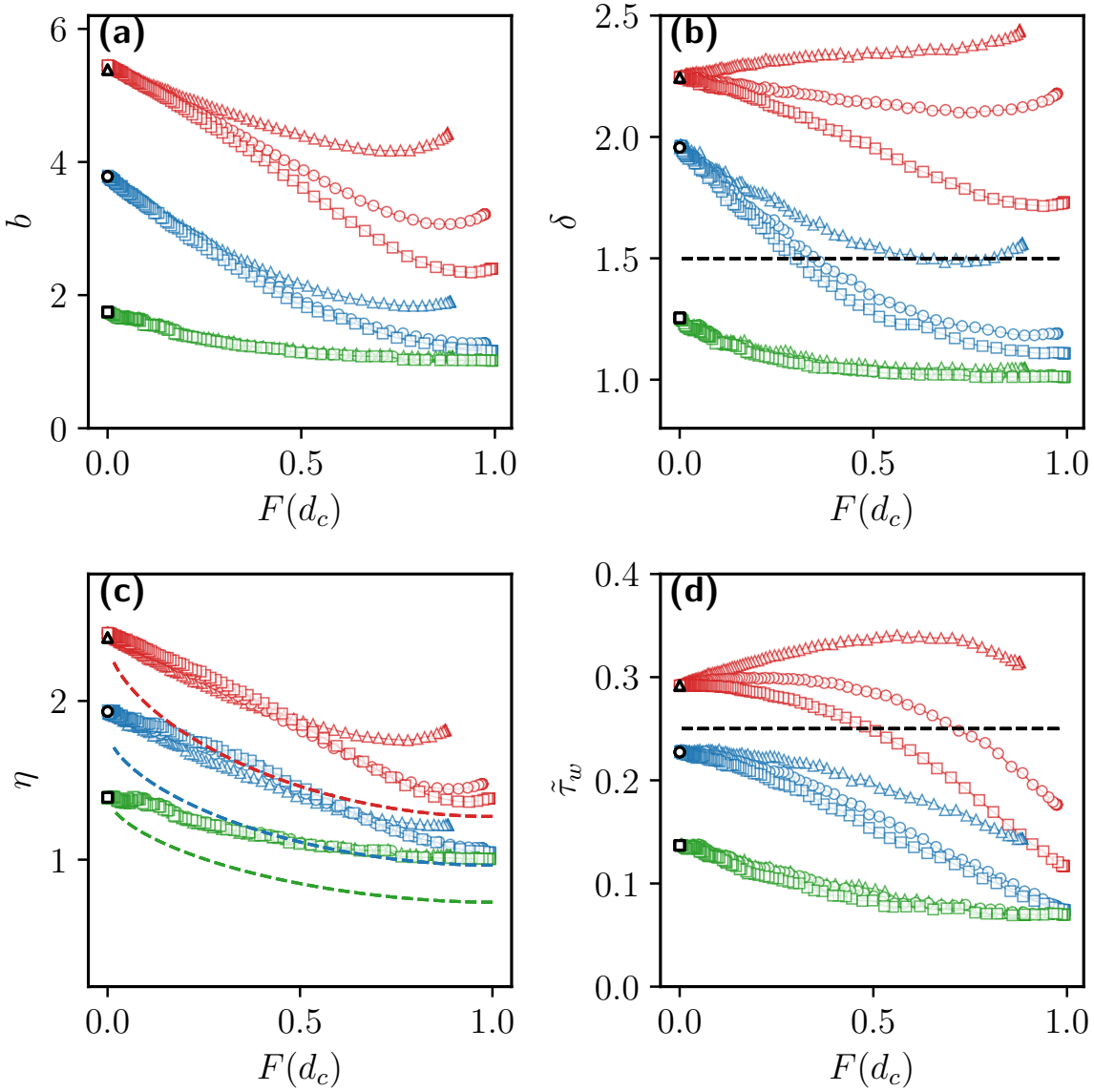

Figure 4.4: **DRRP performance statistics:** DRRP/Shuttle performance parameters are plotted against bi-modal fraction F. Green, blue, and red curves represent $\Lambda = \{13.7, 123, 1201\}$, respectively. Triangles, circles and squares represent $\Theta = \{0, 1, 3\}$, respectively, for all colors. Black square, circle, and triangle represent uni-modal transport (shuttles only) **(a)** Mean DRRP occupancy for non-standing vehicles, b. **(b)** Mean detour, δ, for shuttle users. The black dashed curve represents the detour assumed for theory [39]. **(c)** Mean DRRP pooling efficiency $\eta \equiv b/\delta$. Dashed curves represent the theoretical data for pooling efficiency, as determined by Eq.3.19. **(d)** Mean waiting time, $\tilde{\tau}_w$, for shuttles normalized with t_0. The black dashed curve represents the assumed value for theory [39].

the shuttle during the entire journey. We observe that the effect of intermediate stations on η is mostly insignificant, except for higher demand at a large bi-modal fraction, F.

The dashed curves represent the theoretical prediction for pooling efficiency, determined by Eq. 3.19, which follows a trend similar to the simulations. We observe that the theoretical data underestimates the pooling efficiency when compared with the simulation data. This underestimation can be attributed to the 'common stop effect' mentioned earlier, which is not accounted for in theoretical predictions in Eq. 3.19.

Waiting time

In Fig. 4.4d, we study the mean waiting time for trips with shuttles. Mean waiting time normalized with the average trip duration, t_0, is plotted against the bi-modal fraction F. The black dashed curve represents the assumed value for the theoretical study. We observe a trend of increasing waiting time for higher demands because shuttles become busier. Involvement of line services generally decreases the waiting time for trips with shuttles because of the 'common stop effect' and a lower share of distance traveled in shuttles. The latter holds, too, for more intermediate stations, thus explaining the lower waiting time for larger Θ.

In summary, the main messages from Fig. 4.4 are: 1) Shuttles become more efficient with demand, while user experience suffers due to larger detours and waiting times. 2) Intermediate stations enhance the user experience due to shorter detours and waiting times. The effect on pooling efficiency is insignificant. 3) Trips with shuttles become more convenient for users with the involvement of line services due to reductions in waiting time and detours.

4.3.2 Overall energy consumption and service quality of bi-modal transit

We now analyze the overall objectives, i.e., energy consumption (Eq. 3.14) and service quality (Eq. 3.11) of the combined bi-modal system.

Energy Consumption

In Fig. 4.5a, relative energy consumption, $\mathcal{E}$, is plotted as a function of bi-modal fraction, F, for various numbers of intermediate stations, Θ. We observe a general trend of decreasing energy consumption with the involvement of line services. This is because Δ_{shuttle} decreases with the involvement of line services (see Fig. 4.6a) while Δ_{train} is constant due to a constant service frequency μ, thus decreasing the total energy consumption by the bi-modal system (see Eq. 3.14). We observe that the relative energy consumption is reduced with increasing demand, Λ, as is evident from the direct contribution

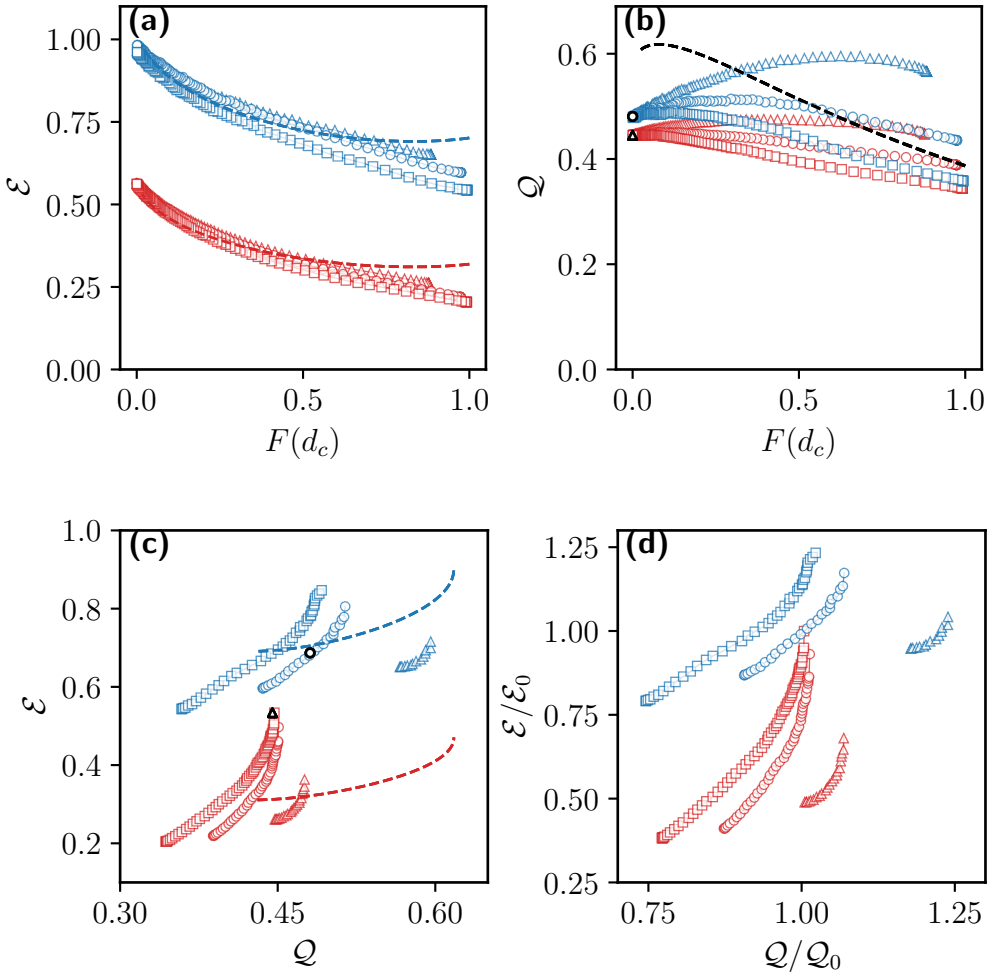

Figure 4.5: **Effect of intermediate stations on the overall performance of bi-modal transit:** The bimodal fraction F has been varied in the range [0,1) in simulations to obtain the data shown. Blue and red curves represent data for $\Lambda = \{123, 1201\}$, respectively. Triangles, circles and squares represent $\Theta = \{0, 1, 3\}$, respectively. **(a)** Energy consumption, $\mathcal{E}$, as a function of F. The dashed curves represent the theoretical data determined by Eq. 3.22. **(b)** Quality, $\mathcal{Q}$, as a function of F. Black dashed curve represents the theoretical data determined by Eq. 3.13. Notice that the theoretical data for quality is assumed the same across all demands. **(c)** Pareto fronts of energy consumption, $\mathcal{E}$, vs. service quality, $\mathcal{Q}$ determined from the data shown in (a), (b). Data not part of Pareto fronts is not shown. The dashed curves represent the theoretical data as in (a), (b). Black circle and triangle represent uni-modal transport (shuttles-only) data for $\Lambda = \{123, 1201\}$, respectively. **(d)** Pareto fronts as in (c), but normalized with respect to the performance, $(\mathcal{Q}_0, \mathcal{E}_0)$, of the uni-modal system (shuttles only).

in Eq. 3.22, as well as via the enhanced pooling efficiency, η (see Fig. 4.4c). Fig. 4.5a reveals that the energy consumption can be lower than 25% of the energy consumption for MIV for demands in large cities like Berlin ($\Lambda \approx 5 \cdot 10^3$, [39]). Energy consumption is observed to decrease slightly with the increasing number of intermediate stations because the normalized distance driven by shuttles is reduced (see Fig. 4.6a). We find reasonable agreement between theoretical data (Eq. 3.22) and simulations.

Quality

In Fig. 4.5b, we plot the overall quality of the system against the bi-modal fraction, F. We observe that $\mathcal{Q}$ is non-monotonic in F. This is due to the competing effects of decreasing waiting time for shuttles with more involvement of trains (see Fig. 4.4d), on the one hand, and additional waiting time for trains at the train stations for a larger user fraction (F), on the other hand.

We observe that the overall service quality, $\mathcal{Q}$, decreases with demand, which is due to the trend we observed for waiting times for trips with shuttles in Fig. 4.4d.

The dashed black curve represents the theoretical predictions determined by Eq. 3.13. Notice that the theoretical prediction for quality does not depend on the demand because the train frequency μ is maintained at a constant value of $0.1\,\mathrm{min}^{-1}$ across all demands (see Subsec. 4.2.3). The difference between theory and simulation data primarily stems from the waiting time of shuttles, which we approximated as $0.25\,t_0$ in our theory, for all demands. However, we see in Fig. 4.4d that the waiting time varies with demand, bi-modal fraction, and the number of intermediate stations.

In Fig. 4.5b, we observe that the overall service quality of the combined bi-modal system decreases with more intermediate stops, despite a trend of decreasing waiting times and detours for trips with shuttles (see Figs. 4.4b, d). Apparently, this trend is dominated by a slowing down of trains due to intermediate stations, which increases the average trip duration.

The general trend of reduction in consumption of energy with increasing demand and involvement of line services hints towards the merit of bi-modal transportation for high-demand scenarios. For service quality, we find that typical values are around one-half the service quality of MIV, i.e., about twice the travel time. This quality is customary for public transport systems [56, 48] and is generally well accepted by users. Note that our data for service quality represent a safe lower bound, as the (sometimes quite substantial) time required for parking spot search [49, 50] is neglected in t_0.

We observe that service quality attains a maximum for a bi-modal fraction, F, where energy consumption is not minimal. Jointly optimizing such conflicting objectives can be done in the framework of Pareto optimization, which we will discuss next.

Optimization

We determine the optimal parameters of operation by using the Pareto frontiers (see Subsec. 3.5.1), keeping in mind that we aim at maximum service quality at minimum energy consumption. Hence, in diagrams spanned by $\mathcal{Q}$ as the abscissa and $\mathcal{E}$ as the ordinate, system operation as far as possible to the lower right is desirable.

In order to study the effect of density of line service stations on the overall performance of the bi-modal transit system, we have introduced $\Theta = \{0, 1, 3\}$ as the number of intermediate stations. For $\Theta = 0$, transit stops are only at the intersection between two transit lines. For each value of Θ, we vary $\boldsymbol{d}_\mathrm{c}$ to obtain the Pareto fronts.

In Fig. 4.5c, we show the Pareto fronts obtained for data in Figs. 4.5a, b. Note that for a better resolution of the curves, we only show the data for $\Lambda = \{123, 1201\}$. We observe that intermediate stations reduce the energy consumption to as low as 20% of MIV for larger demand. However, the service quality is worsened due to the reduced average speed of trains. Black triangles and circles represent the data for the uni-modal system (shuttles only), and dashed curves represent the theoretical estimates. We observe a fair agreement between previous theoretical estimates and simulation results for the overall performance of the bi-modal system. Discrepancies mainly result from the simplifying assumptions for mean waiting time, $\tilde{\tau}_w$ and detour, δ, as described in Subsec. 4.3.1.

In Fig. 4.5d, the same Pareto fronts as in Fig. 4.5c are plotted normalized with respect to energy consumption and service quality of a uni-modal system, $(\mathcal{E}_0, \mathcal{Q}_0)$. We observe that the bi-modal system can provide a service quality superior to a uni-modal (shuttles only) system with a lower energy consumption. This observation holds for both demand values presented.

Traffic volume

Road traffic is a source of local noise and air pollution and occupies significant shares of urban space. Bi-modal transit aims at reduction of road traffic by utilizing line services for trips over larger distances. Fig. 4.1c and Fig. 4.1d provide qualitative evidence by comparing abundance of MIV and shuttles for the same request pattern.

To obtain a quantitative estimate, we define as bi-modal traffic volume, $\tilde{\Delta}_\mathrm{shuttle}$, the cumulative distance driven by shuttles, Δ_shuttle (Eq. 3.15), normalized with respect to the equivalent of total MIV distance requested, Δ_MIV (Eq. 3.21), or, equivalently, the relative number of driving shuttles as compared to MIV.

For our theoretical estimates, we use the analytical expression,

$$\tilde{\Delta}_{\text{shuttle}} \equiv \Delta_{\text{shuttle}}/\Delta_{\text{MIV}} = \eta^{-1}\,(1+F)\,\tilde{D}_{\text{shuttle}}\,, \tag{4.2}$$

with pooling efficiency, η, bimodal fraction, F, and average requested distance for trips by shuttles involved in bi-modal transit, $\tilde{D}_{\text{shuttle}}$.

In Fig. 4.6a, we plot bi-modal traffic in simulations on a vertical axis as a function of bi-modal fraction for various demands and number of intermediate stations. Dashed curves represent the theoretical data (Eq. 4.2) for an idealized square grid network without any intermediate stops ($\Theta = 0$).

We observe a trend of decreasing bi-modal traffic with involvement of line services, i.e., with increasing F. Also, $\tilde{\Delta}_{\text{shuttle}}$ decreases with increasing demand, because shuttles become more efficient due to the possibility of larger pooling (see also Fig. 4.4c). We furthermore observe that, for low demand, bi-modal traffic decreases with more intermediate stations. This is despite an insignificant impact on pooling efficiency, η (see Fig. 4.4c). It is rather the reduced average requested distance for trips with shuttles, $\tilde{D}_{\text{shuttle}}$, due to the increased proximity of train stations, which accounts for the reduced traffic volume (see Eq. 4.2).

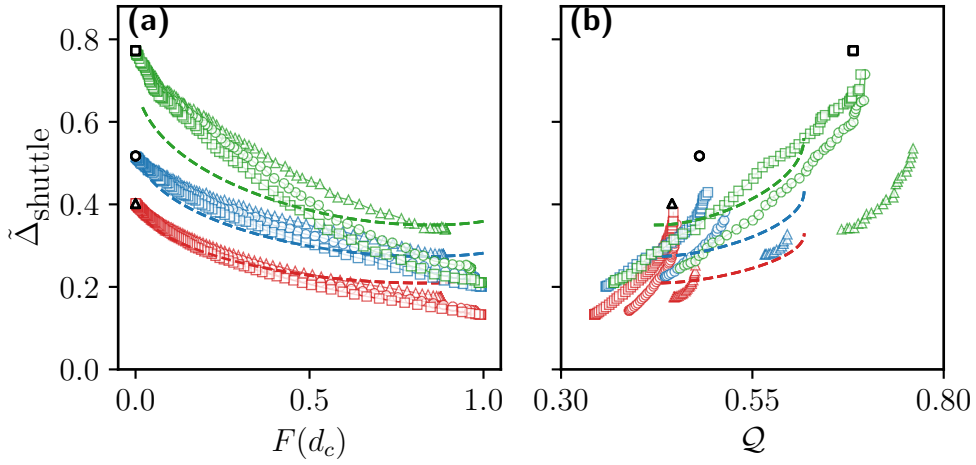

Figure 4.6: **Impact of intermediate stations on traffic volume.** Green, blue, and red curves represent $\Lambda = \{13.7, 123, 1201\}$, respectively. Triangles, circles, and squares represent $\Theta = \{0, 1, 3\}$, respectively. **(a)** Relative bi-modal traffic in simulations, $\tilde{\Delta}_{\text{shuttle}}$, as defined in Eq. 4.2, as a function of the bi-modal fraction, F. Black square, circle, and triangle represent uni-modal transport (shuttles-only) data for $\Lambda = \{13.7, 123, 1201\}$, respectively. Dashed curves represent the theoretical data, determined by Eq. 4.2. **(b)** Relative bi-modal traffic in simulations, $\tilde{\Delta}_{\text{shuttle}}$, determined along the Pareto fronts in Fig. 4.5, against corresponding service quality $\mathcal{Q}$. Dashed curves and black symbols represent the theoretical and uni-modal data, respectively, as in (a).

In Fig. 4.6b, we plot the relative bi-modal traffic volume, $\tilde{\Delta}_{\text{shuttle}}$, for simulations on a vertical scale, determined along the Pareto fronts in Fig. 4.5c, against corresponding

service quality $\mathcal{Q}$. The traffic volume for uni-modal (shuttle-only) scenarios is plotted with black symbols. We observe that the relative traffic volume for uni-modal scenarios decreases with demand due to increased pooling efficiency, η (see Fig. 4.4c). The relative traffic volume for the uni-modal case can be reduced to 80% of MIV for very low demand and down to 50% and 40% for low and medium demand, respectively.

Bi-modal public transportation allows for further reduction in relative traffic volume below the uni-modal case at a superior service quality. For an idealized square grid without any intermediate stations (represented by colored triangles), bi-modal transportation reduces traffic volume down to about 30% of MIV for very low and low demand and even below 20% for medium demand. Intermediate stops allow for further reduction in traffic. This reduction, however, comes at the cost of reduced service quality. Due to computational limitations, we could only simulate scenarios with the demand of the order of $\Lambda = 10^3$. However, the demand can be as high as 10^4 for very dense areas like New York. Earlier findings suggest that bi-modal public transportation can reduce traffic in such areas even below 10% of MIV [39].

4.4 Discussion

Our investigation had two primary goals. First, to study the impact of the number of intermediate line service stops on the performance of bi-modal public transport systems. Second, to evaluate the analytical framework proposed in chapter 3 through simulations. The parameters investigated in this chapter drew inspiration from real-world agglomerations. The grid constant $\tilde{\ell} = \ell/D = 0.4$ in our model is close to what is found for, e.g., New York and Berlin. Other technical parameters, including shuttle speed (v_0) and train speed (v_{train}), have been carefully chosen to reflect the observed real-life environments (see Subsec. 4.2.3).

Below, we first discuss the comparison between agent-based simulations and the analytical study in chapter 3. Simulations reveal that observables characterizing shuttle performance, namely detour and waiting time, vary with demand, bi-modal fraction, and the number of intermediate stops, in contrast to the constant values assumed by the previous chapter.

Furthermore, we observe that the pooling efficiency for shuttles in a bi-modal scenario is higher than the one estimated by power-law (see Eq. 3.19). This is because of the 'common stop effect' (see Subsec¿ 4.3.1). The findings above highlight that shuttle waiting time, detours, and pooling efficiency are complex observables, which, in bi-modal transit, depend on line service operations, and thus must be modeled carefully to assess the performance of bi-modal transit systems accurately.

Adding intermediate stations between line crossings had limited benefits. While there was a marginal reduction in energy consumption and traffic volume, the resulting slow-

down of trains made them less suitable as a faster mode of transportation than MIVs and shuttles, i.e., lead to substantial reduction of service quality. Our research hence suggests that reducing the number of intermediate stops within an existing railway system and complementing an on-demand shuttle service as bi-modal transit may improve the overall performance of public transport.

It should be noted that the network structure employed in our research, although inspired by real-world urban agglomerations, is still a simplified representation. In the next chapter, we consider a more complex and realistic network topology to capture the nuances of the urban environment and evaluate the generalizability of our findings.

In summary, our study confirms that bi-modal transit can provide door-to-door service with satisfactory service quality while consuming only a fraction of the energy required by an equivalent fleet of MIVs, and significantly reducing road traffic volume. These advantages hold for low-demand regions as well as medium-sized cities. Although our simulations were limited to a medium user demand of approximately $\Lambda = 10^3$ due to computational constraints, we anticipate that bi-modal transit would outperform MIVs and uni-modal ride-pooling even more significantly under higher demand conditions, as suggested in previous research [39]. It is important to note that our analysis did not consider other MIV-specific drawbacks, such as parking time or traffic congestion during rush hours [57, 58, 50], which would further enhance the relative performance of bi-modal transit.

It doesn't matter how beautiful your theory is, it doesn't matter how smart you are. If it doesn't agree with experiment, it's wrong.

Richard P. Feynmann

5

Bi-modal transit in Berlin and Brandenburg

5.1 Introduction

In chapters 3 and 4, we considered a spatially uniform demand with constant average request frequency. However, in realistic scenarios, demand is heterogeneous in space, due to non-homogeneous population density and individual mobility patterns, and fluctuating in time due to phenomena like rush hours. Furthermore, the trains were assumed to run periodically at the same constant speed throughout the system and the shuttles were also assumed to operate at a constant speed. These assumptions undermine the nuances in real settings. The network topology, for example, is much more complex in real settings (see Fig. 5.1) and vehicles barely operate at the same constant speed, if at all. It is unclear how these heterogeneities affect the overall performance of the system.

A prevalent assumption in chapters 3 and 4 was that all transportation requests within a given study region exclusively relied on the public transit system, these requests were then assigned to bi-modal (shuttle-train-shuttle) or uni-modal (shuttles only) transportation. However, the reality is far more intricate, as user adoption of public transportation systems exhibits significant variability. In this chapter, we study the effects of such adoption variability on the holistic performance of bi-modal transportation systems for Berlin and Brandenburg (see Fig. 5.2). We explore two distinct scenarios: one where $x = 1\%$ of the total population utilizes public transportation and another where the adoption rate increases to $x = 10\%$ of the total population. For both scenarios, we assume that the rest of the people use private cars or MIVs to commute.

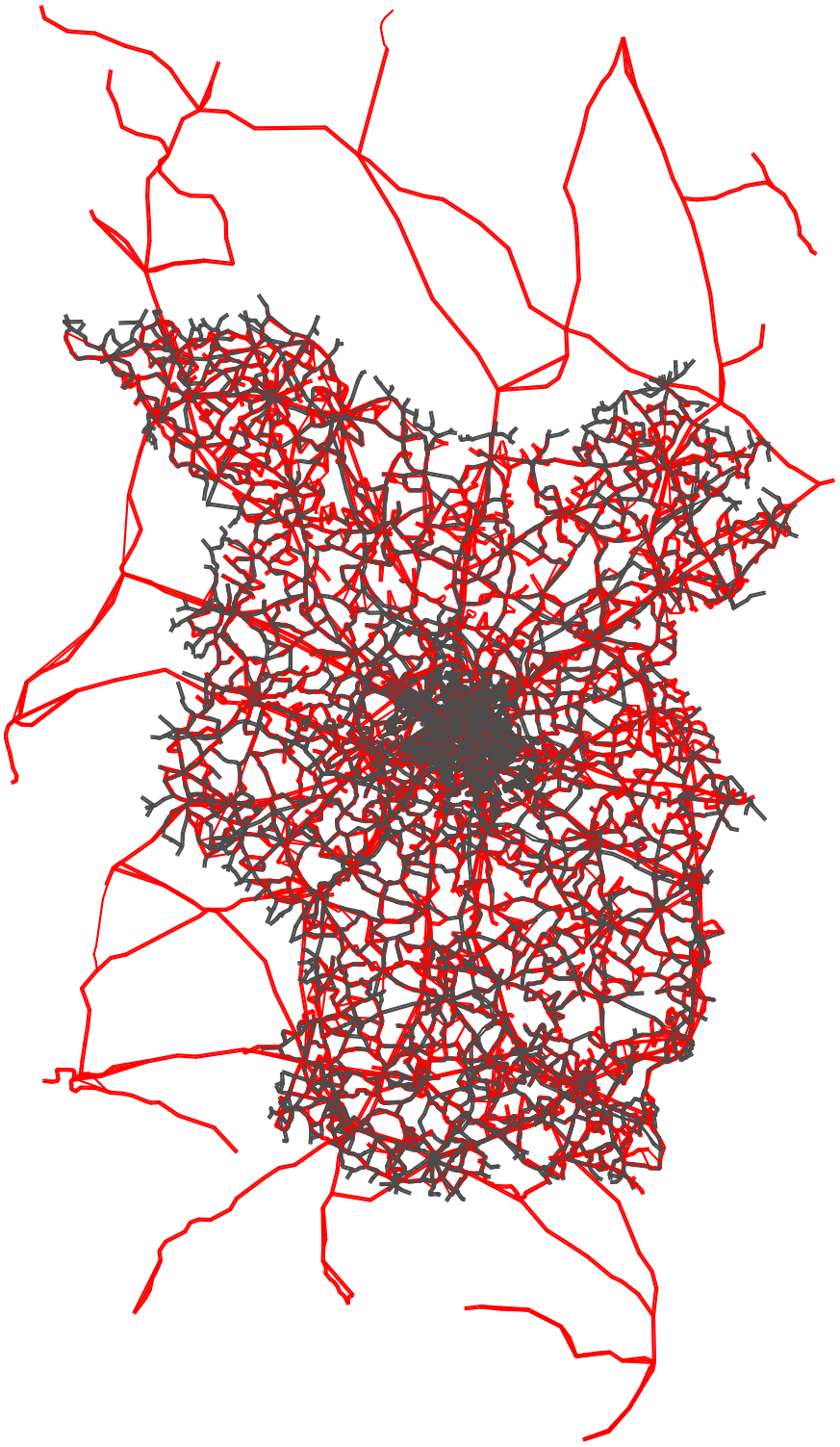

Figure 5.1: Transit network for Berlin and Brandenburg. Black curves represent the road network and red curves represent the public transit network including buses and rails (also long-distance trains) [59].

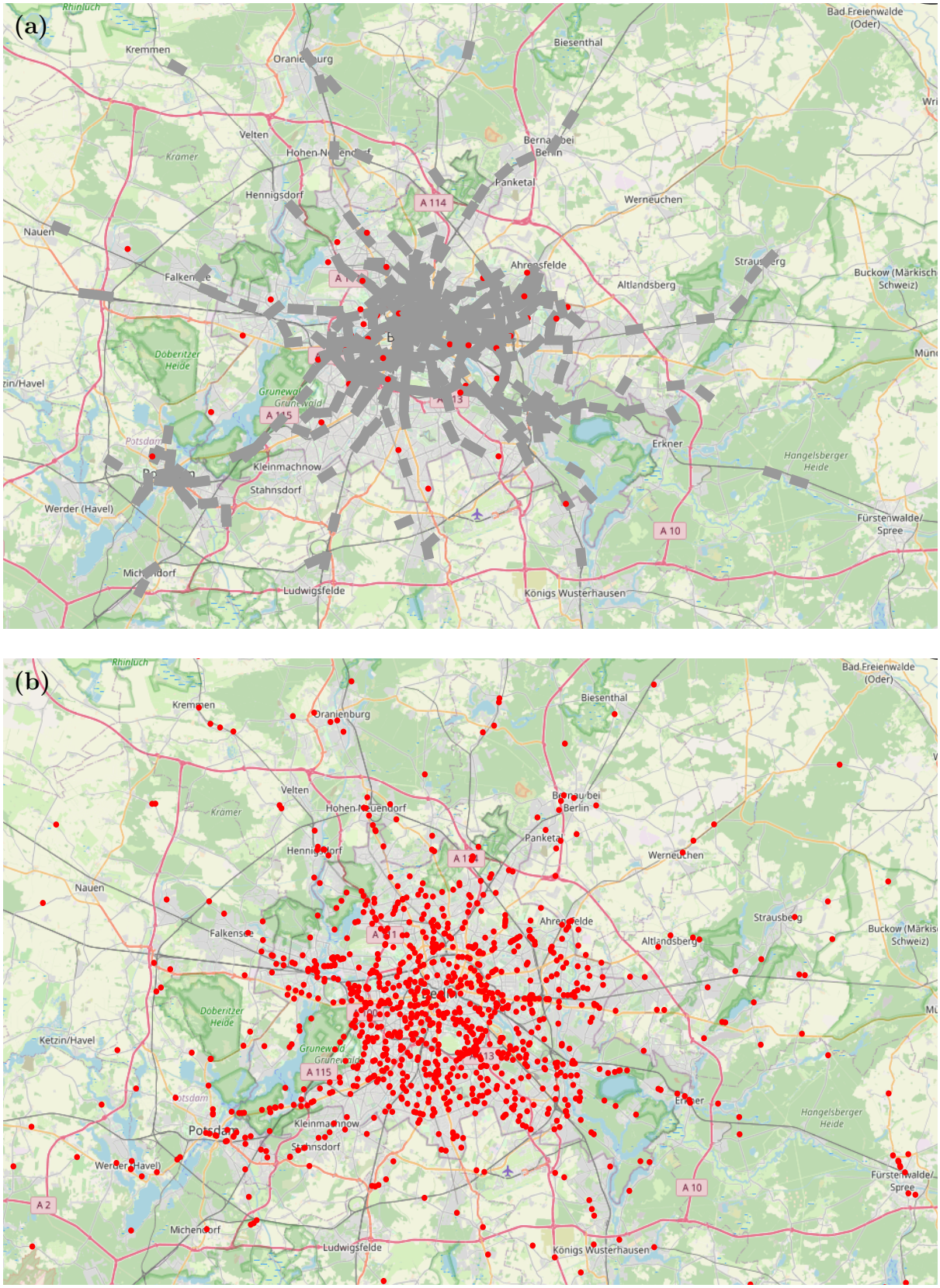

Figure 5.2: **Bi-modal transport network in Berlin and Brandenburg** A snapshot of simulations for 1% user-adoption fraction ($x = 0.01$) zoomen in around Berlin. **(a)** A bi-modal scenario where grey rectangles represent trains and red dots represent the shuttles. **(b)** MIV scenario where people use private cars to commute. Red dots represent private cars. The number of required shuttles in a bi-modal system (a) is much lower than the number of MIVS required in (b). See Subsec. 5.3.3 for quantitative analysis.

5.2 Methods

For simulating a system of bi-modal transport, with on-demand shuttles and trains operating on lines, we deploy the open-source, multi-agent transport simulation framework MATSim [51]. We used the map from [60]. We used the passenger travel patterns that were artificially generated using the census data [59]. The data is provided by the Transport Systems Planning and Transport Telematics group of Technische Universität Berlin. We used an openly available General Transit Feed Specification GTFS dataset for the Berlin-Brandenburg region [61] to generate MATSim public transport schedule and vehicle files and to add public transport links to the network. The dataset provides schedules and vehicles for various transport modes available, however, we only use rail-bound line services as a means of public transport. Each link on the transportation network has an associated speed for the vehicles. We explore two distinct scenarios: one where $x = 1\%$ of the total population utilizes public transportation and another where the adoption rate increases to $x = 10\%$ of the total population. For both scenarios, we assume that the rest of the people use private cars or MIVs to commute. Our study unveils the dynamics between user adoption patterns and the overall performance of bi-modal transportation systems, offering insights essential for optimizing their design and operation.

5.3 Results

Below in Subsec. 5.3.1, we first present how DRRP performs with a bi-modal system when the bi-modal transit system is used by 10%, and 1% population. Then in Subsecs. 5.3.2 and 5.3.3, we describe the overall performance of the bi-modal transit system for the two used cases above. We conclude the results section with an analysis of the potential reduction in traffic volume.

5.3.1 DRRP performance

Occupancy

In Fig. 5.3a, we show the mean DRRP occupancy, b, averaged over non-empty driving vehicles against the bi-modal fraction, F, for 10% and 1% use case. We observe that the shuttles have a higher mean occupancy for larger use case, i.e., larger demand because of the greater possibility of pooling. Mean occupancy decreases with the involvement of trains (increasing F). This is because shuttle trips are shortened causing passengers to spend less time in shuttles during their transit. The black symbols represent mean occupancy for a uni-modal (shuttles only) scenario. We observe that the mean occupancy is larger for uni-modal scenarios.

Detours

In Fig. 5.3b, we observe that higher use case, i.e., 10% population has larger detours. The detour δ and occupancy b trend observed above shows a well-known trade-off between detour and pooling for DRRP, i.e., desirable pooling necessitates undesirable detours for passengers [33]. We observe that the detours decrease with the involvement of line services, this can be attributed to the 'common stop effect', a phenomenon observed in the previous study [62]. With greater involvement of line services, more passengers are picked up and dropped of at the same train station, thereby reducing detours.

Pooling efficiency

The pooling efficiency which is defined as the ratio between mean occupancy and mean detour is shown in Fig. 5.3c. We observe that the pooling efficiency, η, is higher for larger demand, i.e., 10% use case as also reported in previous study [62]. This suggests that the larger use of shuttles or bi-modal service will be favorable for pooling efficiency. We observe that the involvement of line service reduces DRRP pooling efficiency because user requests are diverted toward the line which shortens the average distance a passenger travels on the shuttle during the entire journey.

Waiting time

In Fig. 5.3d, we study the mean waiting time for shuttle-borne trips. We plot the mean waiting time normalized with the average trip duration, t_0, against the bi-modal fraction, F. We observe that larger demand, that is, the use case of ten percent has larger waiting times because shuttles are busier. We also observe that the involvement of line services decreases the waiting time for shuttle trips because of the 'common stop effect' and a lower share of distance traveled in shuttles.

The main messages form Fig. 5.3 are: 1) Shuttles become more efficient with demand, while user experience suffers due to larger detours and waiting times, as also found in the previous study [62]. 2) The involvement of line services makes the shuttle trips more convenient for users by reducing the waiting time and detours.

5.3.2 Overall energy consumption and service quality of bi-modal transit

Now, we will analyze the overall objectives, i.e., energy consumption (Eq. 3.22) and service quality (Eq. 3.13) of the transportation system for the two use cases.

Energy consumption In Fig. 5.4a, relative energy consumption, $\mathcal{E}$, is plotted as a function of bi-modal fraction, F, for the two use cases discussed above. We observe a

general trend of decreasing energy consumption with the involvement of line services. This is because $\tilde{\Delta}_{\text{shuttle}}$ decreases with the involvement of line services (see Fig. 5.6a) while $\tilde{\Delta}_{\text{train}}$ is constant due to a fixed schedule of trains in the simulations, thus reducing the total energy consumption by the bi-modal transportation system. We also observe that energy consumption is reduced with increasing demand, i.e., for a higher used case. This is evident from Eq. 3.22. Note that the emission curves for bi-modal transportation start above the emissions for uni-modal scenarios (black symbols). This is because in our bi-modal simulations, trains are always running at fixed schedules. For low bi-modal fraction, F, trains are underutilized because they operate at low occupancies (see Fig. 5.5b). We observe that for 10% use case, the energy consumption can easily drop below 20%, however, for a 1% use case, it's not advisable to use bi-modal transportation, suggesting that a larger adoption of bi-modal transportation can significantly reduce the energy consumption.

Quality In Fig. 5.4b, the overall quality of the system is plotted against the bi-modal fraction, F, for the two use cases. We observe that the demand doesn't significantly impact the overall service quality and service quality decreases with the involvement of the line services. Large waiting times (see Fig. 5.5a) contribute to degrading quality with the bi-modal fraction, F. This suggests that user quality can be improved by increasing the train frequency and adapting the train capacity, k, depending on the demand. We see in Fig. 5.5b that trains are barely full.

5.3.3 Optimization

We determine the optimal parameters of operation by using the Pareto frontiers. Hence, in diagrams spanned by $\mathcal{Q}$ as the abscissa and $\mathcal{E}$ as the ordinate, system operation as far as possible to the lower right is desirable.

In order to study the overall performance of bi-modal transportation in real scenarios and the impact of user adoption, we explore two distinct scenarios: one where 1% of the total population utilizes bi-modal transportation, and another where the adoption rate increases to 10% of the total population. In each case, we vary $\boldsymbol{d}_{\text{c}}$ to obtain the Pareto fronts.

In Fig. 5.4c, we show the Pareto fronts obtained for data in Figs. 5.4a,b. We observe that the energy consumption can go below 20% for a service quality of around 0.25 for the 10% use case. The black circle represents the uni-modal data for the 10% use case. We observe that bi-modal transportation can significantly reduce emissions as compared to uni-modal (shuttles only) case with a compromise on service quality. This is clear from Fig. 5.4d, where we plot the Pareto-optimal $\mathcal{E}$ and $\mathcal{Q}$ normalized with uni-modal $\mathcal{E}_0$ and $\mathcal{Q}_0$ respectively.

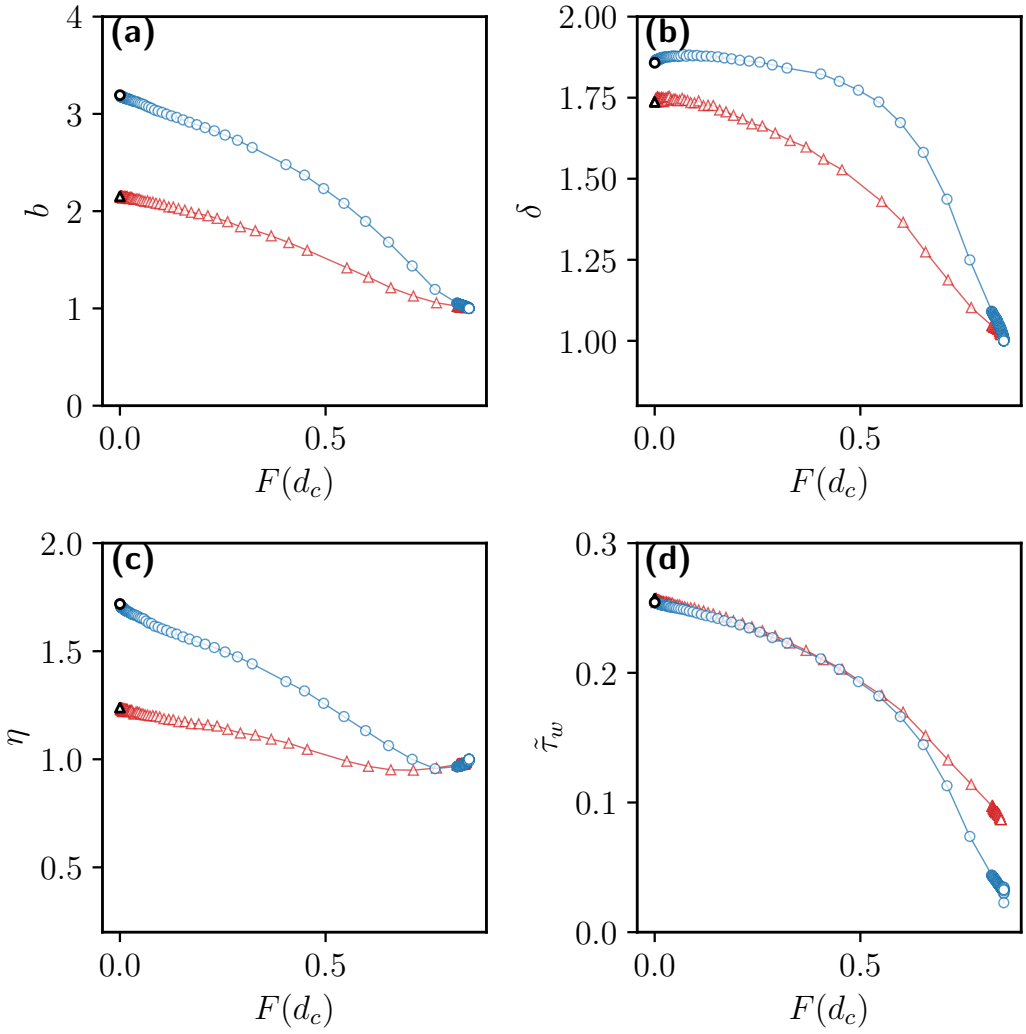

Figure 5.3: **DRRP performance statistics:** DRRP/Shuttle performance parameters are plotted against bi-modal fraction F. Blue circles and red triangles represent 10%, and 1% population of Greater Berlin, respectively. Black circle, and triangle represent uni-modal transport (shuttles only) **(a)** Mean DRRP occupancy for non-standing vehicles, b. **(b)** Mean detour, δ, for shuttle users. **(c)** Mean DRRP pooling efficiency $\eta \equiv b/\delta$. **(d)** Mean waiting time, $\tilde{\tau}_w$, for shuttles normalized with t_0.

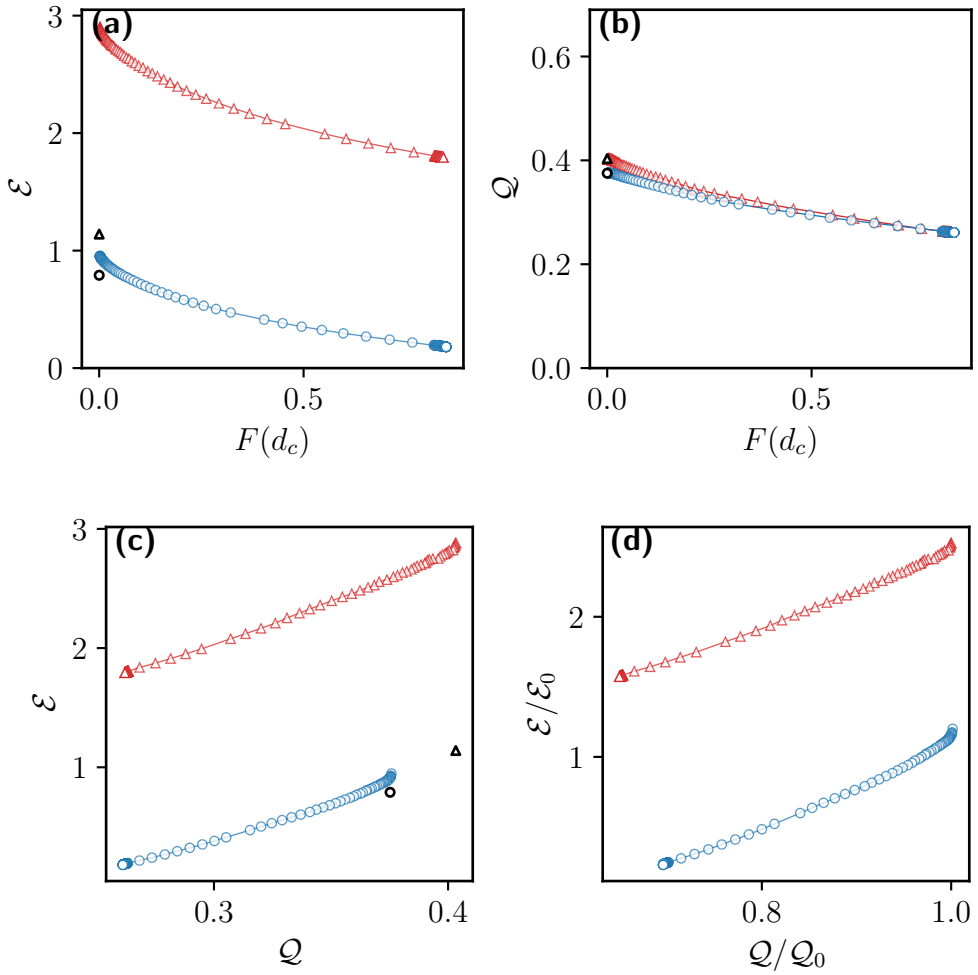

Figure 5.4: **Overall performance of bi-modal transit:** Blue circles and red triangles represent data for 10%, and 1% greater Berlin population respectively. **(b)** Quality, $\mathcal{Q}$, as a function of F. **(c)** Pareto fronts of energy consumption, $\mathcal{E}$, vs. service quality, $\mathcal{Q}$ determined from the data shown in (a), (b). Data not part of Pareto fronts is not shown. The black circle and triangle represent uni-modal transport (shuttles-only) data for 10%, and 1% greater Berlin population respectively. **(d)** Pareto fronts as in (c), but normalized with respect to the performance, $(\mathcal{Q}_0, \mathcal{E}_0)$, of the uni-modal system (shuttles only).

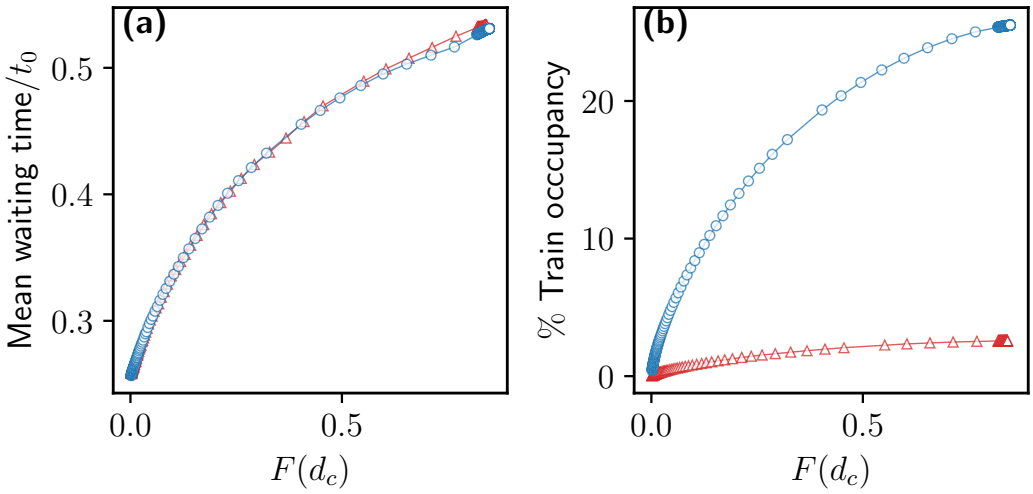

Figure 5.5: **Mean waiting time and Train occupancy:** Blue circles and red triangles represent 10% and 1% population of Greater Berlin, respectively. **(a)** Mean waiting times normalized with t_0. **(b)** Mean train occupancy.

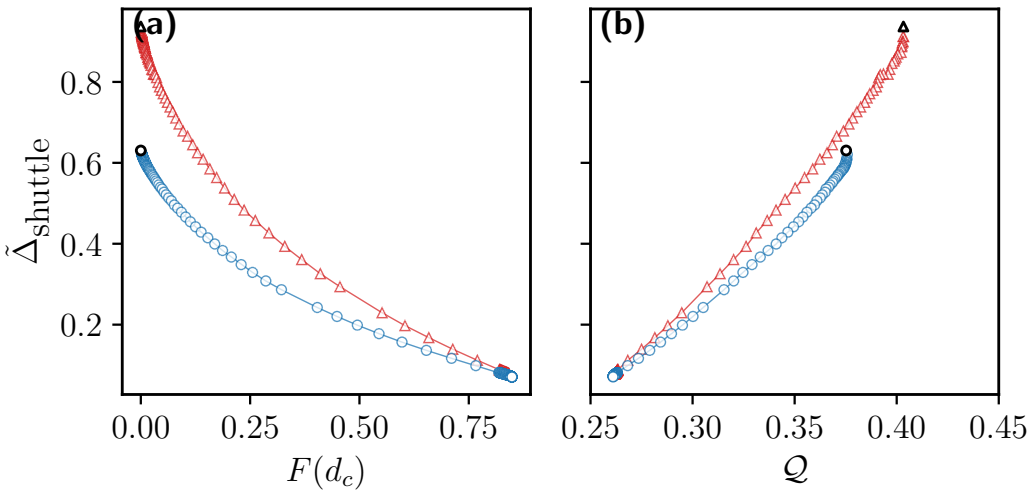

Figure 5.6: **Traffic volume.** Blue circles and red triangles represent 10%, and 1% greater Berlin population respectively. **(a)**Relative bi-modal traffic in simulations, $\tilde{\Delta}_{\text{shuttle}}$, as defined in Eq. 4.2, as a function of the bi-modal fraction, F. Black circle and triangle represent uni-modal transport (shuttles-only) data for 10%, and 1% greater Berlin population respectively. **(b)** Relative bi-modal traffic in simulations, $\tilde{\Delta}_{\text{shuttle}}$, determined along the Pareto fronts in Fig. 5.4, against corresponding service quality $\mathcal{Q}$.

For the 1% use case, it is not advisable to deploy bi-modal transportation at all because requests are better served by uni-modal transportation (black triangle) both in terms of energy consumption and service quality.

Traffic volume

In Fig. 5.6a, we plot the total relative traffic volume, $\tilde{\Delta}_{\text{shuttle}}$, described in Eq. 4.2 on the vertical axis as a function of bi-modal fraction, F, for the two used cases. We observe a trend of decreasing bi-modal traffic with the involvement of line services, i.e., with increasing F. Also, $\tilde{\Delta}_{\text{shuttle}}$ decreases when the user adoption goes from 1% to 10% because the shuttles become more efficient due to the possibility of larger pooling (see also Fig. 5.3c).

In Fig. 5.6b, we plot the total relative traffic volume, $\tilde{\Delta}_{\text{shuttle}}$, for simulations, determined along the Pareto fronts in Fig. 5.4c, against corresponding service quality, $\mathcal{Q}$. The traffic volume for uni-modal (shuttles-only) scenarios is plotted with black symbols. We observe that the relative traffic volume for uni-modal scenarios decreases with demand due to increased pooling efficiency, η (see Fig. 5.3c). The relative traffic volume for uni-modal (shuttles only) scenario for 1% use case is not significantly less than that of MIV because of low pooling efficiency, η (see Fig. 5.3c). The uni-modal traffic volume for the 10% use case is around 60% of MIV traffic. This suggests that the relative uni-modal traffic volume can be further reduced if more people adopt ride pooling.

Bi-modal public transportation allows for further reduction in relative traffic volume Below the uni-modal scenario, albeit, at a lower service quality. The bi-modal traffic can go as low as 15% for 10% user adoption.

5.3.4 Discussion

Our investigation had two primary goals. First to study the feasibility of bi-modal demand-responsive public transportation in Berlin and Brandenburg with the existing rail network. Second, to study the impact of user adoption of public transit on the overall performance of bi-modal demand-responsive public transportation in Berlin and Brandenburg.

Our study suggests that bi-modal demand-responsive transportation can be deployed in Berlin and Brandenburg with the existing rail network of public transportation. We find that the overall performance of bi-modal transportation improves with higher user adoption. While 10% user adoption can significantly reduce emissions and vehicular traffic, it is not advisable to deploy bi-modal transit with existing rail network and train schedules if the user adoption is 1%. This suggests that the overall performance of the bi-modal transit can be further improved by devising strategies to attract users towards bi-modal transportation.

Isn't it funny how day by day nothing changes,
but when you look back everything is different?

C.S. Lewis

6 Conclusion and Outlook

6.1 Conclusion

In this thesis, our aim was to harmonize vital urban convenience with strategies that alleviate traffic challenges and environmental impacts. To that end, we introduce a hybrid model of bi-modal public transit that combines high-speed line service with a fleet of shuttles. In a first approach, we consider an idealized model geometry with a square grid of railways (line service) on which transport occurs via trains. The connection points (train stations) between the two subsystems lie at all railway intersections and are spaced with a lattice constant ℓ. We identify the conflicting objectives for optimization, i.e., service quality and energy consumption. We then ask the following questions in chronology while gradually increasing the complexity of our model to align our model more closely with real-world scenarios. With each step, we gain insights into the operational dynamics that underpin the functionality and efficiency of bi-modal transit systems within the intricate urban landscapes of urban mobility.

1. What performance, regarding energy consumption and convenience, can we achieve for an idealized square grid geometry by diligently choosing the control parameters?
2. How does the performance change with the density of line service stations, i.e., what if we have intermediate train stations between line crossings?
3. Can we deploy the system in real cities like Berlin with an existing network of trains?

By means of simulations and analytical theory, we find that,

1. **Bi-modal transportation is sustainable and convenient.** We find that the energy consumption by bi-modal transportation can reach as low as 30% of the energy consumption by private cars for a service quality of around 50% of private cars. We find that the performance of the system improves with a larger demand. Furthermore, we find that the vehicular traffic can be reduced to 10% of the vehicular traffic when all users use their private cars. The overall performance does not vary dramatically with mesh size (ℓ), as the control parameters at which the system is operated are largely at the operator's discretion, i.e., similar performance can be achieved for different ℓ by tuning the cutoff distance d_c appropriately. This suggests that the density of currently installed rail track systems might already be well suited for deploying a bi-modal on-demand transport systems of the kind we have studied (see [39]).
2. **Intermediate stations are not beneficial.** We find that within a range of realistic technical parameters, additional stops, in excess of the stops at rail crossings, tend to impede train speed without significantly enhancing the overall performance of bi-modal transit in terms of service quality and energy consumption. Hence, reducing the number of stops within an existing railway system and implementing bi-modal transit as a complement can be beneficial (see [62]).
3. **Bi-modal transportation can be deployed in Berlin and Brandenburg with the existing rail network.** With the previous learnings from analytical theory and agent-based simulations, we finally study the feasibility of bi-modal demand-responsive ride-pooling in Berlin and Brandenburg. We deploy the open-source, multi-agent transport simulation framework MATSim. We use the map from OpenStreetMap. We use the passenger travel patterns artificially generated using the census data. We find that the existing network of rails with shuttles can be used to deploy a bi-modal public transit system that can reduce energy consumption and vehicular traffic.

6.2 Outlook

It is important to note that our results represent only a lower bound on bi-modal performance, in particular as far as service quality is concerned because the bi-modal service of the kind studied here potentially provides door-to-door service, while MIV involves the search for parking space, which was completely disregarded in our study due to lack of reliable data. This can be quite significant, and fully adds to the MIV transit time, thus further improving on the relative service quality, $\mathcal{Q}$, of bi-modal service.

Moreover, it should be mentioned that riding the bi-modal transport system neither

involves having to drive nor taking care of vehicle maintenance. In summary, it appears that bi-modal public transport systems have the potential to outperform the MIV in a number of respects.

Following could be the future research directions based on our work:

6.2.1 A better strategy to assign users to uni-modal or bi-modal transportation.

We have based the decision on the type of transport service (uni-modal or bi-modal) on a single scalar parameter, $\boldsymbol{d}_{\mathrm{c}}$, which amounts to representing the decision process by a binary-valued function of a single scalar variable, $d \longrightarrow \{0, 1\}$. The true structure would be a binary-valued field Φ on the four-dimensional space of the pick-up and drop-off coordinates, $\Phi\colon (x_p, y_p, x_d, y_d) \longrightarrow \{0, 1\}$. This would be extremely cumbersome to study in a statistical manner. However, in a real system, data on $\Phi(x_p, y_p, x_d, y_d)$ are being collected on a daily basis, such that over time the system can be ever improving its performance over the data we have presented here.

6.2.2 User adoption coupling with service quality

In reality, demand will couple to service quality and other parameters concerning user satisfaction; a well-functioning system of transportation attracts demand. Since service quality depends on demand, too—as seen in this study—modeling user behavior introduces a feedback loop. Future studies should integrate this feedback loop into the modeling framework, a step towards resolving user adoption dynamically. Broader analysis of user adoption of bi-modal transportation based on incentives, customer convenience, and customer preferences remains to be explored. Recent results from experimental social science, however, point into a very favorable direction [63, 64, 65].

A

Publication: Sustainable and convenient: Bi-modal public transit systems outperforming the private car

Multimodal Transportation 2 (2023) 100083

Contents lists available at ScienceDirect

Multimodal Transportation

journal homepage: www.elsevier.com/locate/multra

Full Length Article

Sustainable and convenient: Bi-modal public transit systems outperforming the private car

Puneet Sharma[a], Knut M. Heidemann[a,*], Helge Heuer[a], Steffen Mühle[a], Stephan Herminghaus[a]

Max Planck Institute for Dynamics and Self-Organization (MPIDS), Am Faßberg 17, Göttingen 37077, Germany

ARTICLE INFO

Keywords:
Sustainable transport
Human mobility
Ride-pooling
Carbon emissions
Traffic reduction

ABSTRACT

Mobility is an indispensable part of modern human societies, but the dominance of motorized individual traffic (MIV, i.e., the private car) leads to a prohibitive waste of energy as well as other resources. Public transportation with line services, such as light rail, can pool many more passengers, thereby saving resources, but often is less convenient (longer transit times). Door-to-door shuttle services, on the other hand, are convenient but have a limited pooling efficiency due to detours scaling with shuttle occupancy. Combining line services with a fleet of shared shuttles in an integrated so-called bi-modal system may provide on-demand door-to-door service at a service level superior to current public transport with significantly less resource consumption than MIV. Here we introduce a generic model of bi-modal public transit and characterize its critical parameters of operation. We identify the conflicting objectives for optimization, i.e., user convenience and energy consumption, and evaluate the system's performance in terms of Pareto fronts. By means of simulation and analytical theory, we find that energy consumption can be as low as 20% of MIV, at line service densities typically found in real settings. Road traffic can be reduced to less than 10% of MIV. Surprisingly, we find favorable performance not only in urban, but also in rural settings. We thereby provide a possible answer to the pressing question of designing sustainable future mobility solutions.

1. Introduction

Transportation accounts for about one fifth of global anthropogenic carbon emissions (Fan et al., 2018; Kontovas and Psaraftis, 2016), owing mainly to the fact that humans rely mostly on motorized individual vehicles (MIV), i.e., private cars (Douglas et al., 2011; Newman and Kenworthy, 1989). Aside from the ensuing logistic (Jang et al., 2016; Manville and Shoup, 2005; Mingardo et al., 2022; Park et al., 2012; Swenseth and Godfrey, 2002) and environmental (eea, 2020; Joireman et al., 2004) problems of traffic congestion (Arnott and Small, 1994; Barth and Boriboonsomsin, 2009; Chin, 1996; Koźlak and Wach, 2018) and air pollution (eeab, 2020; Caiazzo et al., 2013), MIV represents an enormous waste of energy. On average it amounts to moving about a ton of material (MacKenzie et al., 2014) in order to move just one person (Tachet et al., 2017). Nevertheless, it maintains a leading market position (eurostat, 2022; Fiorello et al., 2016) because it is convenient (Kent, 2013) and relatively cheap for its users.

A well-known answer to this problem is ride-pooling (Chen et al., 2017; Shaheen and Cohen, 2019; Zwick et al., 2021), i.e., combining routes of several passengers such that they can be served by one vehicle (Merlin, 2019). This is done most efficiently by line services, like trains, light rail, or the underground. A light rail car easily takes a hundred passengers or more, uses much less

* Corresponding author.
E-mail address: knut.heidemann@ds.mpg.de (K.M. Heidemann).

https://doi.org/10.1016/j.multra.2023.100083
Received 23 November 2022; Received in revised form 16 January 2023; Accepted 14 February 2023

Table 1
City data. Typical values of population density E, average traveled distance D, speeds of shuttles v_0, as well as the resulting dimensionless demand $\Lambda = D^3 E\nu/v_0$, service quality Q (see Eq. 4) and dimensionless mesh size $\tilde{\ell}$, for a few selected areas. $\tilde{\ell} = \sqrt{m}/D$, where m is the average area enclosed by surrounding rail services. We assume $\nu = 2/17\,h^{-1}$, i.e., two trips per day per user given a time of service of 17 h per day. Road vehicle velocities for Ruhr (north) and Emsland, as well as data for Q, have been obtained by averaging Google navigator data over many relations randomly chosen within the respective area.

city/district	type	E $[km^{-2}]$	D $[km]$	v_0 $[km/h]$	m $[km^2]$	$\tilde{\ell}$	Λ	Q	ref.
New York City	dense urban	$1.1 \cdot 10^4$	4.99	11.3	2.0	0.28	$1.5 \cdot 10^4$	0.33	Herminghaus, 2019; NYCDOT, 2018; TLC, 2022; USCB, 2020
Berlin	urban	$4.1 \cdot 10^3$	5.90	19.8	3.6	0.32	$5.0 \cdot 10^3$	0.64	AfS, 2021; Gerike et al., 2018
Ruhr (north)	urban	$3.6 \cdot 10^3$	15.7	44.9	94	0.62	$3.6 \cdot 10^4$	0.34	Haller and Dauth, 2018
Emsland	rural	$1.1 \cdot 10^2$	16.7	58.7	1200	2.1	$1.0 \cdot 10^3$	0.35	IAB, 2018; StBA, 2020

energy than the same number of MIV and contributes next to nothing to traffic congestion (Pietrzak, 2016). Therefore, many large cities (like, e.g., Tokyo) rely heavily on transportation by line services (Ferbrache and Knowles, 2017; Kato et al., 2014; Pietrzak and Pietrzak, 2019).

They come, however, with a serious downside when compared to MIV. With the latter, users can freely choose the starting time and location as well as the destination. This is not possible for line services, which must follow fixed schedules and fixed routes (Alam et al., 2015). Users thus may have to walk significant distances to and from stations, and need to know the schedules of the involved lines. Demand-responsive ride-pooling (DRRP) (Herminghaus, 2019) services try to address this problem by deploying a large number of shuttles which pick up and drop off users at the desired locations. This requires a central facility which collects travel requests, along with a powerful algorithm which combines these requests into appropriate routes of the shuttles (Alonso-Mora et al., 2017). In such systems, users necessarily experience some detour (Herminghaus, 2019; Lobel and Martin, 2020) with respect to the direct route they could have taken via MIV. This trade-off (Daganzo et al., 2020) severely limits the achievable pooling efficiency to well below ten passengers per vehicle (Zwick et al., 2021). Hence while DRRP is more attractive than line services because it provides door-to-door transport, its pooling efficiency is intrinsically much inferior.

The observations above suggest the following question: "Can we achieve both, high pooling efficiency *and* attractive service quality, by combining line services with on-demand door-to-door transport in a single system of transportation?" While there have been quite a number of studies on ride-pooling systems before (Chen et al., 2017; Lotze et al., 2022; Molkenthin et al., 2020; Salonen, Toivonen, 2013; Santi et al., 2014; Sorge et al., 2015; Storch et al., 2021; Sundt et al., 2021; Tachet et al., 2017; Vazifeh et al., 2018; Wolf et al., 2022), the combination of different transport modes has so far been only scarcely addressed and remains to be explored. Thus, in this paper we fill this gap and investigate a bi-modal public transit system, which consists of a combination of both transport modes. A line service, with fixed routes and schedule, shall coexist with a fleet of shuttles which pick-up users and bring them either to and from line service stations, or serve shorter-distance requests directly. This provides both door-to-door transport by virtue of the shuttles and a large average pooling efficiency due to the involvement of line service vehicles.

In Section 2, we first introduce the bi-modal model system with a square-grid geometry together with a mean-field description. We identify the relevant parameters in Section 3, which need to be controlled in such a combined system of transportation to optimize the objectives of operation (see Section 4). By computing Pareto fronts, we explore in Section 5 what performance may be achieved in terms of energy consumption, quality of service, and traffic volume. We find that bi-modal transit has the potential to provide on-demand door-to-door service with a quality superior to customary public transportation, while at the same time consuming only a fraction of the energy a corresponding fleet of MIV would require, and with a road traffic volume reduced by an order of magnitude.

2. Definition of the system

2.1. User environment

For the sake of conciseness and simplicity, we consider a planar area uniformly populated at density E with potential users of the public transit system under study. Users are assumed to place transit requests in an uncorrelated fashion, each consisting of a desired pick-up ($\mathcal{P}$) and drop-off ($\mathcal{D}$) location, at an average rate ν per passenger. Requested travel distances $d = \overline{\mathcal{P}\mathcal{D}}$ are assumed to follow a certain distribution, $p(d)$, with mean D (Herminghaus, 2019).

For a transparent discussion, it is useful to introduce dimensionless parameters characterizing the system under study. By combining the intrinsic length scale D with a characteristic road vehicle velocity, v_0, we obtain an intrinsic time scale, $t_0 = D/v_0$. This is the average time a travel request would need to be completed by MIV. The demand of transport within the system can then be characterized by the dimensionless parameter $\Lambda = E\nu D^3/v_0$[1], which can reach well beyond 10^4 in a densely populated area. Tab. 1 provides a few typical parameters encountered in real systems for reference. Note that $\tilde{\ell} = \ell/D = \sqrt{m}/D$, where m is the average area enclosed by surrounding rail (line) services, and ℓ is the spacing of line service routes (see below, Fig. 2.2).

[1] Average number of incoming requests in an area D^2 in time t_0.

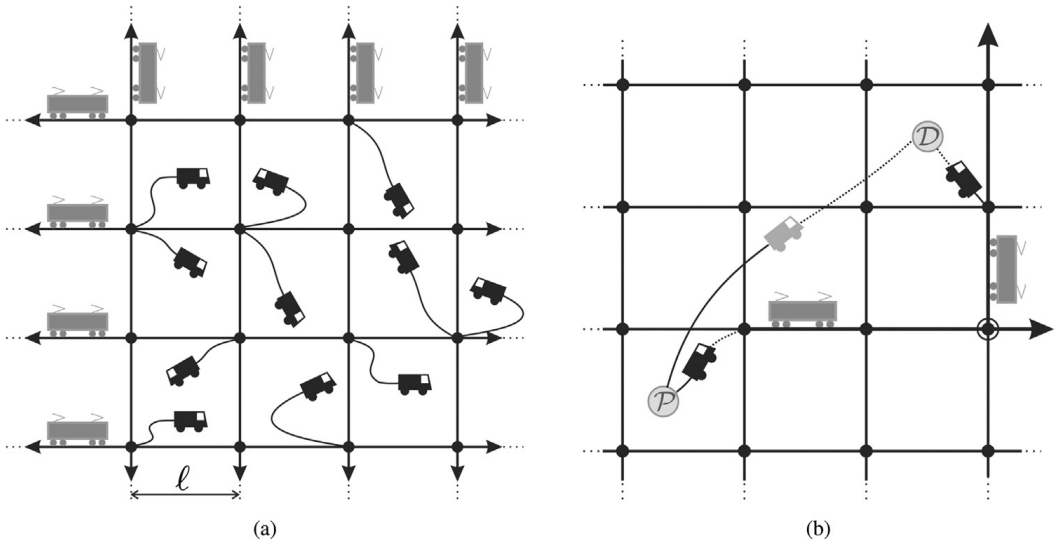

Fig. 1. Bi-modal transport network on a square grid. (a) A bi-modal network with trains (grey vehicles) operating along the solid lines. Shuttles (black vehicles) are used as a feeder service to carry people to and from the train stations (black dots at intersection points) separated by distance ℓ. Trains operate periodically at a frequency μ, with vehicle seating capacity k. **(b)** Two alternative ways to serve a transport request from $\mathcal{P}$ (pick-up) to $\mathcal{D}$ (drop-off). Bi-modal transport involves a shuttle ride from $\mathcal{P}$ to the train station, transport by train (arrows, here with one change (circle)), and another shuttle ride from the train station to $\mathcal{D}$. Uni-modal transport service is a direct shuttle (grey) ride from $\mathcal{P}$ to $\mathcal{D}$. A major task of the system is to appropriately decide which of these two types of transport services to choose.

2.2. Model system geometry

For an overarching systematic study, it is useful to consider an idealized model geometry (see Fig. 2.2). We assume that transport occurs via DRRP shuttle service, combined with a square grid of railways on which transport occurs via trains. The connection points (train stations) between the two subsystems lie at all railway intersections and are spaced with a lattice constant ℓ (see Fig. 2.2). The transit system is further characterized by a shuttle density B in the plane and a train frequency μ at all train stations, with trains having a seating capacity k. Shuttles and trains move with velocities v_0 and v_{train}, respectively. They require energy e_{shuttle} and e_{train}, respectively, per unit distance of travel.

The main goal of the bi-modal system under consideration is to provide high quality (i.e., rapid) door-to-door transportation service at minimal energy consumption, thereby minimal carbon emission. To reach this goal, the provider of bi-modal transit may vary certain parameters of operation. We will first introduce these control parameters in Section 3 and then derive expressions for the system's service quality and energy consumption as functions of these parameters in Section 4.

3. Parameters of operation

3.1. Choosing the type of transport service

A single user in the model system may either be transported by uni-modal service, i.e., by shuttle (DRRP) only, or by bi-modal service, i.e., be brought from $\mathcal{P} = (x_p, y_p)$ to the nearest train station by means of a shuttle, followed by a train journey, which is again followed by a shuttle journey to $\mathcal{D} = (x_d, y_d)$ (see Fig. 2.2). Aside from assembling the routes of the shuttles such as to optimize pooling efficiency, one central task of the dispatcher system will be to decide, for each individual request $(\mathcal{P}, \mathcal{D})$, whether the desired door-to-door service should be completed uni-modally or bi-modally.

If only user convenience were considered relevant, one would just need to calculate which type of transport service (uni-modal or bi-modal) requires less time for completing the transit, and then to choose that one. This requires knowledge of the parameters v_0, v_{train}, and the frequency of line service, μ. The latter can be assumed to be just sufficient to carry the bi-modal passenger load. Its derivation will be discussed further below (see Subsec. 3.2). By sampling random transport requests in the plane, and distances from the probability distribution $p(d)$ of travel distances, we can compile a histogram of relative travel times, t_{bi} and t_{uni}, as shown in Fig. 2a. It displays the resulting ratio $t_{\text{bi}}/t_{\text{uni}}$[2] as a scatter heat map in the plane spanned by the vector $\overline{\mathcal{PD}}$. Requests corresponding to the area within the black curve (contour curve of $t_{\text{bi}}/t_{\text{uni}} = 1$) would then be served uni-modally by a single shuttle services, while for all others, the dispatcher would offer bi-modal transport service.

In order to choose, for an incoming request $(\mathcal{P}, \mathcal{D})$, the type of transport service which consumes the least incremental amount of energy, we have to compute the energy increment $(\Delta\mathcal{E})_{\text{bi}}$ needed for bi-modal transport, and compare it to the energy increment

[2] Subsec. 4.1 displays the mathematical expressions of t_{bi}, t_{uni}.

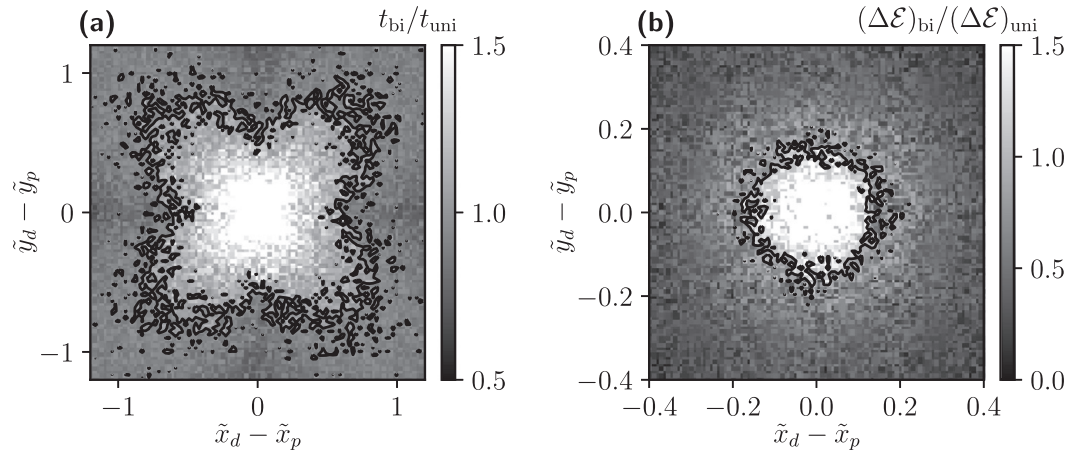

Fig. 2. Choosing the type of transport service. Relative characteristics of either bi-modal (shuttle-train(s)-shuttle) or uni-modal (just shuttle) service, in the plane spanned by the individual trip vector from pick-up $\mathcal{P} = (x_p, y_p)$ to drop-off $\mathcal{D} = (x_d, y_d)$. **(a)** Bi-modal travel time, t_{bi}, divided by uni-modal travel time, t_{uni}. The black curve represents the contour line where both are equal. Requests outside this region are served faster with bi-modal transportation. **(b)** Increment in total energy consumption if a new user is served by bi-modal transportation, $(\Delta\mathcal{E})_{\mathrm{bi}}$ divided by the increment in total energy consumption if the same user is served by uni-modal transportation, $(\Delta\mathcal{E})_{\mathrm{uni}}$. The black curve represents the contour line where both are equal, i.e., from the perspective of energy consumption both types of transport service are equivalent. Requests outside the white region lead to lower energy consumption if served by bi-modal transportation. See Supporting Information for details.

$(\Delta\mathcal{E})_{\mathrm{uni}}$ assuming direct transport via a single shuttle. This ratio of energy increments is equal to the ratio of driven distances by the shuttles for each type of service (see also Fig. 2.2). We assume that a single request does not alter the line service frequency, i.e, the energy consumption of the line service does not change. In analogy to the travel times shown in Fig. 2a, the ratio of the energy consumption increments (i.e., traveled distances by shuttles) is depicted in Fig. 2b. Again, we see that while for small requested distances uni-modal service is advisable, bi-modal service should be preferred for larger distances, corresponding to the area outside the black contour curve.

Comparison of Fig. 2a and 2b reveals that there is a significant range of distances which lie outside the solid curve in Fig. 2b, but still well inside the curve depicted in Fig. 2a. This shows that we may have to deal with conflicting objectives for quite a number of incoming transport requests. The notion of optimality then depends upon the relative valuation of energy consumption and service quality. As a generally accepted way of dealing with conflicting objectives, we will tackle this problem by means of Pareto fronts (Debreu, 1959; Greenwald and Stiglitz, 1959; Magill and Quinzii, 2002) further below (see Subsec. 5.1).

While the plot in Fig. 2b represents a rather isotropic structure, we encounter a shamrock-like shape in Fig. 2a. This reflects the orthogonal geometry of our model line service system (Fig. 2.2). In a real situation, the geometry will in general not be this simple. Instead, the directions at which rails are installed will vary from one station to another. We thus expect a structure like the 'shamrock' to be less pronounced in reality, if discernible at all. Hence although a perfectly isotropic structure may not be expected, the anisotropy will certainly be less pronounced. We assume that it will be a reasonable approximation to consider the contour line of service times as 'sufficiently' circular. Therefore we consider henceforth only the requested travel distance, $d = |\overline{\mathcal{PD}}|$, as the discriminating parameter for the choice of type of transport service, irrespective of its direction. The task of the dispatcher will then be to determine a proper cutoff distance, $\boldsymbol{d}_{\mathbf{c}}$, such that for $d > \boldsymbol{d}_{\mathbf{c}}$, bi-modal service is offered, while for $d \le \boldsymbol{d}_{\mathbf{c}}$, the system will provide uni-modal service, by shuttle only.

Note that the above approximation provides a lower bound of the performance achievable. In a real system, the type of transport service may be decided upon the true expected travel times and energy consumption, for which data will be available with ever improving quality over time.

3.2. Choice of line service frequency

It is clear that the capacity k and frequency μ of the line service must be sufficient to carry the flux of shuttle passengers towards and from the train stations. The total number of requests emanating in unit time in an area of ℓ^2 around a train station is $\nu E\ell^2$. Out of these, only a fraction $F = F(\boldsymbol{d}_{\mathbf{c}}) = \int_{\boldsymbol{d}_{\mathbf{c}}}^{\infty} p(d)\,\mathrm{d}d$ is served by bi-modal transportation. However, trains are also occupied by passengers from previous stations. If D_{train} is the average distance that users travel on trains, then a user travels D_{train}/ℓ stations on train on average. Therefore, the total number of users to be transported at this station per unit time is

$$\mathcal{J}_{\mathrm{in}} = \nu E\ell^2 F \frac{D_{\mathrm{train}}}{\ell}\,. \tag{1}$$

We find that $D_{\mathrm{train}} = \frac{4}{\pi}\langle d\rangle_{d>\boldsymbol{d}_{\mathbf{c}}}$[3], with $\langle d\rangle_{d>\boldsymbol{d}_{\mathbf{c}}}$ the mean of requested distances larger than $\boldsymbol{d}_{\mathbf{c}}$.

[3] Averaging the 1-norm $\|\overline{\mathcal{PD}}\|_1$ over distances and orientations.

A similar relation holds for the number of users per unit time that can be transported by trains arriving at one train station (with frequency μ_0 and going into four directions), namely

$$\mathcal{J}_{\text{out}} = 4 \cdot \mu_0 \cdot k \,. \tag{2}$$

Balancing $\mathcal{J}_{\text{in}}$ with $\mathcal{J}_{\text{out}}$, we obtain

$$\tilde{\mu}_0 = \frac{\Lambda \tilde{\ell}}{\pi k} \langle \tilde{d} \rangle_{\tilde{d} > \tilde{\boldsymbol{d}}_{\mathbf{c}}} F \tag{3}$$

for the minimum frequency required to carry all passengers conveyed by the shuttles. The $\tilde{}$ indicates quantities non-dimensionalized via division by the respective unit, i.e., D or t_0. We refer to Eq. 3 as passenger flux balance.

If we allow trains to operate at a frequency $\tilde{\mu}$ larger than the minimum required frequency $\tilde{\mu}_0$, the train occupancy is given by $\boldsymbol{\alpha} = \tilde{\mu}_0/\tilde{\mu} \in [0, 1]$. As this can be adjusted within some range when operating the line service, $\boldsymbol{\alpha}$ provides an additional free variable in system operation.

4. Objectives of operation

4.1. Service quality

We define the service quality as the ratio between average travel time by MIV and by the bi-modal system

$$\mathcal{Q} = \frac{t_0}{(1-F) \cdot t_{\text{uni}} + F \cdot t_{\text{bi}}} \,. \tag{4}$$

For assessing the overall quality of service, suitable averaging has to be applied. Transportation by shuttles is always assumed to be delayed with respect to MIV by a waiting time, which we assume (on average) to be of order one half the direct travel time, $t_0/2$ (see Supporting Information for motivation). The average time taken to serve a request in a bi-modal system (i.e., the denominator of $\mathcal{Q}$ in Eq. 4) is then

$$t_0\, \mathcal{Q}^{-1} = \quad (1-F) \cdot \underbrace{\left(\frac{t_0}{2} + \frac{\delta \langle d \rangle_{d < \boldsymbol{d}_{\mathbf{c}}}}{v_0} \right)}_{t_{\text{uni}}} + F \cdot \underbrace{\left(t_0 + \frac{2\beta\ell\delta}{v_0} + \frac{1}{\mu} + \frac{4}{\pi} \frac{\langle d \rangle_{d > \boldsymbol{d}_{\mathbf{c}}}}{v_{\text{train}}} \right)}_{t_{\text{bi}}}, \tag{5}$$

where $\langle d \rangle_{d < \boldsymbol{d}_{\mathbf{c}}}$ represents the mean of all requested distances less than $\boldsymbol{d}_{\mathbf{c}}$ (i.e., served uni-modally) and δ is the average detour[4] incurred by the shuttles due to the necessity of pooling several different transport requests into one vehicle route. For the expected detour with a shuttle we set $\delta = 1.5$ (see Supporting Information for details). For the second term (t_{bi}), t_0 is the total average waiting time for two shuttle trips (to and from the station), $1/\mu$ is the average waiting time for two train rides (usually there is a change involved), $\beta\ell$ is the average distance of a randomly chosen point from the next train station, with a geometrical constant $\beta \approx 0.383$[5], and $4\pi^{-1}\langle d \rangle_{d > \boldsymbol{d}_{\mathbf{c}}}$ is the average distance traveled on trains. The effective train velocity, v_{train}, depends on the inter-station distance ℓ and is modeled based on train vehicle data (see Supporting Information for details).

If we use D, t_0, and v_0 as units for length, time, and velocity, respectively, we can write:

$$\mathcal{Q}^{-1} = (1-F) \cdot \left(\tfrac{1}{2} + \delta \langle \tilde{d} \rangle_{\tilde{d} < \tilde{\boldsymbol{d}}_{\mathbf{c}}} \right) + F \cdot \left(1 + 2\beta\tilde{\ell}\delta + \tfrac{1}{\tilde{\mu}} + \tfrac{4}{\pi} \tfrac{\langle \tilde{d} \rangle_{\tilde{d} > \tilde{\boldsymbol{d}}_{\mathbf{c}}}}{\tilde{v}_{\text{train}}} \right). \tag{6}$$

4.2. Energy consumption

In order to assess the efficiency of a transit system in terms of energy consumption, it is essential to consider the total distances over which passengers are being transported in the different vehicles involved (see Eq. 7). The bi-modal energy consumption can be written as

$$\mathcal{E} \equiv \frac{\Delta_{\text{shuttle}} \cdot e_{\text{shuttle}} + \Delta_{\text{train}} \cdot e_{\text{train}}}{\Delta_{\text{MIV}} \cdot e_{\text{MIV}}}, \tag{7}$$

where $\Delta_{\cdot}$ denotes the (mode-specific) total distance traveled in a unit cell of size ℓ^2 per unit time, and $e_{\text{shuttle/train}}$ is the vehicle-specific energy consumption per unit distance. Note that this expression is already normalized with respect to the MIV energy consumption (denominator), as this is the door-to-door transportation system we intend to compare with. For $\mathcal{E} > 1$ (< 1) energy requirement for bi-modal transportation is more (less) than for private cars serving the same requests.

For the simulations we will describe below, we use numbers found for frequently used transport vehicles. Specifically, we consider electric light rails with a maximum seating-capacity $k = 100$ and $e_{\text{train}} = 9.72$ kN (Knörr et al. (2016)) for the line service. For MIV we consider Diesel cars with $e_{\text{MIV}} = 2.47$ kN (BMDV, 2022). For the shuttle we choose Mercedes Sprinter (8.8 liters of Diesel per 100 km (mbenz, 2022), thus $e_{\text{shuttle}} = 3.28$ kN.

[4] driven distance / direct distance

[5] A simple calculation shows that $\beta = \frac{1}{6}(\sqrt{2} + \log(1+\sqrt{2})) = 0.383$.

Shuttles Both uni-modal (shuttle only) and bi-modal trips contribute to the total distance driven by shuttles per unit time due to requests from a unit cell of size ℓ^2, hence

$$\Delta_{\text{shuttle}} = \frac{\nu E \ell^2}{\eta}\left(\underbrace{\langle d\rangle_{d<\boldsymbol{d}_c}(1-F)}_{\text{shuttleonly}} + \underbrace{2\beta\ell F}_{\text{twoshuttletrips}}\right), \tag{8}$$

where η is the DRRP pooling efficiency, which is the ratio of requested direct distance by the users and the driven distance by the shuttles (for MIV, $\eta = 1$).

In simulations of the uni-modal system (shuttles only), it has been observed that η scales with demand Λ roughly in an algebraic manner, $\eta(\Lambda) \propto \Lambda^{\gamma}$, with $\gamma \approx 0.12$ (Mühle (2022)). In a bi-modal system, however, some of the demand Λ is directed towards trains, therefore, we need to compute an adjusted demand, $\Lambda_{\text{shuttle}} \equiv (E\nu_{\text{shuttle}} D^3_{\text{shuttle}})/v_0$, considering shuttle trips only; ν_{shuttle} is the effective request frequency for shuttle trips and D_{shuttle} is the average distance of a shuttle trip. Bi-modal trips consist of two shuttle trips (from and to the station), therefore

$$\nu_{\text{shuttle}} = \underbrace{2\nu F}_{\text{twoshuttletrips}} + \underbrace{\nu(1-F)}_{\text{shuttlesonly}} = \nu(1+F)\,. \tag{9}$$

Similarly, the average requested distance for shuttle-borne trips involved in bi-modal transport is

$$D_{\text{shuttle}} = \Big(\underbrace{2\beta\ell F}_{\text{twoshuttletrips}} + \underbrace{\langle d\rangle_{d<\boldsymbol{d}_c}(1-F)}_{\text{shuttlesonly}}\Big)/(1+F), \tag{10}$$

where $(1+F)$ is due to normalization. The bi-modal demand for shuttles is thus given by:

$$\begin{aligned}\Lambda_{\text{shuttle}} &= (E\nu_{\text{shuttle}} D^3_{\text{shuttle}})/v_0 \\ &= \Lambda(1+F)^{-2}((1-F)\langle\tilde{d}\rangle_{\tilde{d}<\tilde{\boldsymbol{d}}_c} + 2\beta\tilde{\ell}F)^3\,.\end{aligned} \tag{11}$$

In simulations we observe a higher efficiency than suggested by $\eta \propto \Lambda^{0.12}_{\text{shuttle}}$ (see Supporting Information for simulation data). We call this the *common stop effect*, meaning that pooling gets more efficient because bi-modal requests are spatially correlated due to shared pick-up and drop-off locations, i.e., the train stations. We account for this effect via an empirical function $h(F)$ ($1 \le h \le 1.35$, see Supporting Information for details). In particular, we set

$$\eta \equiv \Lambda^{0.12}_{\text{shuttle}} \cdot h(F)\,. \tag{12}$$

Line Service and MIV Trains are recurrent every $1/\mu$ time units. Therefore, the cumulative distance driven by all trains in a unit cell of side length ℓ per unit time is

$$\Delta_{\text{train}} = 4 \cdot \mu \cdot \ell\,. \tag{13}$$

There is a multiplicative factor of 4 because trains go in four directions at every train station. The total distance driven via MIV for requests from the unit cell amounts to

$$\Delta_{\text{MIV}} = \nu E \ell^2 D. \tag{14}$$

Replacing Δ_{shuttle}, Δ_{train}, and Δ_{MIV} in Eq. 7 from Eq. 8, 13, and 14 we obtain the final expression for the energy consumption of bi-modal transit normalized with respect to MIV

$$\mathcal{E} = \underbrace{\eta^{-1}\left(\langle\tilde{d}\rangle_{\tilde{d}<\tilde{\boldsymbol{d}}_c}(1-F) + 2\beta\tilde{\ell}F\right)\cdot\frac{e_{\text{shuttle}}}{e_{\text{MIV}}}}_{\text{shuttles}} + \underbrace{\frac{4\tilde{\mu}}{\Lambda\tilde{\ell}}\cdot\frac{e_{\text{train}}}{e_{\text{MIV}}}}_{\text{train}}. \tag{15}$$

5. Results

We now analyze how the objectives, i.e., energy consumption (Eqs. 7, 15) and quality (Eqs. 4, 6), can be optimized by choice of parameters of operation, i.e., cutoff distance $\boldsymbol{d}_c$ and train occupancy $\boldsymbol{\alpha}$, under different 'external' conditions, Λ and $\tilde{\ell}$. Notice that the two control parameters, $\boldsymbol{\alpha}$ and $\boldsymbol{d}_c$, enter the objectives, $\mathcal{Q}$ and $\mathcal{E}$, via $\langle\tilde{d}\rangle_{\tilde{d}\le\tilde{\boldsymbol{d}}_c}$, $F(\boldsymbol{d}_c)$, and $\tilde{\mu} = \tilde{\mu}_0(\boldsymbol{d}_c)/\boldsymbol{\alpha}$ (Eq. 3).

In Fig. 3, energy consumption, $\mathcal{E}$, and service quality, $\mathcal{Q}$, for the combined system are shown as a function of the share of bi-modal transport $F(\boldsymbol{d}_c)$ at $\tilde{\ell} = 0.8$ for three different values of dimensionless demand, Λ. Trains are operated at full occupancy, i.e., $\boldsymbol{\alpha} = 1$. The general trend of reduction of energy consumption with increasing demand and involvement of line services is obvious from the data for $\mathcal{E}$. We encounter a minimum of energy consumption at around $F \approx 0.6$ for all values of Λ investigated. Energy consumption can be less than 30% of MIV for sufficiently large (but realistic, see Table 1) demand. For service quality, we find that typical values are around one half the service quality of MIV, i.e., about twice the travel time. This is customary for public transport systems (Liao et al., 2020; Salonen and Toivonen, 2013b) and generally well accepted by users. Note that our data for service quality represent a safe lower bound, as the (sometimes quite substantial) time required for parking spot search (Chaniotakis and Pel, 2015; Fulman and Benenson, 2021) is neglected here in t_0. While for low Λ the involvement of line service seems to generally increase travel times (i.e., reduce service quality), we find an optimum at $F \approx 0.25$ for large Λ. The primary message from Fig. 3, however, is that minimizing energy consumption and maximizing service quality cannot be simultaneously achieved.

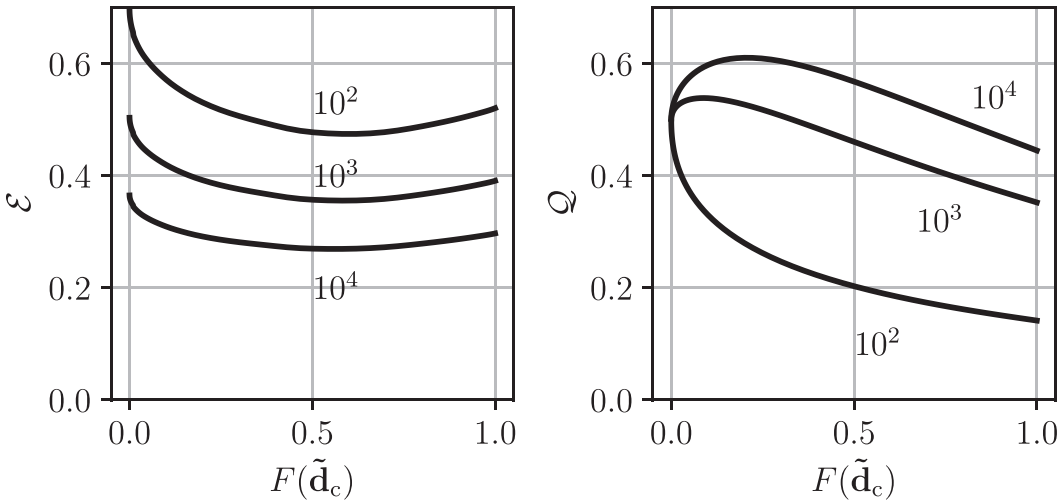

Fig. 3. Bi-modal performance characteristics. Energy consumption $\mathcal{E}$ and service quality $\mathcal{Q}$ for bi-modal transport, normalized with respect to MIV, as a function of the bi-modal fraction $F(\boldsymbol{d}_\mathrm{c})$, for three different values of demand $\Lambda = \{10^2, 10^3, 10^4\}$. All data for $\tilde{\ell} = 0.8$ and fully-occupied trains, $\boldsymbol{\alpha} = 1$.

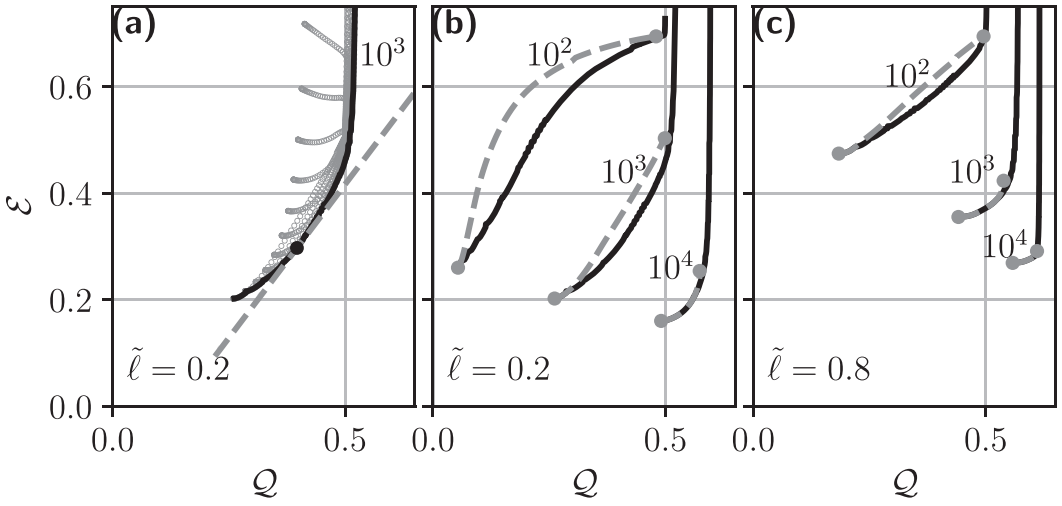

Fig. 4. Emergence of Pareto fronts and effects of train occupancy. **(a)** Grey circles: admissible data for full variation of $\boldsymbol{\alpha}$ and $\boldsymbol{d}_\mathrm{c}$, at $\tilde{\ell} = 0.2$ and $\Lambda = 10^3$. Black curve: Pareto front, i.e., the boundary of the full data set towards optimality (low $\mathcal{E}$ and high $\mathcal{Q}$). The slope of the dashed tangent to the Pareto front represents the ratio of valuations (see text). **(b)**. Black curves: Pareto fronts for variable train occupancy $\boldsymbol{\alpha} < 1$ at $\Lambda = \{10^2, 10^3, 10^4\}$ and $\tilde{\ell} = 0.2$. Grey dashed curves: degenerate Pareto fronts obtained at full train occupancy ($\boldsymbol{\alpha} = 1$) at corresponding values of Λ. Grey circles mark the ends of these fronts which are determined by minimum achievable energy consumption and maximum achievable service quality, specific to Λ and $\tilde{\ell}$. **(c)** Same as (b) but for $\tilde{\ell} = 0.8$.

5.1. Pareto fronts in energy consumption and service quality

A tuple of parameter values, in our case $(\mathcal{E}, \mathcal{Q})$, is called Pareto optimal if none of the parameters (or objectives) can be further optimized without compromising on at least one of the others. The set of all such tuples of parameters is called the Pareto front. To illustrate this concept, in Fig. 4a, we show all values $\{\mathcal{E}(\boldsymbol{d}_\mathrm{c}, \boldsymbol{\alpha}), \mathcal{Q}(\boldsymbol{d}_\mathrm{c}, \boldsymbol{\alpha})\}$ obtained for different values of $\boldsymbol{d}_\mathrm{c}$ and $\boldsymbol{\alpha}$ as grey dots. The solid black line represents the Pareto-optimal subset, i.e., the Pareto front.

In order to choose the truly optimal point on the Pareto front, one needs to define the relative valuation of the objectives, $\mathcal{E}$ and $\mathcal{Q}$. In other words, the authorities operating the system have to decide how much reduction in service quality they (i.e., the users) would be willing to accept for how much savings in energy. The ratio of these valuations is then expressed in the slope of the dashed line in Fig. 4a, which is a tangent to the Pareto front. The point where it touches the front (black dot) represents the optimal set of parameters, under the given valuation.

For our analysis, we fix the train capacity to $k = 100$, and choose a representative set of values for line service mesh size $\tilde{\ell} = \{0.2, 0.4, 0.8\}$ and demand $\Lambda = \{10^2, 10^3, 10^4\}$, corresponding to a typical parameter range encountered in real systems (see Table 1). Note that fixing k does not reduce the generality of our study, because a different k can be compensated for by properly readjusting μ_0 (see Eq. 3).

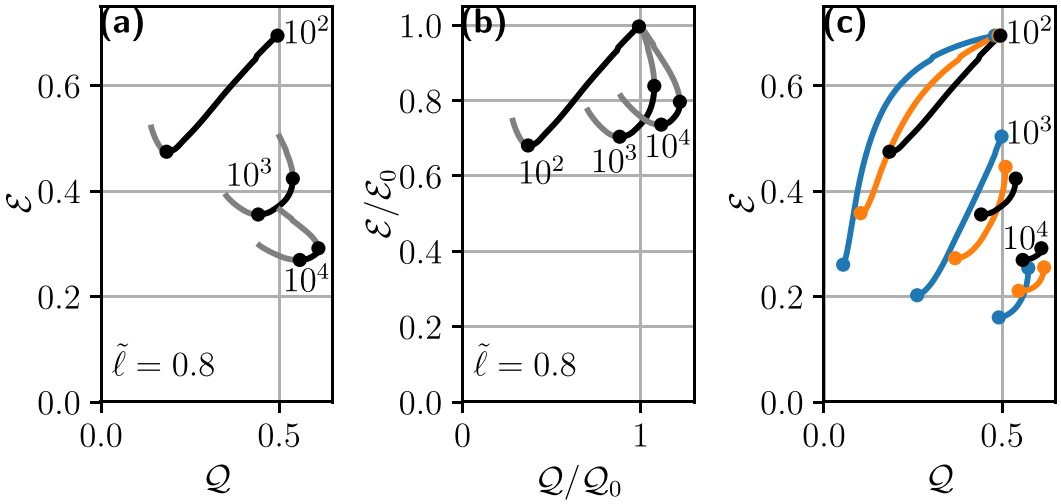

Fig. 5. Bi-modal performance with fully-occupied trains. (a) Black curves show degenerate Pareto fronts for fully-occupied trains ($\boldsymbol{\alpha} = 1$) for varying demands $\Lambda = \{10^2, 10^3, 10^4\}$ shown as annotations and $\tilde{\ell} = 0.8$. Black circles mark the end points of the Pareto fronts which are determined by the minimum achievable energy consumption and the maximum achievable service quality. Grey curves show the entire data, i.e., not only the Pareto-optimal set, but all admissible values with $\boldsymbol{d}_c$ as the control parameter. **(b)** Data as in (a), but normalized with respect to the performance, $(\mathcal{Q}_0, \mathcal{E}_0)$, of the uni-modal system (shuttles only). **(c)** Degenerate Pareto fronts as in (a), but for $\tilde{\ell} = \{0.2, 0.4, 0.8\}$ in blue, orange, and black, respectively. (For interpretation of the references to colour in this figure legend, the reader is referred to the web version of this article.)

Fig. 4 b demonstrates the effect of Λ on the overall performance of the system. Pareto fronts are shown in black. We see that for typical values of Λ, as listed in Table 1, energy consumption reaches down to well below 40% (even below 20%) of MIV for large values of Λ. At the same time, quality levels are comparable to, mostly even in excess of, what is found in existing public transport in terms of transit time (see Table 1). Note, however, that our system even provides on-demand door-to-door service, comparable to MIV.

The dashed grey curves indicate the subset of data for train occupancy $\boldsymbol{\alpha} = 1$. We will henceforth call them degenerate Pareto fronts, as they correspond to the variation of only one parameter. They are lying, slightly but consistently, above the Pareto fronts. This indicates that by reducing train occupancy below its maximum ($\boldsymbol{\alpha} < 1$), i.e., operating trains at higher frequency than necessary, one can enhance the overall performance of the system. Service quality increases because the time spent waiting for trains, which is proportional to $1/\mu$, is smaller when trains are operated more frequently. The increase in service quality is found to overcompensate the increase in energy consumption due to higher operation frequency. Since waiting time is inversely proportional to both Λ and $\tilde{\ell}$ (see Eq. 3), this effect is more pronounced for small Λ and $\tilde{\ell}$, which is qualitatively corroborated in Fig. 4c which shows corresponding data for large mesh size ($\tilde{\ell} = 0.8$). At the resolution of the figure, the Pareto fronts (black) and their degenerate partner (dashed grey) are distinguishable only for smallest values of Λ. Hence for typical values of Λ and $\tilde{\ell}$ it appears sufficient to discuss the degenerate Pareto fronts, which only need one parameter ($\boldsymbol{d}_c$) to be varied. We keep in mind that the true Pareto optimum will still be superior.

Degenerate Pareto fronts are shown in Fig. 5 in various presentations. Fig. 5a has basically the same information as Fig. 4c, but here we show the full data set (grey), where the black curves are the Pareto-optimal subset, i.e., the degenerate Pareto fronts. They terminate wherever the tangent becomes either vertical or horizontal (black dots), thus offsetting any tradeoff between the objectives.

Fig. 5 b shows these data normalized with respect to the performance of a uni-modal (shuttles only) DRRP system, represented by $\mathcal{E}_0$ and $\mathcal{Q}_0$. Clearly in relevant parameter regions the combined bi-modal system outperforms the uni-modal system in both energy consumption ($\mathcal{E} < \mathcal{E}_0$) and service quality ($\mathcal{Q} > \mathcal{Q}_0$).

The effect of inter-station distance (mesh size) on the (degenerate) Pareto fronts is explored in Fig. 5c. We see that a dense network of rails (small $\tilde{\ell}$, blue fronts) achieves the best results concerning energy consumption, reaching down to below 20% of MIV, but compromises on achievable service quality. For admissible quality $\mathcal{Q} \approx 0.5$, sparse train networks (black fronts) are Pareto-optimal for low demands. For larger demands, denser train networks (orange and blue fronts) are advantageous.

However, it is remarkable that the overall position of the Pareto fronts in the plane spanned by $\mathcal{Q}$ and $\mathcal{E}$ does not vary dramatically with mesh size, as the position on the front at which the system is operated is largely at the discretion of the operator. This suggests that the density of currently installed rail track systems might already be well suited for deploying a bi-modal on-demand transport systems of the kind we have studied.

5.2. Traffic volume

Energy consumption and service quality are not the only possible objectives for optimization of public transport. Road traffic, for example, is a source of noise and local air pollution and occupies significant shares of urban space. Bi-modal ride-pooling reduces traffic by use of shared shuttles, and by directing certain trips towards trains. We quantify this reduction by introducing the relative bi-modal traffic $\tilde{\Gamma}$ as the ratio of the number of on-road vehicles necessary for bi-modal transportation (i.e., shuttles) to the number

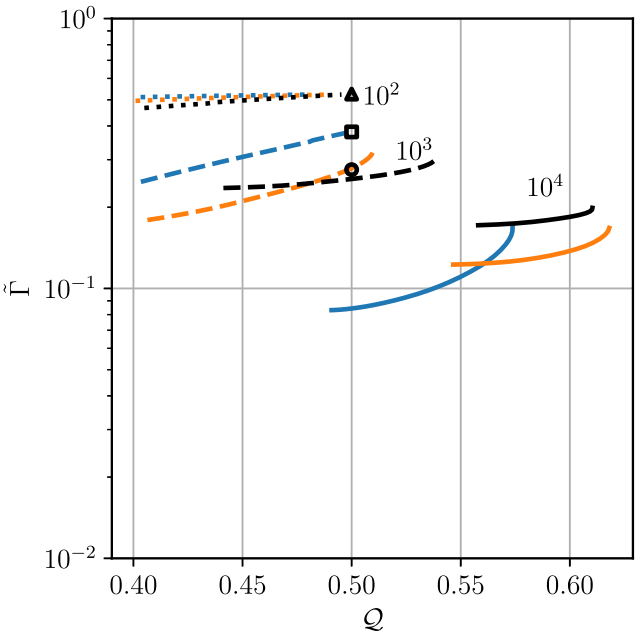

Fig. 6. Traffic volume in bi-modal transit. Relative bi-modal traffic $\tilde{\Gamma}$, as defined in Eq. 16, determined along the Pareto fronts in Fig. 5c, against corresponding service quality $\mathcal{Q}$. Data are presented for $\Lambda = 10^2$ (triangle, dotted), $\Lambda = 10^3$ (square, dashed), and $\Lambda = 10^4$ (circle, solid). Symbols represent uni-modal traffic volume, $1/\eta$. Color code is as in Fig. 5, i.e., $\tilde{\ell} = \{0.2, 0.4, 0.8\}$ in blue, orange, and black, respectively. (For interpretation of the references to colour in this figure legend, the reader is referred to the web version of this article.)

of MIV (i.e., cars) needed to serve the same demand. We have (see Supporting Information for details)

$$\tilde{\Gamma} = \eta^{-1}(1 + F)\,\tilde{D}_{\text{shuttle}}\,. \tag{16}$$

In Fig. 6, $\tilde{\Gamma}$ is plotted against service quality $\mathcal{Q}$ as determined along the degenerate Pareto fronts shown in Fig. 5c. For low demand ($\Lambda = 10^2$), uni-modal (shuttles only) transportation allows for about 50% reduction in traffic as compared to MIV (triangle). Bi-modal transportation allows for further reduction in traffic at the cost of service quality. For intermediate and high demand ($\Lambda = \{10^3, 10^4\}$), uni-modal transportation allows for about 70% to 80% reduction in traffic as compared to MIV (square, circle). In these cases, bi-modal transportation allows for truly dramatic reductions in traffic (> 90%), at equal or even higher service quality than for uni-modal transport. Combining this finding with typical parameter values in Table 1, we recognize that even in rural settings, traffic volume is expected to decrease by an order of magnitude, relative to MIV. In urban environments, traffic volume may even be reduced by more than a factor of ten.

6. Discussion

The goal of this study was to find whether and under what circumstances bi-modal transport, i.e., on-demand ride-pooling with shared shuttles combined with fixed schedule line services (railway), can be a viable alternative to customary public transportation (line services or DRRP alone) or MIV. For that purpose we introduced a simple model system for bi-modal transport, combined with a mean-field approach, which allowed us to parameterize the user environment (dimensionless demand) as well as the bi-modal service operations (cutoff distance, train occupancy) with few variables, and to write down analytic expressions for key performance characteristics, namely energy consumption and service quality (i.e., transit times), as well as road traffic volume. Our results, in form of Pareto fronts, indicate that bi-modal public transportation systems have the potential to provide on-demand door-to-door service with a quality superior to customary public transportation, while at the same time consuming only a fraction of the energy a corresponding fleet of MIV would require, and with a road traffic volume reduced by an order of magnitude.

In our model, we assume customer demand to be given, more precisely, we assume a spatially uniform demand with constant average request frequency. However, in realistic scenarios, demand will be heterogeneous in space, due to non-homogeneous population density and individual mobility patterns, and fluctuating in time due to phenomena like rush hours or workdays versus weekends. Such spatio-temporal demand patterns can be taken into account by structured railway networks (e.g., more dense in highly-populated areas), spatially varying shuttle densities, and variable service frequencies. In future case studies or real-world applications, these context-specific adjustments can be implemented to provide tailored solutions.

Although demand patterns can be estimated from historical data, there will be fundamental uncertainties in predicting future demand. Such uncertainties will alter the performance of a bi-modal system. Nevertheless, our considerations based on known (average) transportation demand give a valuable estimate of the performance potential of bi-modal transport under various external conditions.

Moreover, in reality, demand will couple to service quality and other parameters concerning user satisfaction; a well-functioning system of transportation attracts demand. Since service quality depends on demand, too—as seen in this study—modeling user

behavior introduces a feedback loop. In a forthcoming study we will integrate this feedback loop into our modeling framework, a step towards resolving user adoption dynamically. Broader analysis of user adoption of bi-modal transportation based on incentives, customer convenience, and customer preferences remains to be explored. Recent results from experimental social science, however, point into a very favorable direction (Avermann and Schlüter, 2019; Nyga et al., 2020; Sörensen et al., 2021).

It is important to note that our results, represent only a lower bound on bi-modal performance, in particular as far as service quality is concerned. First, we have based the decision on the type of transport service (uni-modal or bi-modal) on a single scalar parameter, $\boldsymbol{d_c}$, which amounts to representing the decision process by a binary-valued function of a single scalar variable, $d \longrightarrow \{0,1\}$. The true structure would be a binary-valued field Φ on the four-dimensional space of the pick-up and drop-off coordinates, $\Phi : (x_p, y_p, x_d, y_d) \longrightarrow \{0,1\}$. This would be extremely cumbersome to study in a statistical manner. However, in a real system, data on $\Phi(x_p, y_p, x_d, y_d)$ are being collected on a daily basis, such that over time the system can be ever improving its performance over the data we have presented here.

Second, bi-modal service of the kind studied here provides door-to-door service, while MIV involves the search for parking space, which was disregarded in our study due to lack of reliable data. This can be quite significant, and fully adds to the MIV transit time, thus further improving on the relative service quality, Q, of bi-modal service.

Moreover, it should be mentioned that riding a bi-modal transport system neither involves having to drive nor taking care of vehicle maintenance.

In summary, bi-modal public transport systems have the potential of outperforming customary public transportation and the private car in a number of ways. With this study, we provided broad fundamental evidence and laid the foundation for taking the idea of bi-modal public transit systems to real-world applications.

Declaration of interests

The authors declare that they have no known competing financial interests or personal relationships that could have appeared to influence the work reported in this paper.

Acknowledgements

The authors would like to appreciate fruitful discussions with Tariq Baig-Meininghaus, Michael Patscheke and Prakhar Godar

Supplementary material

Supplementary material associated with this article can be found, in the online version, at doi:10.1016/j.multra.2023.100083

References

AfS, 2021. Bevölkerungsstand Jahresergebnisse. https://www.statistik-berlin-brandenburg.de/a-i-3-j. Accessed: 2022-10-04.
Alam, B.M., Nixon, H., Zhang, Q., 2015. Investigating the determining factors for transit travel demand by bus mode in US metropolitan statistical areas.
Alonso-Mora, J., Samaranayake, S., Wallar, A., Frazzoli, E., Rus, D., 2017. On-demand high-capacity ride-sharing via dynamic trip-vehicle assignment. Proc. Natl. Acad. Sci. 114 (3), 462–467.
Arnott, R., Small, K., 1994. The economics of traffic congestion. Am. Sci. 82 (5), 446–455. http://www.jstor.org/stable/29775281.
Avermann, N., Schlüter, J., 2019. Determinants of customer satisfaction with a true door-to-door DRT service in rural germany. Res. Transp. Bus. Manag. 32, 100420.
Barth, M., Boriboonsomsin, K., 2009. Traffic congestion and greenhouse gases. Access Mag. 1 (35), 2–9.
BMDV, 2022. Verkehr in Zahlen 2021/2022. Technical Report. Bundesministerium für Verkehr und digitale Infrastruktur.
Caiazzo, F., Ashok, A., Waitz, I.A., Yim, S.H.L., Barrett, S.R.H., 2013. Air pollution and early deaths in the united states. part i: quantifying the impact of major sectors in 2005. Atmos. Environ. 79, 198–208. doi:10.1016/j.atmosenv.2013.05.081.
Chaniotakis, E., Pel, A.J., 2015. Drivers' Parking location choice under uncertain parking availability and search times: a stated preference experiment. Transp. Res. Part A: 82, 228–239. doi:10.1016/j.tra.2015.10.004.
Chen, M.H., Jauhri, A., Shen, J.P., 2017. Data driven analysis of the potentials of dynamic ride pooling. In: Proceedings of the 10th ACM SIGSPATIAL Workshop on Computational Transportation Science. Association for Computing Machinery, New York, NY, USA, pp. 7–12. doi:10.1145/3151547.3151549.
Chin, A.T.H., 1996. Containing air pollution and traffic congestion: transport policy and the environment in singapore. Atmos. Environ. 30 (5), 787–801. doi:10.1016/1352-2310(95)00173-5. Supercities: Environment Quality and Sustainable Development
Daganzo, C.F., Ouyang, Y., Yang, H., 2020. Analysis of ride-sharing with service time and detour guarantees. Transp. Res. Part B: Methodological 140, 130–150.
Debreu, G., 1959. Valuation equilibrium and pareto optimum. Proc. Natl. Acad. Sci. 40, 588–592.
Douglas, M.J., Watkins, S.J., Gorman, D.R., Higgins, M., 2011. Are cars the new tobacco? J. Public Health (Bangkok) 33 (2), 160–169. doi:10.1093/pubmed/fdr032.
eea, 2020. European environment agency: are we moving in the right direction? Indicators on transport and environmental integration in the EU. https://www.eea.europa.eu/ds_resolveuid/0c1c4a6acf289ffdefa1876ea5d60f07, Accessed: 2022-07-14.
eeab, 2020. Air quality in Europe 2020 report. https://www.eea.europa.eu/publications/air-quality-in-europe-2020-report. Accessed: 2022-05-18.
eurostat, 2022. Passenger mobility statistics. https://ec.europa.eu/eurostat/statistics-explained/index.php?title=Passenger_mobility_statistics#Urban_trips. Accessed: 2022-09-29.
Fan, Y.V., Perry, S., Kleme, J.J., Lee, C.T., 2018. A review on air emissions assessment: transportation. J. Clean. Prod. 194, 673–684. doi:10.1016/j.jclepro.2018.05.151.
Ferbrache, F., Knowles, R.D., 2017. City boosterism and place-making with light rail transit: a critical review of light rail impacts on city image and quality. Geoforum 80, 103–113.
Fiorello, D., Martino, A., Zani, L., Christidis, P., Navajas-Cawood, E., 2016. Mobility data across the EU 28 member states: results from an extensive CAWI survey. Transp. Res. Procedia 14, 1104–1113.
Fulman, N., Benenson, I., 2021. Approximation method for estimating search times for on-street parking. Transp. Sci. 55 (5), 1046–1069.
Gerike, R., Hubrich, S., Ließke, F., Wittig, S., Wittwer, R., 2018. Mobilität in Städten – SrV 2018 https://tu-dresden.de/bu/verkehr/ivs/srv/ressourcen/dateien/SrV2018_Staedtevergleich.pdf?lang=en.
Greenwald, B., Stiglitz, J.E., 1959. Externalities in economies with imperfect information and incomplete markets. Q. J. Econ. 40, 229–264.
Haller, P., Dauth, W., 2018. Wirtschaftsdienst 98, 608–610. doi:10.1007/s10273-018-2339-y.

Herminghaus, S., 2019. Mean field theory of demand responsive ride pooling systems. Transp. Res. Part A: Policy Pract. 119, 15–28.
IAB, 2018. Kurzbericht 10.
Jang, Y.J., Jeong, S., Lee, M.S., 2016. Initial energy logistics cost analysis for stationary, quasi-dynamic, and dynamic wireless charging public transportation systems. Energies 9 (7). doi:10.3390/en9070483.
Joireman, J.A., Van Lange, P.A.M., Van Vugt, M., 2004. Who cares about the environmental impact of cars? those with an eye toward the future. Environ. Behav. 36 (2), 187–206.
Kato, H., Kaneko, Y., Soyama, Y., 2014. Economic benefits of urban rail projects that improve travel-time reliability: evidence from tokyo, japan. Transp. Policy (Oxf.) 35, 202–210.
Kent, J., 2013. Secured by automobility: why does the private car continue to dominate transport practices?. UNSW Sydney.
Knörr, W., Heidt, C., Gores, S., Bergk, F., 2016. Aktualisierung GDaten- und Rechenmodell: Energieverbrauch und Schadstoffemissionen des motorisierten Verkehrs in Deutschland 1960–2035æ (TREMOD) für die Emissionsberichterstattung 2016 (Berichtsperiode 1990–2014) Anhang. Technical Report.
Koźlak, A., Wach, D., 2018. Causes of traffic congestion in urban areas. case of poland. SHS Web Conf. 57, 01019. doi:10.1051/shsconf/20185701019.
Kontovas, C.A., Psaraftis, H.N., 2016. Transportation Emissions: Some Basics. Springer International Publishing, Cham.
Liao, Y., Gil, J., Pereira, R.H.M., Yeh, S., Verendel, V., 2020. Disparities in travel times between car and transit: spatiotemporal patterns in cities. Sci. Rep. 10 (1), 1–12.
Lobel, I., Martin, S., 2020. Detours in shared rides. Available at SSRN 3711072.
Lotze, C., Marszal, P., Schröder, M., Timme, M., 2022. Dynamic stop pooling for flexible and sustainable ride sharing. N. J. Phys. 24 (2), 023034. doi:10.1088/1367-2630/ac47c9.
Mühle, S., 2022. An analytical framework for modeling ride pooling efficiency and minimum fleet size. under review.
MacKenzie, D., Zoepf, S., Heywood, J., 2014. Determinants of US passenger car weight. Int. J. Veh. Des. 65 (1), 73–93.
Magill, M., Quinzii, M., 2002. Theory of Incomplete Markets. MIT Press.
Manville, M., Shoup, D., 2005. Parking, people, and cities. J. Urban Plann. Dev. 131 (4), 233–245.
mbenz, 2022. Mercedez-Benz configurator. https://voc.mercedes-benz.com/voc/de_de?_ga=2.230012379.695886780.1664812666-1473138929.1664499805. Accessed: 2022-10-03.
Merlin, L.A., 2019. Transportation sustainability follows from more people in fewer vehicles, not necessarily automation. J. Am. Plan. Assoc. 85 (4), 501–510.
Mingardo, G., Vermeulen, S., Bornioli, A., 2022. Parking pricing strategies and behaviour: evidence from the netherlands. Transp. Res. Part A: Policy Pract. 157, 185–197. doi:10.1016/j.tra.2022.01.005.
Molkenthin, N., Schröder, M., Timme, M., 2020. Scaling laws of collective ride-sharing dynamics. Phys. Rev. Lett. 125, 248302. doi:10.1103/PhysRevLett.125.248302.
Newman, P.W.G., Kenworthy, J.R., 1989. Cities and Automobile Dependence : A Sourcebook. Gower Technical Aldershot, Hants., England ; Brookfield, Vt., USA.
NYCDOT, 2018. New York City mobility report. https://www1.nyc.gov/html/dot/html/about/mobilityreport.shtml. Accessed: 2022-10-05.
Nyga, A., Minnich, A., Schlüter, J., 2020. The effects of susceptibility, eco-friendliness and dependence on the consumer's willingness to pay for a door-to-door DRT system. Transp. Res. A 132, 540–558.
Park, D., Kim, N.S., Park, H., Kim, K., 2012. Estimating trade-off among logistics cost, CO2 and time: a case study of container transportation systems in korea. Int. J. Urban Sci. 16 (1), 85–98. doi:10.1080/12265934.2012.668322.
Pietrzak, K., 2016. Analysis of the possibilities of using ælight freight railwayg for the freight transport implementation in agglomeration areas (example of west pomerania province). Transp. Res. Procedia 16, 464472.
Pietrzak, O., Pietrzak, K., 2019. The role of railway in handling transport services of cities and agglomerations. Transp. Res. Procedia 39, 405416.
Sörensen, L., Bossert, A., Jokinen, J.-P., Schlüter, J., 2021. How much flexibility does rural public transport need? - implications from a fully flexible DRT system. Transp. Policy (Oxf.) 100, 5–20.
Salonen, M., Toivonen, T., 2013. Modelling travel time in urban networks: comparable measures for private car and public transport. J. Transp. Geogr. 31, 143–153. doi:10.1016/j.jtrangeo.2013.06.011.
Santi, P., Resta, G., Szell, M., Sobolevsky, S., Strogatz, S.H., Ratti, C., 2014. Quantifying the benefits of vehicle pooling with shareability networks. Proc. Natl. Acad. Sci. 111 (37), 13290–13294. doi:10.1073/pnas.1403657111.
Shaheen, S., Cohen, A., 2019. Shared ride services in north america: definitions, impacts, and the future of pooling. Transp. Rev. 39 (4), 427–442. doi:10.1080/01441647.2018.1497728.
Sorge, A., Manik, D., Herminghaus, S., Timme, M., 2015. Towards a unifying framework for demand-driven directed transport (d3t). In: Proceedings of the 2015 Winter Simulation Conference. IEEE Press, p. 28002811.
StBA, 2020. Regionalatlas deutschland. https://regionalatlas.statistikportal.de/. Accessed: 2022-10-04.
Storch, D.-M., Timme, M., Schröder, M., 2021. Incentive-driven transition to high ride-sharing adoption. Nat. Commun. 12 (1), 3003. doi:10.1038/s41467-021-23287-6.
Sundt, A., Luo, Q., Vincent, J., Shahabi, M., Yin, Y., 2021. Heuristics for customer-focused ride-pooling assignment. 10.48550/ARXIV.2107.11318
Swenseth, S.R., Godfrey, M.R., 2002. Incorporating transportation costs into inventory replenishment decisions. Int. J. Prod. Econ. 77 (2), 113–130. doi:10.1016/S0925-5273(01)00230-4.
Tachet, R., Sagarra, O., Santi, P., Resta, G., Szell, M., Strogatz, S.H., Ratti, C., 2017. Scaling law of urban ride sharing. Sci. Rep. 7 (1), 1–6.
TLC, N., 2022. NYC taxi and limousine commission trip record data. https://www1.nyc.gov/site/tlc/about/tlc-trip-record-data.page. Accessed: 2022-10-05.
USCB, 2020. QuickFacts – New York City. https://www.census.gov/quickfacts/fact/table/newyorkcitynewyork/PST045221. Accessed: 2022-10-04.
Vazifeh, M.M., Santi, P., Resta, G., Strogatz, S.H., Ratti, C., 2018. Addressing the minimum fleet problem in on-demand urban mobility. Nature 557, 534–538.
Wolf, H., Storch, D.-M., Timme, M., Schröder, M., 2022. Spontaneous symmetry breaking in ride-sharing adoption dynamics. Phys. Rev. E 105, 044309. doi:10.1103/PhysRevE.105.044309.
Zwick, F., Kuehnel, N., Moeckel, R., Axhausen, K.W., 2021. Ride-pooling efficiency in large, medium-sized and small towns -simulation assessment in the munich metropolitan region. Procedia Comput. Sci. 184, 662–667. doi:10.1016/j.procs.2021.03.083. The 12th International Conference on Ambient Systems, Networks and Technologies (ANT) / The 4th International Conference on Emerging Data and Industry 4.0 (EDI40) / Affiliated Workshops

Supplementary material for the article "Sustainable and convenient: bi-modal public transit systems outperforming the private car"

Puneet Sharma[a], Knut M. Heidemann[a,], Helge Heuer[a], Steffen Mühle[a], Stephan Herminghaus[a]

[a]*Max Planck Institute for Dynamics and Self-Organization (MPIDS), Am Faßberg 17, 37077 Göttingen, Germany*

1. Traffic volume

To derive an expression for road traffic due to shuttles we connect the distance served by busses (left hand side) and the distance traveled by customers (right hand side), with average distance $\langle d \rangle$ traveled on road, for an area of reference A during time $t_0 = D/v_0$, with shuttle speed v_0

$$\underbrace{BA\, v_0 \langle b \rangle\, p_{\text{driving}}\, t_0}_{\text{distance served by busses}} = \underbrace{\nu E A\, t_0\, \langle d \rangle \langle \delta \rangle\, p_{\text{accept}}}_{\text{distance traveled by customers}} . \tag{1}$$

Here B is the shuttle density, $\langle b \rangle$ is the average shuttle occupancy, $\nu E A t_0$ is the number of requests in the reference area A during reference time t_0 (with request frequency ν, population density E), $\langle \delta \rangle$ is the average relative detour of customers (no detour means $\langle \delta \rangle = 1$), p_{driving} is the probability of vehicles driving (i.e., not being idle), and p_{accept} is the probability that a user request is accepted. In this study, we assume that all requests can be served ($p_{\text{accept}} = 1$), i.e., no request has to be rejected because certain constraints (like a maximum waiting time) cannot be fulfilled (see (1) for a detailed analysis of p_{accept}). Substituting $\eta \equiv \langle b \rangle / \langle \delta \rangle$[1] in Eq. 1, we define the traffic volume, Γ, by the number of driving vehicles, i.e.:

$$\Gamma \equiv BA \cdot p_{\text{driving}} = \frac{\nu E \langle d \rangle A}{\eta v_0} . \tag{2}$$

Note that for private cars, $\eta = 1$ and $\langle d \rangle \equiv D$, and for a bi-modal service, $\langle d \rangle = D_{\text{shuttle}}$ and $\nu_{\text{shuttle}} = (1 + F)\nu$ (Eq. 10, 11 in the main manuscript). Substituting these expressions in Eq. 2, we define the normalized traffic volume, $\tilde{\Gamma}$, as the ratio of traffic volume by shuttles in the bi-modal system, Γ_{bi}, and the traffic volume by private cars, Γ_{MIV}, i.e.,

$$\tilde{\Gamma} \equiv \Gamma_{\text{bi}} / \Gamma_{\text{MIV}} = \eta^{-1} (1 + F)\, \tilde{D}_{\text{shuttle}} . \tag{3}$$

2. DRRP pooling efficiency in bi-modal transport

Simulations (2) show that the DRRP pooling efficiency η in a bi-modal system of transportation is larger than expected by the relation $\eta \propto \Lambda_{\text{shuttle}}^{\gamma}$, with $\gamma \approx 0.12$, as derived in (1). This observation we attribute to what we call *'common stop effect'*, meaning that pooling gets more efficient because bi-modal requests are spatially correlated due to shared pick-up and drop-off

[1] See (1) for details on why this identity holds.

locations, i.e., the train stations. Here we present the empirical scaling function $h(F)$ accounting for this effect (see Eq. 12 in the main manuscript), assuming that the 'common stop effect' is only governed by the fraction F of people assigned to bi-modal transportation. We plot the empirical data for $h(F)$ as a function of F in Fig. 1. As expected the 'common stop effect' is maximal for $F = 1$.

3. Waiting time (τ_w) and detour (δ)

We use simulation results to determine the average waiting time for shuttles, τ_w, and the average detour, δ. In Fig. 2, mean detour and mean waiting time are plotted as a function of user demand. Users are assumed to have a maximum accepted waiting time of t_0. We observe that mean waiting time τ_w grows with demand and saturates around 0.65. Similarly the mean detour δ grows with demand and saturates around 1.65.

4. Decision on transport service type

We compare the time it takes to serve a new user request $(\mathcal{P}, \mathcal{D})$ by bi-modal and uni-modal transportation. In order to do so we sample $N = 10^5$ pick-up $(\mathcal{P})$ and drop-off $(\mathcal{D})$ pairs. The trains operate at $\tilde{\mu} = 2$.

The time it takes to serve a randomly sampled user request $(\mathcal{P}, \mathcal{D})$ by bi-modal transportation (t_{bi}) comprises of driving time in two shuttles to the nearest train station, driving time in train between the two train stations, waiting time due to shuttles and waiting time at the train station. If $\mathcal{S}_\mathcal{P}$ and $\mathcal{S}_\mathcal{D}$ represent the location of the train station next to $\mathcal{P}$ and $\mathcal{D}$, respectively, then

$$t_{\text{bi}} = \underbrace{2t_w^{\text{shuttle}} + \delta\frac{\overline{\mathcal{P}\mathcal{S}_\mathcal{P}}}{v_0} + \delta\frac{\overline{\mathcal{D}\mathcal{S}_\mathcal{D}}}{v_0}}_{\text{two shuttle trips}} + \underbrace{t_w^{\text{train}} + \frac{\overline{\mathcal{S}_\mathcal{P}\mathcal{S}_\mathcal{D}}}{v_{\text{train}}}}_{\text{train}}, \tag{4}$$

where $t_w^{\text{shuttle}}, t_w^{\text{train}}$ are the waiting times incurred due to shuttles and trains and are assumed to take the values $t_0/2$ and $1/2\mu$, respectively.

The time taken to serve the same request by uni-modal transportation (shuttles only) is:

$$t_{\text{uni}} = t_w^{\text{shuttle}} + \delta\frac{\overline{\mathcal{P}\mathcal{D}}}{v_0}. \tag{5}$$

The ratio, $t_{\text{bi}}/t_{\text{uni}}$ is plotted in Fig.2a in the main text.

In order to obtain Fig.2b, we plot the ratio of increment in energy usage for serving a new user request. The increment in energy usage when serving a new request by bi-modal transportation comprises of the increment in energy usage by two shuttle trips,

$$(\Delta\mathcal{E})_{\text{bi}} = \eta^{-1} \cdot e_{\text{shuttle}} \cdot (\overline{\mathcal{P}\mathcal{S}_\mathcal{P}} + \overline{\mathcal{D}\mathcal{S}_\mathcal{D}}). \tag{6}$$

The increment in energy usage when served by uni-modal transportation comprises of only a single shuttle trip,

$$(\Delta\mathcal{E})_{\text{uni}} = \eta^{-1} \cdot e_{\text{shuttle}} \cdot \overline{\mathcal{P}\mathcal{D}}. \tag{7}$$

The ratio $(\Delta\mathcal{E})_{\text{bi}}/(\Delta\mathcal{E})_{\text{uni}}$, i.e., $\frac{\overline{\mathcal{P}\mathcal{S}_\mathcal{P}}+\overline{\mathcal{D}\mathcal{S}_\mathcal{D}}}{\overline{\mathcal{P}\mathcal{D}}}$ is plotted in Fig. 2b in the main text. This ratio, if greater than 1 (less than 1), indicates whether the two trips to/from the train stations are longer (shorter) than a direct trip.

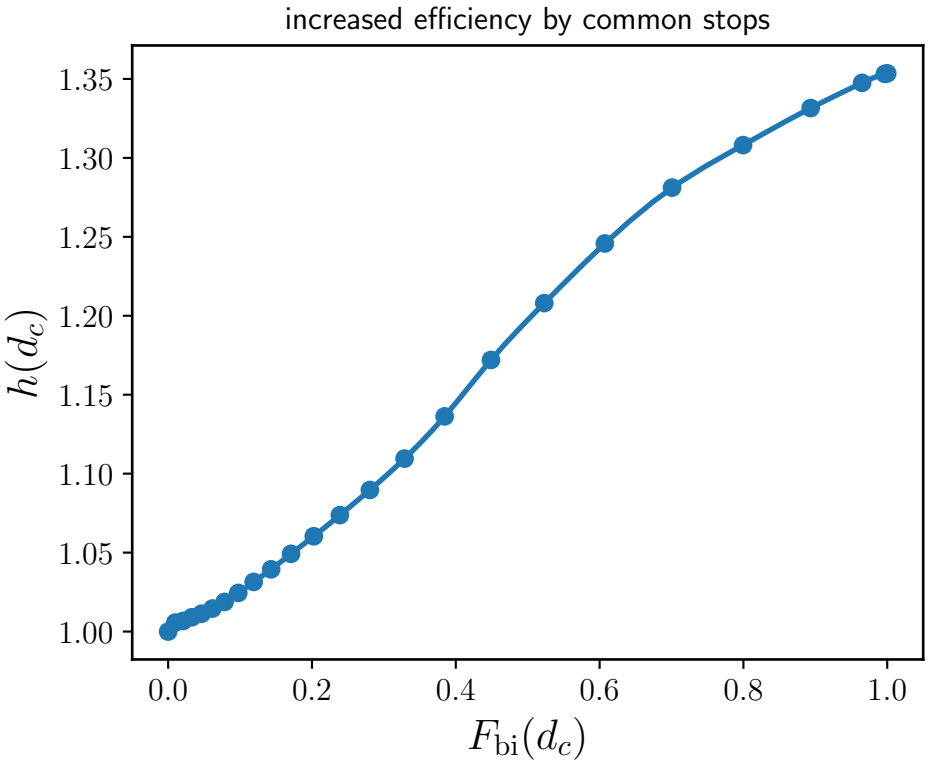

Figure 1: $h(F(\boldsymbol{d}_c))$ as a function of $F(\boldsymbol{d}_c)$. The 'common stop effect' is maximal for $F = 1$, this is when all trips are served by bi-modal transport and all trips have either common origin or destination.

Note that only shuttles contribute to $\Delta\mathcal{E}$ because a single user request is assumed to have no effect on train operations.

5. Dependence of train speed on inter-station distance.

Trains are assumed to have a maximum operating speed of v_m, acceleration and deceleration time t_a and a stop time of t_s at every station. The effective average train speed is therefore

$$v_{\text{train}} = \begin{cases} \frac{\ell}{\frac{\ell}{v_m}+t_a+t_s}, & \text{if } \ell \geq v_m \cdot t_a \\ \frac{\ell}{2\sqrt{\frac{t_a}{v_m}}+t_s}, & \text{otherwise} \end{cases} . \tag{8}$$

For New York, we use $v_m = 89\,\text{km/h}$ and $v_{\text{train}} = 28\,\text{km/h}$ (3) at $\tilde{\ell} = 0.28$ (see Tab. 1 in the main text). We use Eq. 8 to determine t_a and t_s by assuming that $t_a = t_s$. Similarly, for Berlin we use $v_m = 72\,\text{km/h}$ and $v_{\text{train}} = 30.7\,\text{km/h}$ (4) at $\tilde{\ell} = 0.32$. For our analysis, we use New York train speed as a proxy for $\Lambda = 10^4$ and Berlin train speed for $\Lambda = \{10^3, 10^2\}$.

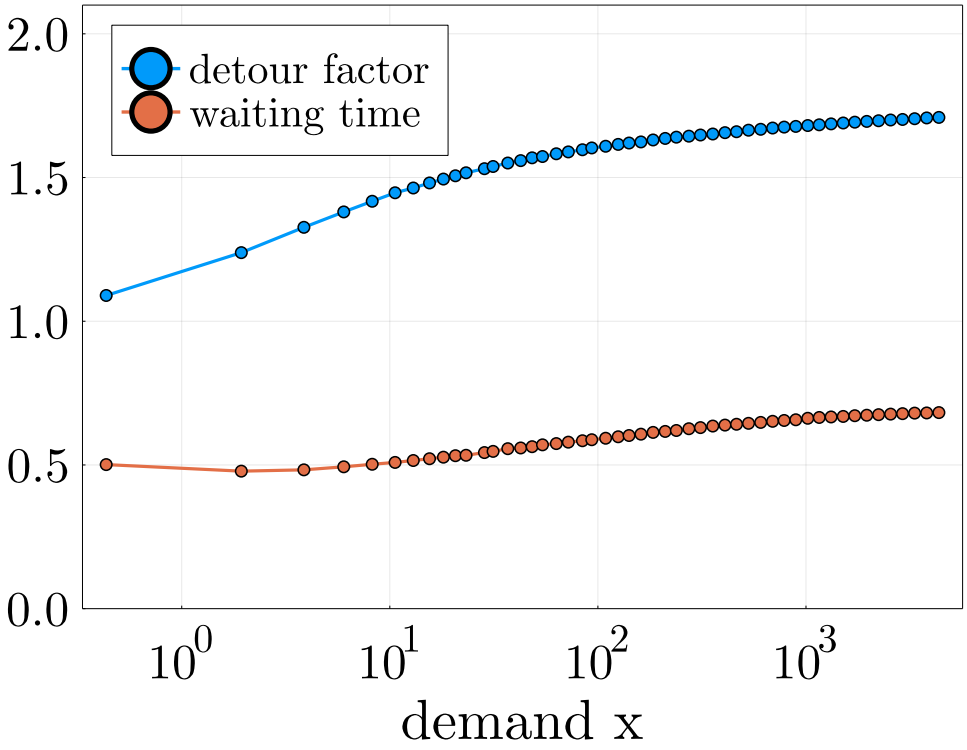

Figure 2: Detour factor (δ) and mean waiting time (τ_w) for various demands.

References

[1] S. Mühle, An analytical framework for modeling ride pooling efficiency and minimum fleet size, under review, 2022.

[2] A. Horni, K. Nagel, K. Axhausen (Eds.), Multi-Agent Transport Simulation MATSim, Ubiquity Press, London, 2016. doi:10.5334/baw.

[3] Wikipedia, https://en.wikipedia.org/wiki/New$_{}$York$_{}$City$_{}$Subway, *accessed* : 26 – 10 – 2022(2022).

[4] Wikipedia, https://en.wikipedia.org/wiki/Berlin$_{U}$ − *Bahn*, *accessed* : 26 – 10 – 2022(2022).

B

Manuscript: Impact of the density of line service stations on overall performance in bi-modal public transport settings

Impact of the density of line service stations on overall performance in bi-modal public transport settings

Abstract

Human mobility is mostly dominated by the use of private cars, leading to disproportionate carbon emissions, resource consumption, traffic jams, and pollution. Public transport, with buses, trains, etc., can mitigate these issues via its higher pooling potential. However, often times, public transport is considered less convenient and is therefore avoided. Here, we study a bi-modal public transport system consisting of a rail bound line service and a fleet of on-demand shuttles providing connections to the line service stops, aiming at fast transit at low energy and resource consumption. By means of agent-based simulations and analytical theory, we demonstrate that bi-modal transit indeed has the potential to significantly reduce energy consumption of human mobility at reasonable service quality. We further investigate the influence of the stop density along the rails upon the performance of the bi-modal system. We find that within a range of realistic technical parameters, additional stops tend to impede train speed without significantly enhancing the overall performance of bi-modal transit in terms of service quality and energy consumption. Hence, it can be beneficial to reduce the number of stops within an existing railway system and to implement bi-modal transit as a complement.

Keywords:
Sustainable public transport, human mobility, ride-pooling, carbon emissions, traffic reduction, agent-based simulations

1. Introduction

Transportation plays a vital role in our society, enabling people to move from one place to another. However, the traditional motorized individual vehicle (MIV, i.e., the private car) used for passenger transportation is highly inefficient, requiring the movement of a ton of material to transport just one person (MacKenzie et al., 2014; Tachet et al., 2017). This wastefulness, causing air pollution (European Environment Agency, 2020; Caiazzo et al., 2013) and other environmental impact (European Environment Agency, 2020; Joireman et al., 2004) as well as traffic congestion (Chin, 1996; Koźlak, Aleksandra and Wach, Dagmara, 2018; Arnott and Small, 1994; Barth and Boriboonsomsin, 2009), highlights the need for more sustainable and efficient transportation solutions.

In stark contrast to MIV, line services can carry hundreds of passengers at a time (e.g., light rails). This makes them an ideal candidate for sustainable public transportation (PT) (Pietrzak, 2019; Ferbrache, 2017; Kato and Kaneko Y. & Soyama, 2014). However, owing to its seemingly higher convenience (Kent, 2013), the MIV dominates the global mobility market (Eurostat, 2022; Fiorello et al., 2016), compared to line services, with their downsides of fixed routes, fixed schedules, and a limited set of fixed stops for accessing and leaving the vehicles.

Demand responsive ride-pooling (DRRP) services, on the other hand, offer flexible routes and schedules by deploying shuttles which pick up and drop off users at the desired locations.

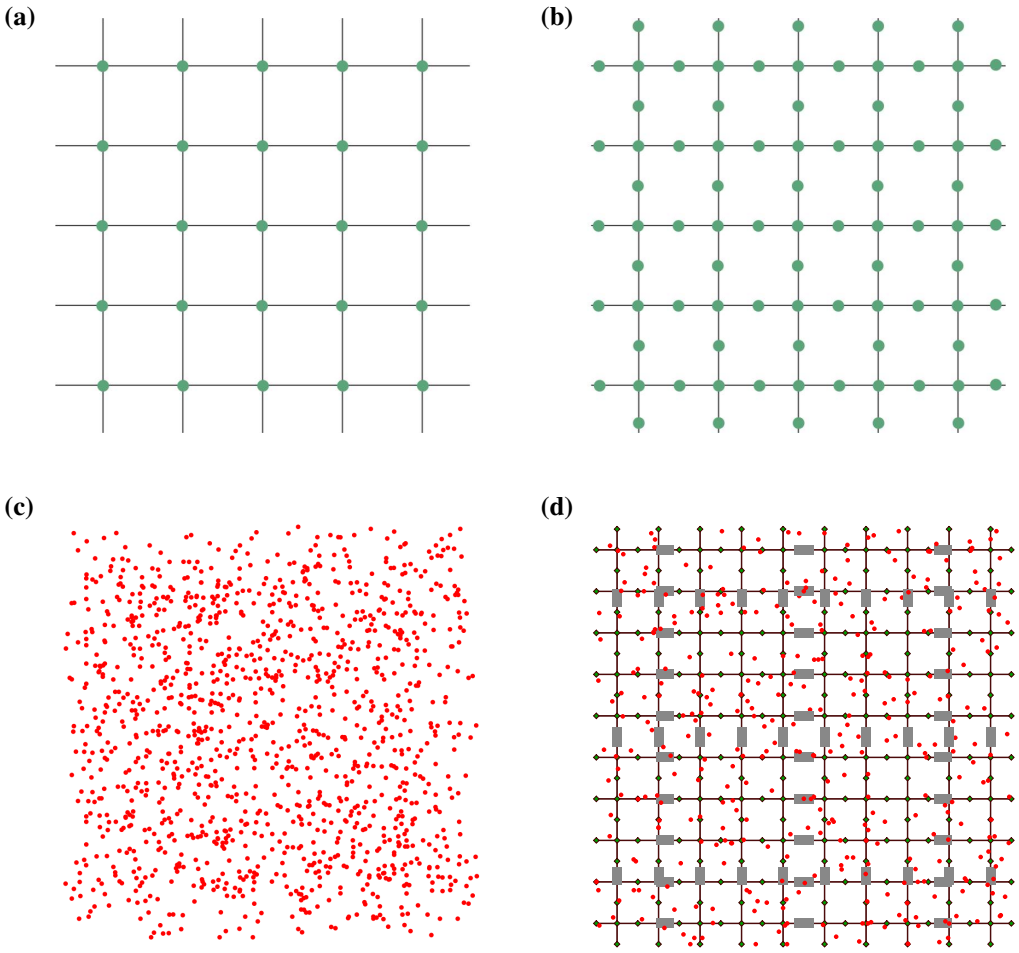

Figure 1: **Bi-modal transport network on a square grid.** **(a)** Idealized line service network. Green nodes at the intersection of railway lines represent the train stations. **(b)** A network as in (a), but with additional (intermediate) stations. **(c)** A snapshot of a simulation where passengers use MIVs (red dots) as the only mode of transportation. **(d)** A snapshot of bi-modal simulations on a network with one intermediate station ($\Theta = 1$). Demand is the same as in (c). Red dots represent shuttles (DRRP), gray rectangles represent trains, green diamonds represent train stations. The number of required shuttles in a bi-modal system (d) is much lower than the number of MIVS required in (c). See Subsec. 3.4 for a quantitative analysis.

Combining individual user requests into an appropriate set of routes of the shuttles (Alonso-Mora et al., 2017), they provide door-to-door transport, similar to the MIV, but at higher occupancy. In such systems, however, users necessarily experience some undesirable detour with respect to the direct route due to the necessity to pick up and drop off other passengers (Herminghaus, 2019; Lobel and Martin, 2020). This trade-off between pooling and detouring severely limits the achievable pooling efficiency (Zwick et al., 2021), and therefore the achievable reduction in traffic and emissions.

A promising solution is bi-modal transport, in which DRRP is combined with line services. Line services, with their fixed routes and schedules, facilitate high vehicle occupancy, while DRRP shuttles provide on-demand transport to and from the line service stops. Additionally, shuttles can serve short distance requests door-to-door, where usage of line services is inefficient. This integration of line services and DRRP has the potential to achieve high pooling efficiency while maintaining user convenience.

In a previous, mean-field based approach, Sharma et al. (2023) identified user convenience and energy consumption as the relevant conflicting objectives for optimization of bi-modal transit. They found that with a diligent choice of system parameters, energy consumption may be reduced to about 20% relative to MIV, and traffic volume to less than 10% relative to MIV. Their findings suggested that bi-modal public transport systems have the potential to outperform customary public transportation as well as MIV in several respects. This appears promising, because most agglomerations have a passenger transport line service system already in place, and DRRP shuttles can be deployed on the streets in between. It therefore suggests itself to study bi-modal transport in a geometry akin to what one finds in real settings, in order to come close to advising authorities and policy makers.

Sharma et al. (2023) adopted a simplified 'cartesian' network as sketched in Fig. 1a, where they assumed line service stations to exist at each crossing. In most cities, however, a line has more stops than crossings with other lines, as sketched in Fig. 1b. The impact of these intermediate stops on the overall performance of the system is hitherto not known. On the one hand, intermediate stops increase the user's proximity to transit stations, resulting in shorter shuttle trips to and from train stations. On the other hand, additional stations slow down the trains, potentially impacting the service quality for longer trips.

In the present paper, we investigate the impact of intermediate stops on bimodal-transit via agent-based simulations. By studying realistic sets of parameters, we aim to provide valuable insights into how the addition of intermediate stops affects factors such as travel time, passenger waiting time, and vehicle occupancy. In addition, we validate the findings of our previous study (Sharma et al., 2023), which were based on a mean-field approach.

We find that 1) intermediate stops reduce average shuttle occupancy, detours, and waiting times. The maximum size of this effect increases with demand. 2) Intermediate stops do not improve overall performance because reduction in quality due to slower trains dominates over slight improvements in energy consumption and traffic volume. 3) With or without intermediate stops, average shuttle occupancy, detours, and waiting times vary significantly with the fraction of bi-modal trips, and increase with demand, in contrast with the assumption of constant waiting times and detours in Sharma et al. (2023). 4) None the less, our agent-based simulations validate the performance potential of bi-modal transit as suggested in Sharma et al. (2023), however, they provide a refined quantitative picture, especially regarding achievable service quality.

In the following, we first introduce the geometry and parameters of the system under consideration (Sec. 2.1). Subsequently, we describe the objectives of optimization and the parameters of operation (Sec. 2.2). We then present results from our simulations and compare them to theo-

retical modeling in Sec. 3. In the results part we discuss performance of DRRP (shuttles) within bi-modal transit (Subsec. 3.1), energy consumption and service quality of bi-modal transit as a whole (Subsec. 3.2), Pareto-optimal solutions (Subsec. 3.3), and potential for traffic reduction (Subsec. 3.4). We end with a discussion of our findings (Sec. 4).

2. Methods

2.1. Definition of the system

For simulating a system of bi-modal transport, with on-demand shuttles and trains operating on lines, we deploy the open-source, multi-agent transport simulation framework, MATSim (Horni et al., 2016). In contrast to the mean-field study by Sharma et al. (2023), where observables like waiting time, vehicle occupancy, or mean detour were estimated by heuristics, in this agent-based framework, transportation requests are served explicitly by individual vehicles (the agents), such that the aforementioned quantities emerge solely based on the user environment and the parameters of operation of the bi-modal transit system. Our methodological contribution lies in the implementation of a bi-modal transit system within an agent-based simulation framework.

To assess the validity of the assumptions, as well as findings on potential reductions in energy consumption and traffic volume in Sharma et al. (2023), we choose the same parameters in our simulations as in Sharma et al. (2023), where applicable. In addition, we introduce intermediate stations between line crossings (see Fig. 1 b) to study the impact of the density of line service stations on the overall performance in bi-modal public transport settings. We refer to Supporting Information for algorithmic details of this framework. In the following we present the characteristic parameters of this model.

User environment. In simulations, we consider a uniformly populated planar region of side length $\mathcal{L} = 20\,\mathrm{km}$, i.e., an area of $\mathcal{A} = 400\,\mathrm{km}^2$, and a total number of transit requests $\mathcal{N}$, uniformly randomly spread over a time $\mathcal{T} = 1\,\mathrm{h}$. Introducing population density E and average request frequency per inhabitant ν, the number of transit requests per time $\mathcal{N}/\mathcal{T} = \nu E \mathcal{A}$. Users are assumed to place transit requests in an uncorrelated fashion, each consisting of a desired pick-up ($\mathcal{P}$) and drop-off ($\mathcal{D}$) location with a requested distance $d = \overline{\mathcal{P}\mathcal{D}}$ following a distribution $p(\cdot)$[1]. As average requested distance we choose $D = 5\,\mathrm{km}$ in simulations. We define D as the intrinsic length scale of our system. Shuttles and MIV are assumed to have a characteristic road vehicle velocity, v_0, which we choose to be $30\,\mathrm{km/h}$ in simulations. We can thus obtain the intrinsic time scale[2] $t_0 = D/v_0 = 10\,\mathrm{min}$. This is the average time a travel request would need to be completed by MIV[3]. We denote (non-dimensional) variables measured in these units (D, t_0) with the $\tilde{}$ symbol. The demand of transport within the system can be characterized by the dimensionless parameter $\Lambda = \frac{\mathcal{N} D^3}{\mathcal{A}\mathcal{T} v_0} = \tilde{\nu}\tilde{E}$, which measures the number of requests for transport in an area of D^2 during time D/v_0 (Sharma et al., 2023). Typical values range from $\Lambda = 10^2$ to 10^4 for rural up to dense urban transportation scenarios (Sharma et al., 2023).

[1] We are using the inverse-gamma distribution as it has been observed in NYC, for example (Herminghaus, 2019).

[2] Introduction of intrinsic length and time scales, D and t_0, as units reduces the number of parameters by two.

[3] $D = 5\,\mathrm{km}$ is at the lower end of typical values for cities/regions and $v_0 = 30\,\mathrm{km/h}$ is at the upper end (see table in Sharma et al. (2023)), leading to a comparatively short estimate for the average driving time by car.

Bi-modal transit system. We distinguish two types of train stations. Train stations at railway intersections are called junction stations. They are separated by the lattice constant ℓ. Additional train stations are called intermediate stations. The distance between two adjacent train stations along a train line is ℓ'. The number of intermediate stations between two junctions is then $\Theta = \ell/\ell' - 1$. All train stations (intermediate and junction) serve as the connection points between DRRP and line service (see Fig. 1b). We restrict our analysis to values of up to three ($\Theta \in \{0, 1, 3\}$) intermediate stations, motivated by agglomerations like Berlin and New York, where we find about one intermediate stop on average, and only rarely more than two (see Supporting Information for details). We choose a grid of length $\ell = 2\,\mathrm{km}$ (Sharma et al., 2023), since we observed previously that the performance of the system is optimal for $\ell/D \approx 0.4$ across an extensive range of user demand (Sharma et al., 2023). This value is also close to what is found, e.g., for Berlin (Sharma et al., 2023). Therefore, we fix $\ell/D = 0.4$ throughout this study.

The trains operate along orthogonal lines from source to end, the first and the last station of the transit network line in the direction of travel (see Fig. 1). The trains arrive at stations with a frequency $\mu = 1/10\,\mathrm{min}^{-1}$ (as in metropolitan regions like Berlin (S-Bahn Berlin, 2023)) and travel at an average speed v_{train}. We assume that trains attain a maximum speed of $3 \cdot v_0$ and the time taken to reach this speed starting from rest is assumed to be $0.05 \cdot t_0$. The trains stop at each connecting station for $0.05 \cdot t_0$. These values are inspired from real data (see Supporting Information for details) and are equal to the ones in Sharma et al. (2023). Note that due to these factors, the effective train velocity, v_{train}, depends on the inter-station distance ℓ'. Trains require energy e_{train} per unit distance of travel.

The transit system is further characterized by a number of shuttles, $\mathcal{S}$, in the plane. For the sake of conciseness and simplicity, we assume that the number of shuttles $\mathcal{S}$ is just sufficient to serve all user requests emanating in the system over time $\mathcal{T}$. Shuttles require energy e_{shuttle} per unit distance of travel. User requests served by DRRP/shuttles are subject to the constraint that the maximum accepted detour (traveled distance / direct distance) is $\delta_m = 3$, the maximum waiting time is $\tau_{w,\max} = 5\,\mathrm{min} = 0.5 \cdot t_0$ and the maximum travel time is $\alpha \cdot t_{\mathrm{direct}} + \gamma$, where $\alpha = 3$, $\gamma = 10\,\mathrm{min}$ are simulation parameters and t_{direct} is the direct travel time[4]. Requests are assigned to feasible shuttles so as to minimize the total distance driven by the shuttles.

We let trains and DRRP operate for a time $2\mathcal{T} = 2\,\mathrm{h}$ in order to ensure that all user requests are served during simulation time.

2.2. Parameters and objectives of operation

Choosing the type of transport service. A single user in the model system may either be transported by uni-modal service, i.e., by shuttle (DRRP) only, or by bi-modal service, i.e., be brought from $\mathcal{P} = (x_p, y_p)$ to the nearest train station by means of a shuttle, followed by a train journey, which is again followed by a shuttle journey to $\mathcal{D} = (x_d, y_d)$. It is the task of the dispatcher system to decide, for each individual request $(\mathcal{P}, \mathcal{D})$, whether the desired door-to-door service should be completed by uni-modal transportation (shuttles only) or bi-modal transportation (shuttle-train(s)-shuttle). Sharma et al. (2023) showed that the requested travel distance, $d = |\overline{\mathcal{P}\mathcal{D}}|$, irrespective of the direction of travel, may serve as a reasonable discriminating parameter. Therefore, in order to choose the mode of transportation for an individual user request, we adhere to the previous policy (Sharma et al., 2023) of assigning user requests with travel distance $d > \boldsymbol{d}_{\mathrm{c}}$ to bi-modal transportation (shuttle-train(s)-shuttle). Shorter trips, i.e., user requests

[4]For the mean-field theory, Sharma et al. (2023) require averages, they assume $\langle\delta\rangle = \delta_m/2$ and $\langle\tau_w\rangle = \tau_{w,\max}/2$.

with travel distance $d \leq \boldsymbol{d}_\mathrm{c}$, are assigned to uni-modal transportation (shuttle only). The cut-off distance, $\boldsymbol{d}_\mathrm{c}$, is the control parameter we will use to optimize the performance of the system. It is in one-to-one correspondence to the fraction of bi-modal transportation $F(\boldsymbol{d}_\mathrm{c}) = \int_{\boldsymbol{d}_\mathrm{c}}^{\infty} p(x)\,dx$, with $p(\cdot)$ the probability density of requested distances.

Service quality. We define the service quality as the ratio between the average travel times by MIV and bi-modal transit, respectively,

$$Q = \frac{t_0}{(1-F)\cdot t_\mathrm{uni} + F \cdot t_\mathrm{bi}}\,, \tag{1}$$

where $F = F(\boldsymbol{d}_\mathrm{c})$ is the fraction of requests served by bi-modal transportation.

To compute the average travel time by MIV for a simulated scenario, we perform independent simulations where the MIV is the only allowed mode of transportation. If t_i^MIV represents the travel time for user i, then t_0 can be obtained by averaging over all users in the system, i.e., $t_0 = 1/\mathcal{N}\sum t_i^\mathrm{MIV}$. Similarly, we compute the denominator in Eq. 1, from simulations by averaging over all users in the system.

In a mean-field approach, Sharma et al. (2023) derived an analytical expression for Q as

$$Q^{-1} = (1-F)\cdot \underbrace{\left(\tilde{\tau}_w + \delta\langle\tilde{d}\rangle_{\tilde{d}\leq\tilde{\boldsymbol{d}}_\mathrm{c}}\right)}_{\tilde{t}_\mathrm{uni}} + F\cdot \underbrace{\left(2\tilde{\tau}_w + 2\beta\tilde{\ell}\delta + \frac{1}{\tilde{\mu}} + \frac{4}{\pi}\frac{\langle\tilde{d}\rangle_{\tilde{d}>\tilde{\boldsymbol{d}}_\mathrm{c}}}{\tilde{v}_\mathrm{train}}\right)}_{\tilde{t}_\mathrm{bi}}. \tag{2}$$

The $\tilde{}$ indicates quantities non-dimensionalized via division by the respective unit (D, t_0, and v_0 as units for length, time, and velocity, respectively). $\langle\tilde{d}\rangle_{\tilde{d}>\tilde{\boldsymbol{d}}_\mathrm{c}}$ is the mean of requested distances larger than $\boldsymbol{d}_\mathrm{c}$ and δ is the average detour incurred by a user during the DRRP trip, $\tilde{\tau}_w$ is the average waiting time for shuttles and $\tilde{\mu}$ the train frequency. $\beta = \frac{1}{6}(\sqrt{2} + \log(1+\sqrt{2})) \approx 0.383$ is a geometrical constant, and $4\pi^{-1}\langle\tilde{d}\rangle_{\tilde{d}>\tilde{\boldsymbol{d}}_\mathrm{c}}$ is the average distance traveled on trains.

Energy consumption. To assess the overall energy consumption by the bi-modal transportation system, we define the dimensionless energy consumption $\mathcal{E}$ as the ratio of total energy consumed by bi-modal transportation and a fleet of MIV, mathematically, $\mathcal{E}$ can be written as

$$\mathcal{E} \equiv \frac{\Delta_\mathrm{shuttle}\cdot e_\mathrm{shuttle} + \Delta_\mathrm{train}\cdot e_\mathrm{train}}{\Delta_\mathrm{MIV}\cdot e_\mathrm{MIV}}\,, \tag{3}$$

where $\Delta_\cdot$ denotes the (mode-specific) total distance traveled in a unit cell of area ℓ^2 per unit time. $e_\cdot$ is the vehicle-specific energy consumption per unit distance. Note that $\mathcal{E}$ is already normalized with respect to the MIV energy consumption (denominator), as this is the door-to-door transportation system we intend to compare with. For $\mathcal{E} > 1$ (< 1), energy requirement for bi-modal transportation is larger (smaller) than for MIV serving the same requests.

Both, uni-modal (shuttle only) and bi-modal trips, contribute to the total distance driven by shuttles per unit time due to requests from a unit cell of area ℓ^2, hence

$$\Delta_\mathrm{shuttle} = \frac{\nu E\ell^2}{\eta}\left(\underbrace{\langle d\rangle_{d<\boldsymbol{d}_\mathrm{c}}(1-F)}_{\text{shuttle only}} + \underbrace{2\beta\ell F}_{\text{two shuttle trips}}\right), \tag{4}$$

where η is the DRRP pooling efficiency, which is the ratio of direct distance requested by the users and the distance actually driven by the shuttles (for MIV, $\eta = 1$). Mühle (2023) has observed that η scales with demand Λ roughly in an algebraic manner, $\eta(\Lambda) \approx \Lambda^{\gamma}$, with $\gamma \approx 0.12$. In a bi-modal system, however, some of the demand Λ is directed towards trains. Therefore, we need to compute an adjusted demand, $\Lambda_{\text{shuttle}} \equiv (E\nu_{\text{shuttle}} D_{\text{shuttle}}^3)/v_0$, considering shuttle trips only. ν_{shuttle} is the effective request frequency for shuttle trips and D_{shuttle} is the average distance of a shuttle trip. One can show that (Sharma et al., 2023)

$$\Lambda_{\text{shuttle}} = \Lambda\,(1+F)^{-2}((1-F)\langle\tilde{d}\rangle_{\tilde{d}\leq\tilde{d}_c} + 2\beta\tilde{\ell}F)^3\,. \tag{5}$$

We compute the theoretical pooling efficiency, η, according to the power law mentioned above

$$\eta \equiv \Lambda_{\text{shuttle}}^{0.12}\,. \tag{6}$$

The distance travelled per unit cell by line service, Δ_{train}, remains constant throughout our study because trains operate at a constant frequency μ, mathematically,

$$\Delta_{\text{train}} = 4 \cdot \mu \cdot \ell\,. \tag{7}$$

Δ_{MIV} is the total distance requested by users per unit time,

$$\Delta_{\text{MIV}} = \nu E \ell^2 D\,. \tag{8}$$

Analytically, Eq. 3 can then be written as

$$\mathcal{E} = \underbrace{\eta^{-1}\left(\langle\tilde{d}\rangle_{\tilde{d}\leq\tilde{d}_c}(1-F) + 2\beta\tilde{\ell}F\right)\cdot\frac{e_{\text{shuttle}}}{e_{\text{MIV}}}}_{\text{shuttles}} + \underbrace{\frac{4\tilde{\mu}}{\Lambda\tilde{\ell}}\cdot\frac{e_{\text{train}}}{e_{\text{MIV}}}}_{\text{train}}\,. \tag{9}$$

In analogy to Sharma et al. (2023), we consider electric light rails with a maximum seating-capacity $k = 100$ and $e_{\text{train}} = 9.72\,\text{kN}$ (Knörr et al., 2016) for the line service. For MIV we consider Diesel cars with $e_{\text{MIV}} = 2.47\,\text{kN}$ (BMDV, 2022). For the shuttles we choose Mercedes Sprinter (8.8 liters of Diesel per 100 km (Mercedes-Benz, 2022)), resulting in $e_{\text{shuttle}} = 3.28\,\text{kN}$.

In order to compute the ratio above in Eq. 3 for a simulated scenario, we perform independent simulations for MIV and bi-modal transit with identical user requests. The denominator in Eq. 3 is obtained from MIV simulations by multiplying the total driven distance by e_{MIV}. The numerator in Eq. 3 is obtained from bi-modal simulations by multiplying mode-specific total driven distance[5] with the respective vehicle-specific energy consumption per unit distance.

3. Results

We organize our results as follows. First we present how DRRP performs within a bi-modal system in Subsec. 3.1. Then we characterize the overall performance of bi-modal transit systems in terms of energy consumption and service quality in Subsecs. 3.2 and 3.3. We conclude the results section with an analysis of potential reductions in traffic volume (Subsec. 3.4).

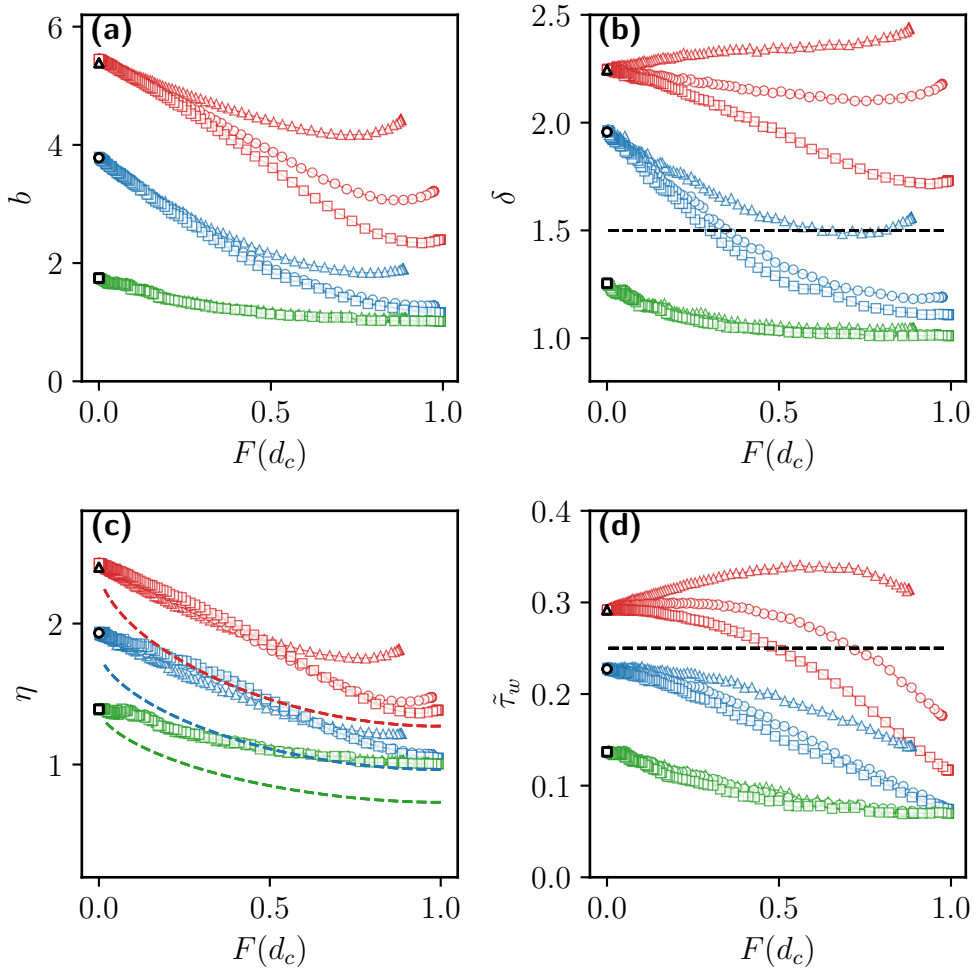

Figure 2: **DRRP performance statistics:** DRRP/Shuttle performance parameters are plotted against bi-modal fraction F. Green, blue and red curves represent $\Lambda = \{13.7, 123, 1201\}$, respectively. Triangles, circles and squares represent $\Theta = \{0, 1, 3\}$, respectively, for all colors. Black square, circle and triangle represent uni-modal transport (shuttles only) **(a)** Mean DRRP occupancy for non-standing vehicles, b. **(b)** Mean detour, δ, for shuttle users. Black dashed curve represents the detour assumed for theory (Sharma et al., 2023). **(c)** Mean DRRP pooling efficiency $\eta \equiv b/\delta$. Dashed curves represent the theoretical data for pooling efficiency, as determined by Eq.6. **(d)** Mean waiting time, $\tilde{\tau}_w$, for shuttles normalized with t_0. Black dashed curve represents the assumed value for theory (Sharma et al., 2023).

3.1. DRRP performance

Occupancy. Fig. 2a shows the mean DRRP occupancy averaged over driving vehicles, namely b, against the bi-modal fraction, F, for various numbers of intermediate stations, Θ, and demands, Λ. We observe that shuttles generally have a higher mean occupancy for large demands because of the greater possibility of pooling. Mean occupancy is observed to decrease with the involvement of trains (increasing F) because trips by shuttles are shortened, resulting in passengers spending less time in shuttles during their transit. We also observe a general trend of decreasing mean occupancy with more intermediate stations, because trips by shuttles for the users assigned to bi-modal transportation become 1) more dispersed and 2) shorter due to the higher number and proximity of train stations, therefore providing less opportunity for pooling.

Detours. From Fig. 2b, the general trend of increasing detour with demand is evident. This trend, together with the trend for mean occupancy, b, in Fig. 2a, shows the well known trade-off between detour and pooling for DRRP, i.e., desirable pooling necessitates undesirable detours for passengers (Herminghaus, 2019). A trend of decreasing detours with increasing involvement of line services (increasing F) can be attributed to a 'common stop effect', that is, passengers are picked up or dropped off at the same train station, thereby reducing detours. We also observe a trend of decreasing detours with more intermediate stations which is due to the lower potential for pooling due to shorter trips, as well as a reduced 'common stop effect'.

Notice that the black dashed curve represents the assumed value of $\delta = 1.5$ for the theoretical analysis (Sharma et al., 2023). We observe in Sec. 3.3, that this assumption does not severely impact the agreement between the theoretical and simulated overall performance of the system.

Pooling efficiency. The ratio between mean occupancy and mean detour, shown in Fig. 2c, provides a reasonable estimate for pooling efficiency, η (Mühle, 2023), which is defined as the ratio of requested direct distance by the users and driven distance by the shuttles (for MIV, $\eta = 1$). In Fig. 2c, we observe a general trend of increasing pooling efficiency, η, with demand, which suggests that deploying shuttles in a region with high demand is favourable. Involvement of line services decreases the DRRP pooling efficiency because user requests are diverted toward the lines, thus shortening the average distance a passenger travels on the shuttle during the entire journey. We observe that the effect of intermediate stations on η is mostly insignificant, except for higher demand at large bi-modal fraction, F.

The dashed curves represent the theoretical prediction for pooling efficiency, determined by Eq. 6, which follows a trend similar to the simulations. We observe that the theoretical data underestimates the pooling efficiency when compared with the simulation data. This underestimation can be attributed to the 'common stop effect' mentioned earlier, which is not accounted for in theoretical predictions in Eq. 6.

Waiting time. In Fig. 2d, we study the mean waiting time for trips with shuttles. Mean waiting time normalized with the average trip duration, t_0, is plotted against bi-modal fraction F. The black dashed curve represents the assumed value for the theoretical study (see Supporting Information for details). We observe a trend of increasing waiting time for higher demands because shuttles become busier. Involvement of line services generally decreases the waiting time for trips with shuttles because of the 'common stop effect' and a lower share of distance travelled in

[5]Note that we only consider the total distance that trains drive during the time interval $\mathcal{T}$.

shuttles. The latter holds, too, for more intermediate stations, thus explaining the lower waiting time for larger Θ.

In summary, the main messages from Fig. 2 are: 1) Shuttles become more efficient with demand, while user experience suffers due to larger detours and waiting times. 2) Intermediate stations enhance the user experience due to shorter detours and waiting times. The effect on pooling efficiency is insignificant. 3) Trips with shuttles become more convenient for users with involvement of line services due to reductions in waiting time and detours.

3.2. Overall energy consumption and service quality of bi-modal transit

We now analyze the overall objectives, i.e., energy consumption (Eq. 3) and service quality (Eq. 1) of the combined bi-modal system.

Energy consumption. In Fig. 3a, relative energy consumption, $\mathcal{E}$, is plotted as a function of bi-modal fraction, F, for various numbers of intermediate stations, Θ. We observe a general trend of decreasing energy consumption with involvement of line services. This is because Δ_{shuttle} decreases with involvement of line services (see Fig. 4a) while Δ_{train} is constant due to a constant service frequency μ, thus decreasing the total energy consumption by the bi-modal system (see Eq. 3). We observe that the relative energy consumption is reduced with increasing demand, Λ, as is evident from the direct contribution in Eq. 9, as well as via the enhanced pooling efficiency, η (see Fig. 2c). Fig. 3a reveals that the energy consumption can be lower than 25% of the energy consumption for MIV for demands in large cities like Berlin ($\Lambda \approx 5 \cdot 10^3$, Sharma et al. (2023)). Energy consumption is observed to decrease slightly with increasing number of intermediate stations, because the normalized distance driven by shuttles is reduced (see Fig. 4a). We find reasonable agreement between theoretical data (Eq. 9) and simulations.

Quality. In Fig. 3b, we plot the overall quality of the system against the bi-modal fraction, F. We observe that Q is non-monotonic in F. This is due to the competing effects of decreasing waiting time for shuttles with more involvement of trains (see Fig. 2d), on the one hand, and additional waiting time for trains at the train stations for a larger user fraction (F), on the other hand.

We observe that the overall service quality, Q, decreases with demand, which is due to the trend we observed for waiting times for trips with shuttles in Fig. 2d.

The dashed black curve represents the theoretical predictions determined by Eq. 2. Notice that the theoretical prediction for quality does not depend on the demand because the train frequency μ is maintained at a constant value of 0.1 min^{-1} across all demands (see Subsec. 2.1). The difference between theory and simulation data primarily stems from the waiting time of shuttles, which we approximated as $0.25\, t_0$ in our theory, for all demands (see Supporting Information for motivation). However, we see in Fig. 2d that the waiting time varies with demand, bi-modal fraction and number of intermediate stations.

In Fig. 3b, we observe that the overall service quality of the combined bi-modal system decreases with more intermediate stops, despite a trend of decreasing waiting times and detours for trips with shuttles (see Figs. 2b, d). Apparently, this trend is dominated by a slowing down of trains due to intermediate stations, which increases the average trip duration.

The general trend of reduction in consumption of energy with increasing demand and involvement of line services hints towards the merit of bi-modal transportation for high-demand scenarios. For service quality, we find that typical values are around one-half the service quality of MIV, i.e., about twice the travel time. This quality is customary for public transport systems

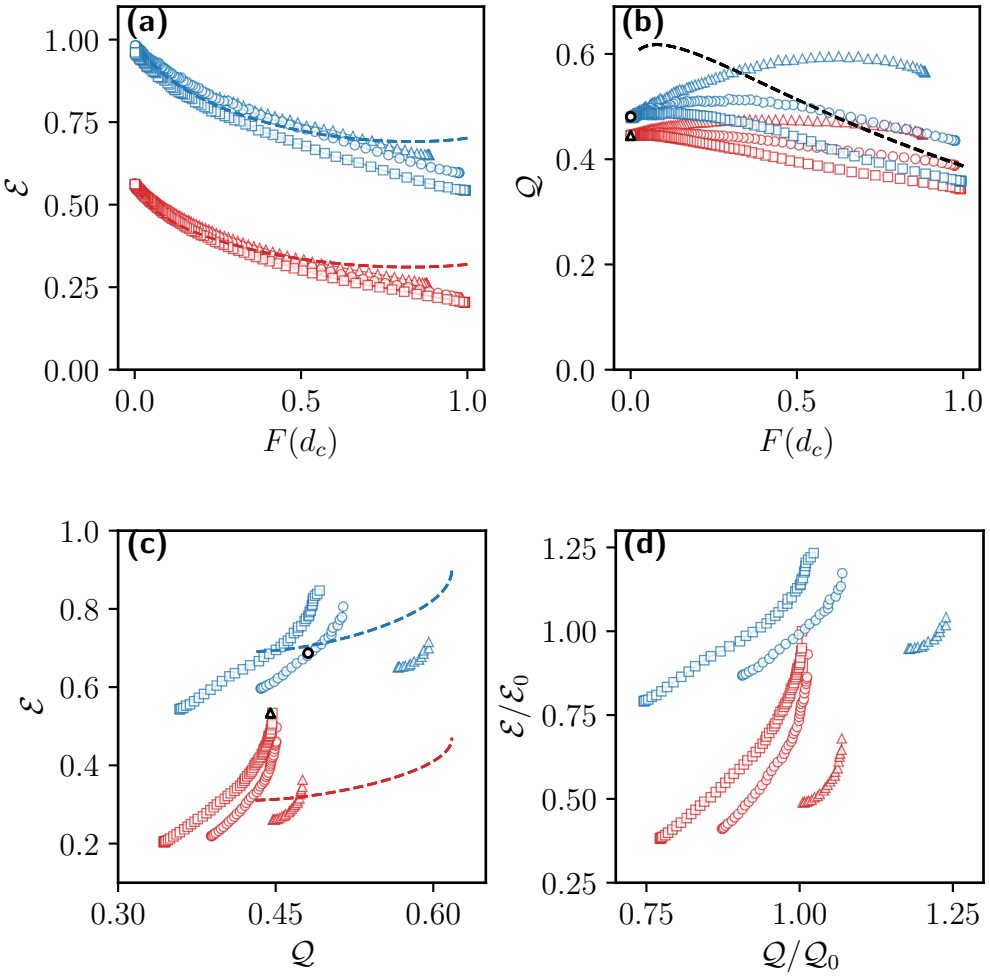

Figure 3: **Effect of intermediate stations on the overall performance of bi-modal transit:** The bimodal fraction F has been varied in the range [0,1) in simulations to obtain the data shown. Blue and red curves represent data for $\Lambda = \{123, 1201\}$, respectively. Triangles, circles and squares represent $\Theta = \{0, 1, 3\}$, respectively. **(a)** Energy consumption, $\mathcal{E}$, as a function of F. The dashed curves represent the theoretical data determined by Eq. 9. **(b)** Quality, $\mathcal{Q}$, as a function of F. Black dashed curve represents the theoretical data determined by Eq. 2. Notice that the theoretical data for quality is assumed the same across all demands. **(c)** Pareto fronts of energy consumption, $\mathcal{E}$, vs. service quality, $\mathcal{Q}$ determined from the data shown in (a), (b). Data not part of Pareto fronts is not shown. The dashed curves represent the theoretical data as in (a), (b). Black circle and triangle represent uni-modal transport (shuttles-only) data for $\Lambda = \{123, 1201\}$, respectively. **(d)** Pareto fronts as in (c), but normalized with respect to the performance, $(\mathcal{Q}_0, \mathcal{E}_0)$, of the uni-modal system (shuttles only).

(Salonen, 2013; Liao et al., 2020) and is generally well accepted by users. Note that our data for service quality represent a safe lower bound, as the (sometimes quite substantial) time required for parking spot search (Fulman and Benenson, 2021; Chaniotakis and Pel, 2015) is neglected in t_0.

We observe that service quality attains a maximum for a bi-modal fraction, F, where energy consumption is not minimal. Jointly optimizing such conflicting objectives can be done in the framework of Pareto optimization, which we will discuss next.

3.3. Pareto optimization

A tuple of parameter values, in our case $(\mathcal{E}, Q)$, is called Pareto-optimal if none of the parameters (or objectives) can be further optimized without compromising on at least one of the others. The set of all such tuples of parameters is called the Pareto front (Debreu, 1959; Greenwald and Stiglitz, 1959; Magill and Quinzii, 2002). We now apply this concept to our results, keeping in mind that we aim at maximum service quality at minimum energy consumption. Hence, in diagrams spanned by Q as the abscissa and $\mathcal{E}$ as the ordinate, system operation as far as possible to the lower right is desirable.

In order to study the effect of density of line service stations on the overall performance of the bi-modal transit system, we have introduced $\Theta = \{0, 1, 3\}$ as the number of intermediate stations. For $\Theta = 0$, transit stops are only at the intersection between two transit lines. For each value of Θ, we vary $\boldsymbol{d}_\mathrm{c}$ to obtain the Pareto fronts.

In Fig. 3c, we show the Pareto fronts obtained for data in Figs. 3a, b. Note that for a better resolution of the curves, we only show the data for $\Lambda = \{123, 1201\}$. We observe that intermediate stations reduce the energy consumption to as low as 20% of MIV for larger demand. However, the service quality is worsened due to reduced average speed of trains. Black triangle and circle represent the data for the uni-modal system (shuttles only), and dashed curves represent the theoretical estimates. We observe a fair agreement between previous theoretical estimates and simulation results for the overall performance of the bi-modal system. Discrepancies mainly result from the simplifying assumptions for mean waiting time, $\tilde{\tau}_w$ and detour, δ, as described in Subsec. 3.1.

In Fig. 3d, the same Pareto fronts as in Fig. 3c are plotted normalized with respect to energy consumption and service quality of a uni-modal system, $(\mathcal{E}_0, Q_0)$. We observe that the bi-modal system can provide a service quality superior to a uni-modal (shuttles only) system with a lower energy consumption. This observation holds for both demand values presented.

3.4. Traffic volume

Road traffic is a source of local noise and air pollution and occupies significant shares of urban space. Bi-modal transit aims at reduction of road traffic by utilizing line services for trips over larger distances. Fig. 1c and Fig. 1d provide qualitative evidence by comparing abundance of MIV and shuttles for the same request pattern.

To obtain a quantitative estimate, we define as bi-modal traffic volume, $\tilde{\Delta}_\mathrm{shuttle}$, the cumulative distance driven by shuttles, Δ_shuttle (Eq. 4), normalized with respect to the equivalent of total MIV distance requested, Δ_MIV (Eq. 8), or, equivalently, the relative number of driving shuttles as compared to MIV. For our theoretical estimates, we use the analytical expression,

$$\tilde{\Delta}_\mathrm{shuttle} \equiv \Delta_\mathrm{shuttle}/\Delta_\mathrm{MIV} = \eta^{-1}\,(1+F)\,\tilde{D}_\mathrm{shuttle}\,, \tag{10}$$

with pooling efficiency, η, bimodal fraction, F, and average requested distance for trips by shuttles involved in bi-modal transit, $\tilde{D}_{\text{shuttle}}$.

In Fig. 4a, we plot bi-modal traffic in simulations on a vertical logarithmic axis as a function of bi-modal fraction for various demands and number of intermediate stations. Dashed curves represent the theoretical data (Eq. 10) for an idealized square grid network without any intermediate stops ($\Theta = 0$).

We observe a trend of decreasing bi-modal traffic with involvement of line services, i.e., with increasing F. Also, $\tilde{\Delta}_{\text{shuttle}}$ decreases with increasing demand, because shuttles become more efficient due to the possibility of larger pooling (see also Fig. 2c). We furthermore observe that, for low demand, bi-modal traffic decreases with more intermediate stations. This is despite an insignificant impact on pooling efficiency, η (see Fig. 2c). It is rather the reduced average requested distance for trips with shuttles, $\tilde{D}_{\text{shuttle}}$, due to increased proximity of train stations, which accounts for the reduced traffic volume (see Eq. 10).

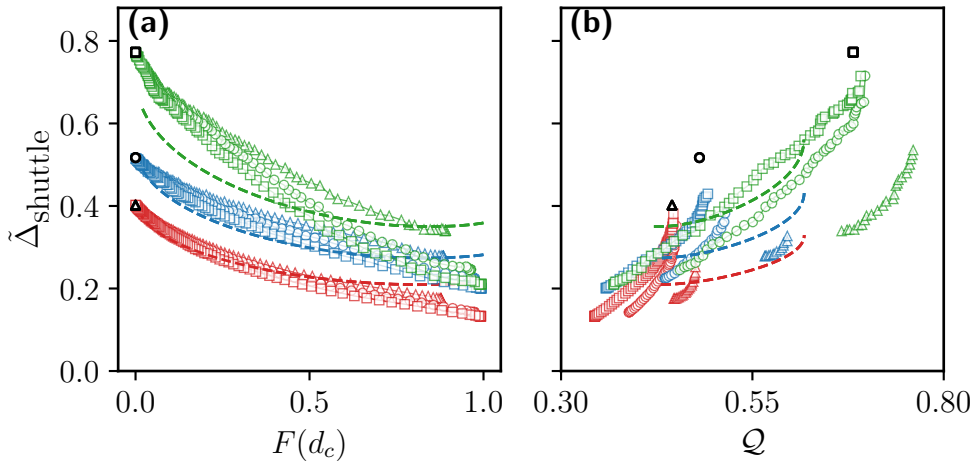

Figure 4: **Impact of intermediate stations on traffic volume.** Green, blue and red curves represent $\Lambda = \{13.7, 123, 1201\}$, respectively. Triangles, circles and squares represent $\Theta = \{0, 1, 3\}$, respectively. **(a)** Relative bi-modal traffic in simulations, $\tilde{\Delta}_{\text{shuttle}}$, as defined in Eq. 10, as a function of the bi-modal fraction, F. Black square, circle, and triangle represent uni-modal transport (shuttles-only) data for $\Lambda = \{13.7, 123, 1201\}$, respectively. Dashed curves represent the theoretical data, determined by Eq. 10. **(b)** Relative bi-modal traffic in simulations, $\tilde{\Delta}_{\text{shuttle}}$, determined along the Pareto fronts in Fig. 3, against corresponding service quality $\mathcal{Q}$. Dashed curves and black symbols represent the theoretical and uni-modal data, respectively, as in (a).

In Fig. 4b, we plot the relative bi-modal traffic volume, $\tilde{\Delta}_{\text{shuttle}}$, for simulations on a vertical axis, determined along the Pareto fronts in Fig. 3c, against corresponding service quality $\mathcal{Q}$. The traffic volume for uni-modal (shuttle-only) scenarios is plotted with black symbols. We observe that the relative traffic volume for uni-modal scenarios decreases with demand due to increased pooling efficiency, η (see Fig. 2c). The relative traffic volume for the uni-modal case can be reduced to 80% of MIV for very low demand and down to 50% and 40% for low and medium demand, respectively.

Bi-modal public transportation allows for further reduction in relative traffic volume below the uni-modal case at a superior service quality. For an idealized square grid without any interme-

diate stations (represented by coloured triangles), bi-modal transportation reduces traffic volume down to about 30% of MIV for very low and low demand and even below 20% for medium demand. Intermediate stops allow for further reduction in traffic. This reduction, however, comes at the cost of reduced service quality. Due to computational limitations, we could only simulate scenarios with the demand of the order of $\Lambda = 10^3$. However, the demand can be as high as 10^4 for very dense areas like New York. Earlier findings suggest that bi-modal public transportation can reduce traffic in such areas even below 10% of MIV (Sharma et al., 2023).

4. Discussion

Our investigation had two primary goals. First, to study the impact of the number of intermediate line service stops on the performance of bi-modal public transport systems. Second, to evaluate the analytical framework proposed by Sharma et al. (2023) through simulations. The parameters investigated in our study drew inspiration from real-world agglomerations. The grid constant $\tilde{\ell} = D/\ell = 0.4$ in our model is close to what is found for, e.g., New York and Berlin. Other technical parameters, including shuttle speed (v_0) and train speed (v_{train}) have been carefully chosen to reflect the observed real-life environments (see Subsec. 2.1).

Below, we first discuss the comparison between agent-based simulations and the analytical study by Sharma et al. (2023). Simulations reveal that observables characterizing shuttle performance, namely detour and waiting time, vary with demand, bi-modal fraction and the number of intermediate stops, in contrast to the constant values assumed by the previous analytical study (Sharma et al., 2023). Furthermore, the previous analytical study approximated the pooling efficiency using an algebraic power-law (see Eq. 6), which underestimated the actual pooling efficiency due to a 'common stop effect' (see Subsec. 3.1). The findings above highlight that shuttle waiting time, detours, and pooling efficiency are complex observables, which, in bi-modal transit, depend on line service operations, and thus must be modeled carefully to assess the performance of bi-modal transit systems accurately.

Adding intermediate stations between line crossings had limited benefits. While there was a marginal reduction in energy consumption and traffic volume, the resulting slowdown of trains made them less suitable as a faster mode of transportation than MIVs and shuttles, i.e., lead to substantial reduction of service quality.

It should be noted that the network structure employed in our research, although inspired by real-world urban agglomerations, is still a simplified representation. Future studies should consider more complex and realistic network typologies to capture the nuances of different urban environments and evaluate the generality of our findings. Moreover, realistic demand patterns, like rush hours and spatial commuting patterns can be included.

In summary, our study confirms that bi-modal transit can provide door-to-door service with satisfactory service quality while consuming only a fraction of the energy required by an equivalent fleet of MIVs, and significantly reducing road traffic volume. These advantages hold for low-demand regions as well as medium-sized cities. Although our simulations were limited to a medium user demand of approximately $\Lambda = 10^3$ due to computational constraints, we anticipate that bi-modal transit would outperform MIVs and uni-modal ride-pooling even more significantly under higher demand conditions, as suggested in previous research (Sharma et al., 2023). It is important to note that our analysis did not consider other MIV-specific drawbacks, such as parking time or traffic congestion during rush hours (Mingardo et al., 2022; Manville and Shoup, 2005; Chaniotakis and Pel, 2015), which would further enhance the relative performance of bi-modal transit.

The findings of this research paper have significant implications for the improvement of public transportation systems. One practical application of these findings is in the design and optimization of line service networks. Public transit authorities and city planners can consider reducing the number of intermediate stops within existing railway systems and complementing on-demand shuttle services to improve the overall performance of public transport. Furthermore, the research suggests that bi-modal transit is not only suitable for high-demand regions but also holds promise for medium-sized cities. As humanity must reduce its carbon footprint, insights from this study can guide the development of more sustainable and efficient public transportation solutions, benefiting both the environment and the quality of life for residents.

References

D. MacKenzie, S. Zoepf, J. Heywood, Determinants of US passenger car weight, Int. J. Veh. Des 65 (2014) 73–93.

R. Tachet, O. Sagarra, P. Santi, G. Resta, M. Szell, S. H. Strogatz, C. Ratti, Scaling law of urban ride sharing, Scientific Reports 7 (2017) 1–6.

European Environment Agency, Air quality in europe — 2020 report, https://www.eea.europa.eu/publications/air-quality-in-europe-2020-report, 2020. Accessed: 2022-05-18.

F. Caiazzo, A. Ashok, I. A. Waitz, S. H. Yim, S. R. Barrett, Air pollution and early deaths in the united states. part i: Quantifying the impact of major sectors in 2005, Atmospheric Environment 79 (2013) 198–208. URL: https://www.sciencedirect.com/science/article/pii/S1352231013004548. doi:https://doi.org/10.1016/j.atmosenv.2013.05.081.

European Environment Agency, Are we moving in the right direction? Indicators on transport and environmental integration in the EU, https://www.eea.europa.eu/ds_resolveuid/0c1c4a6acf289ffdefa1876ea5d60f07, 2020. Accessed: 2022-07-14.

J. A. Joireman, P. A. Van Lange, M. Van Vugt, Who cares about the environmental impact of cars? Those with an eye toward the future, Environment and behavior 36 (2004) 187–206.

A. T. Chin, Containing air pollution and traffic congestion: Transport policy and the environment in singapore, Atmospheric Environment 30 (1996) 787–801. URL: https://www.sciencedirect.com/science/article/pii/1352231095001735. doi:https://doi.org/10.1016/1352-2310(95)00173-5, supercities: Environment Quality and Sustainable Development.

Koźlak, Aleksandra, Wach, Dagmara, Causes of traffic congestion in urban areas. case of poland, SHS Web Conf. 57 (2018) 01019. URL: https://doi.org/10.1051/shsconf/20185701019. doi:10.1051/shsconf/20185701019.

R. Arnott, K. Small, The economics of traffic congestion, American Scientist 82 (1994) 446–455. URL: http://www.jstor.org/stable/29775281.

M. Barth, K. Boriboonsomsin, Traffic congestion and greenhouse gases, Access Magazine 1 (2009) 2–9.

K. Pietrzak, O. & Pietrzak, The role of railway in handling transport services of cities and agglomerations., Transportation Research Procedia 39 (2019) 405–416.

R. D. Ferbrache, F. & Knowles, City boosterism and place-making with light rail transit: A critical review of light rail impacts on city image and quality., Geoforum 80 (2017) 103–113.

H. Kato, Y. Kaneko Y. & Soyama, Economic benefits of urban rail projects that improve travel-time reliability: Evidence from tokyo, japan., Transport Policy 35 (2014) 202–210.

J. Kent, Secured by automobility: why does the private car continue to dominate transport practices?, Ph.D. thesis, UNSW Sydney, 2013.

Eurostat, Passenger mobility statistics, https://ec.europa.eu/eurostat/statistics-explained/index.php?title=Passenger_mobility_statistics#Urban_trips, 2022. Accessed: 2022-09-29.

D. Fiorello, A. Martino, L. Zani, P. Christidis, E. Navajas-Cawood, Mobility data across the eu 28 member states: Results from an extensive cawi survey, Transportation research procedia 14 (2016) 1104–1113.

J. Alonso-Mora, S. Samaranayake, A. Wallar, E. Frazzoli, D. Rus, On-demand high-capacity ride-sharing via dynamic trip-vehicle assignment, Proceedings of the National Academy of Sciences 114 (2017) 462–467.

S. Herminghaus, Mean field theory of demand responsive ride pooling systems, Transportation Research Part A: Policy and Practice 119 (2019) 15–28.

I. Lobel, S. Martin, Detours in shared rides, Available at SSRN 3711072 (2020).

F. Zwick, N. Kuehnel, R. Moeckel, K. W. Axhausen, Ride-pooling efficiency in large, medium-sized and small towns -simulation assessment in the munich metropolitan region, Procedia Computer Science 184 (2021) 662–667. URL: https://www.sciencedirect.com/science/article/pii/S1877050921007195. doi:https://

doi.org/10.1016/j.procs.2021.03.083, the 12th International Conference on Ambient Systems, Networks and Technologies (ANT) / The 4th International Conference on Emerging Data and Industry 4.0 (EDI40) / Affiliated Workshops.

P. Sharma, K. M. Heidemann, H. Heuer, S. Mühle, S. Herminghaus, Sustainable and convenient: Bimodal public transit systems outperforming the private car, Multimodal Transportation 2 (2023) 100083. URL: https://www.sciencedirect.com/science/article/pii/S2772586323000151. doi:https://doi.org/10.1016/j.multra.2023.100083.

A. Horni, K. Nagel, K. Axhausen (Eds.), Multi-Agent Transport Simulation MATSim, Ubiquity Press, London, 2016. doi:10.5334/baw.

S-Bahn Berlin, Route timetables, https://sbahn.berlin/en/plan-a-journey/journey-planner/timetables-by-line/., 2023. Accessed: 2023-10-10.

S. Mühle, An analytical framework for modeling ride pooling efficiency and minimum fleet size, Multimodal Transportation 2 (2023) 100080. URL: https://www.sciencedirect.com/science/article/pii/S2772586323000126. doi:https://doi.org/10.1016/j.multra.2023.100080.

W. Knörr, C. Heidt, S. Gores, F. Bergk, Aktualisierung Daten- und Rechenmodell: Energieverbrauch und Schadstoffemissionen des motorisierten Verkehrs in Deutschland 1960-2035“ (TREMOD) für die Emissionsberichterstattung 2016 (Berichtsperiode 1990-2014) Anhang, Technical Report, 2016.

BMDV, Verkehr in Zahlen 2021/2022, Technical Report, Bundesministerium für Verkehr und digitale Infrastruktur, 2022.

Mercedes-Benz, Mercedez-Benz Configurator, https://voc.mercedes-benz.com/voc/de_de?_ga=2.230012379.695886780.1664812666-1473138929.1664499805, 2022. Accessed:2022-10-03.

T. Salonen, M. & Toivonen, Modelling travel time in urban networks: comparable measures for private car and public transport., Journal of Transport Geography 31 (2013) 143–153.

Y. Liao, J. Gil, R. H. Pereira, S. Yeh, V. Verendel, Disparities in travel times between car and transit: Spatiotemporal patterns in cities, Scientific Reports 10 (2020) 1–12.

N. Fulman, I. Benenson, Approximation method for estimating search times for on-street parking, Transportation Science 55 (2021) 1046–1069.

E. Chaniotakis, A. J. Pel, Drivers' parking location choice under uncertain parking availability and search times: A stated preference experiment, Transportation Research Part A: Policy and Practice 82 (2015) 228–239. URL: https://www.sciencedirect.com/science/article/pii/S0965856415002542. doi:https://doi.org/10.1016/j.tra.2015.10.004.

G. Debreu, Valuation equilibrium and pareto optimum, Proceedings of the National Academy of Sciences 40 (1959) 588–592.

B. Greenwald, J. E. Stiglitz, Externalities in economies with imperfect information and incomplete markets, Quarterly Journal of Economics 40 (1959) 229–264.

M. Magill, M. Quinzii, Theory of incomplete markets, MIT Press, 2002.

G. Mingardo, S. Vermeulen, A. Bornioli, Parking pricing strategies and behaviour: Evidence from the netherlands, Transportation Research Part A: Policy and Practice 157 (2022) 185–197. URL: https://www.sciencedirect.com/science/article/pii/S0965856422000052. doi:https://doi.org/10.1016/j.tra.2022.01.005.

M. Manville, D. Shoup, Parking, people, and cities, Journal of urban planning and development 131 (2005) 233–245.

Supplementary material for the article "Impact of the density of line service stations on overall performance in bi-modal public transport settings"

Puneet Sharma[a], Stephan Herminghaus[a], Helge Heuer[a], Knut M. Heidemann[a,]

[a]*Max Planck Institute for Dynamics and Self-Organization (MPIDS), Am Faßberg 17, 37077 Göttingen, Germany*

1. Average train speed

We assume that trains achieve a maximum speed of $v_m = 3 \cdot v_0$. This values is inspired from data found for New York City subway (1). The time taken to reach this speed starting from rest is assumed to be $t_a = 0.05 \cdot t_0$. The trains stop at each connecting station for $t_s = 0.05 \cdot t_0$. The average train speed can then be obtained as

$$v_{\text{train}} = \begin{cases} \frac{\ell'}{\frac{\ell'}{v_m}+t_a+t_s}, & \text{if } \ell' \geq v_m \cdot t_a \\ \frac{\ell}{2\sqrt{\frac{t_a}{v_m}}+t_s}, & \text{otherwise} \end{cases}, \tag{1}$$

with ℓ' being the inter-station distance. See Fig. 1 for a explicit values of train speed as function of inter-station distance.

2. DRRP waiting time and detour

Similarly to our previous study (2), we used estimates from simulations (3) to determine the average waiting time and detours. In Fig. 2, mean detour and mean waiting time are plotted as a function of user demand. Users are assumed to have a maximum accepted waiting time of $\tau_{w,\max} = t_0$. We observe that mean waiting time, τ_w, grows with demand and saturates around $0.65\, t_0$. The variation for realistic demands is small. In the theoretical model used in the main manuscript we thus approximate the average waiting time as $\tau_w = 0.5\, \tau_{w,\max}$.

Similarly, the mean detour, δ, grows with demand and saturates around 1.65. Again, variation for realistic demands is limited. In our theory we thus assume a constant average detour of $\delta = 1.5$.

3. Intermediate stops in real cities

We analyzed the subway networks of the cities of Berlin (4) and New York (NYC) (5) with respect to the average number of intermediate stops, Θ, between crossings of disjunct lines. For NYC, we considered Manhattan south of Central Park because in that part of the city the network is closest to a grid-like structure, as assumed in our study. North of Manhattan, lines are mostly unidirectional (north-south). For Berlin, we took the subway lines inside the "S-Bahn-Ring" (closed loop of suburban rail system, see Fig. 3) from 2016, as reference. We find on average, $\Theta = 1.08$ for Berlin and $\Theta = 0.983$ for NYC.

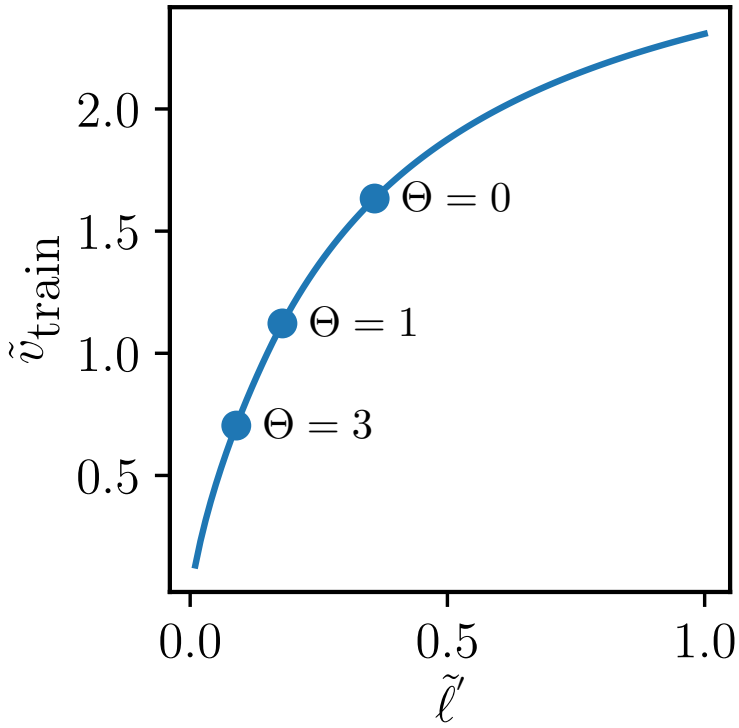

Figure 1: **Train speed as a function of station density.** Train speed is plotted as a function of ℓ'. Values of Θ are annotated in the figure. Data for mesh size $\tilde{\ell} = 0.4$.

4. Simulation framework

We use an open-source, multi-agent transport simulation framework, MATSim (6). It can be used for large-scale simulations of microscopic dynamics on (street) networks. The routing is performed using the AStarLandmarks algorithm, which is a modified version of the A* algorithm.

MATSim simulation comprises individual users, which are called agents. An initial demand characterizes the trips of the agents. Other inputs for simulations like traffic network, transit schedules for trains and a configuration file that define specific parameters used in the simulations characterize the system under study. Mobility simulations are performed for the specified demand and input parameters. Mobility simulations reported in this paper are queue-based and time-step-based. The links or allowed routes for vehicles are modelled as first-in-first-out (FIFO) queues. Vehicles in the queue leave the link after a time equal to the free flow travel time specific to the link is elapsed. A link is also characterized by the maximum number of vehicles that can be queued. For the purpose of the simulations reported here, we assume that the link capacity is large enough. For the simulations reported here, we consider the uniformly populated planar region of area $\mathcal{A}$ and edges of length $\mathcal{L} = 20\,\text{km}$. The distance ℓ' that separates adjacent transit stations is chosen to be 0.5, 1.0 and 2.0 km, corresponding to $\Theta = 3, 1,$ and 0, respectively. The

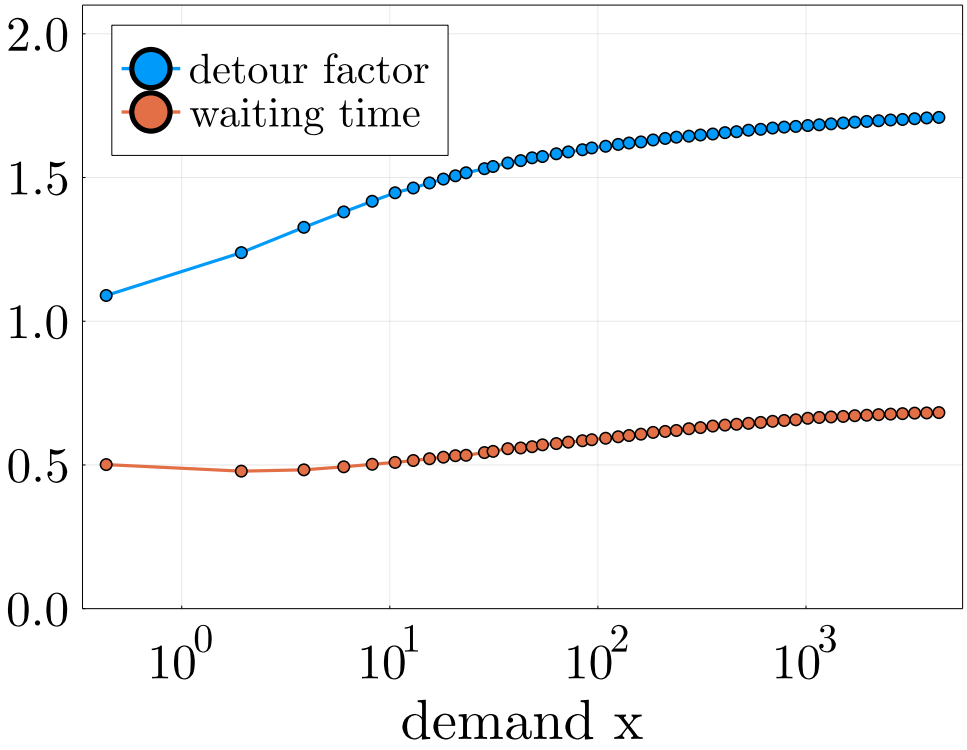

Figure 2: Detour factor, δ and mean waiting time, τ_w for various demands determined from simulations (3).

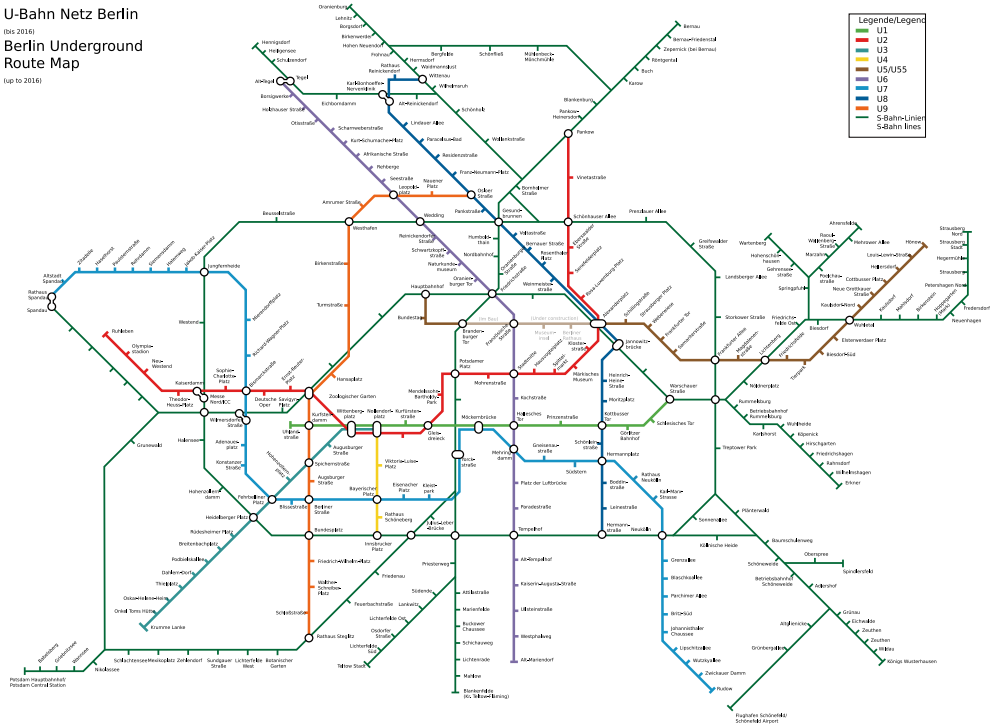

Figure 3: Berlin subway and S-Bahn network (4).

distance between major junction stations is fixed to a value of 2 km. For each simulation, $\mathcal{N}$ uncorrelated requests are generated in the region $\mathcal{A}$ over the time $\mathcal{T} = 1$ hr.

References

[1] New york city subway, `https://en.wikipedia.org/wiki`, accessed: 2023-04-06 (2023).

[2] P. Sharma, K. M. Heidemann, H. Heuer, S. Muehle, S. Herminghaus, Sustainable and convenient: bi-modal public transit systems outperforming the private car (2022). `doi:10.48550/ARXIV.2211.10221`.
URL `https://arxiv.org/abs/2211.10221`

[3] S. Mühle, An analytical framework for modeling ride pooling efficiency and minimum fleet size, Multimodal Transportation 2 (2) (2023) 100080. `doi:https://doi.org/10.1016/j.multra.2023.100080`.
URL `https://www.sciencedirect.com/science/article/pii/S2772586323000126`

[4] Berlin underground network, `https://commons.wikimedia.org/wiki/File:Berlin_U-bahn_und_S-bahn.svg`.

[5] MTA, New York City Subway, `https://new.mta.info/map/5256`.

[6] A. Horni, K. Nagel, K. Axhausen (Eds.), Multi-Agent Transport Simulation MATSim, Ubiquity Press, London, 2016. `doi:10.5334/baw`.

C

Manuscript: Bi-modal public transit system for Berlin and Brandenburg.

Bi-modal demand responsive transport in Berlin and Brandenburg.

Puneet Sharma,* Stephan Herminghaus, and Knut M. Heidemann
Max-Planck Institute for Dynamics and Self-Organization (MPIDS), Am Faßberg 17, 37077 Göttingen, Germany
(Dated: October 26, 2023)

Bi-modal public transport system consisting of a rail-bound line service and a fleet of on-demand shuttles providing connections to the line service stops is studied for the states of Berlin and Brandenburg for user adoption of $x = 1\%$ and $x = 10\%$ of the total population.

Keywords: Sustainability | Mobility | Carbon footprint | Traffic | Public transport

* puneet.sharma@ds.mpg.de

I. INTRODUCTION

The energy-intensive nature of transportation, largely reliant on fossil fuels, has triggered a concerning surge in greenhouse gas (GHG) emissions. In the USA and Europe, this sector is a major contributor, accounting for more than a quarter of total GHG emissions from anthropogenic activities [1]. The prevalent use of motorized individual vehicles (MIVs), i.e., private cars, for passenger transportation is a cause for concern. MIVs exhibit inefficiencies, as they involve the movement of over a ton of materials to transport a single person [2, 3]. This wastefulness has dire consequences, including air pollution and adverse environmental impacts [4–7], as well as contributing to traffic congestion [8–11].

Line services, represented by systems like light rails, have the potential to accommodate large numbers of passengers simultaneously, making them an ideal candidate for sustainable public transportation (PT) [12–14]. Despite their advantages, MIVs continue to dominate the global mobility market[15, 16] due to their perceived convenience[17], flexible routes, and schedules.

Demand-responsive ride-pooling (DRRP) services present an alternative to both MIVs and line services. These services employ shuttle vehicles that adapt their routes and schedules based on user requests to combine individual user requests into an appropriate set of routes of the shuttle [18], thus providing door-to-door transportation. However, the trade-off between pooling and detour [19, 20] limits the achievable pooling efficiency of DRRP services [21], hindering their potential to reduce traffic and emissions significantly.

Previous studies [22] have suggested a promising solution to this challenge, i.e., bi-modal transport. In a bi-modal public transport system, DRRP services are integrated with line services. Line services, characterized by fixed routes and schedules facilitate high vehicle occupancy and faster service. Meanwhile, DRRP shuttles offer seamless on-demand transportation to and from line service stops. Furthermore, shuttles are well-suited to serve short-distance routes with door-to-door service, where the use of line services is inefficient. This integration of line services and DRRP has been found to achieve high pooling efficiency for a simplified square grid geometry while ensuring user convenience.

In a previous, mean-field-based approach, [22] identified the key conflicting objectives of optimization as user convenience and energy consumption. It was found that the energy consumption may be reduced significantly relative to MIV, and traffic volume can be reduced by an order of magnitude relative to MIV. This suggested that bi-modal public transport systems have the potential to outperform customary public transportation as well as MIV in several respects. They also found that the overall performance of the system based on the objectives of emission and quality, does not vary dramatically with mesh size. Motivated by this, [23] studied the bi-modal transportation by means of agent-based simulation on a geometry akin to what one finds in real settings. The study further reinforced the previous claim by [22].

While previous studies were motivating, they considered a spatially uniform demand with constant average request frequency. However, in realistic scenarios, demand is heterogeneous in space, due to non-homogeneous population density and individual mobility patterns, and fluctuating in time due to phenomena like rush hours. Furthermore, the trains were assumed to run periodically at the same constant speed throughout the system and the shuttles were also assumed to operate at a constant speed. These assumptions undermine the nuances in real settings. The network topology, for example, is much more complex in real settings and vehicles barely operate at the same constant speed, if at all. It is unclear how these heterogeneities affect the overall performance of the system.

In previous studies, a prevalent assumption was that all transportation requests within a given study region exclusively relied on the public transit system, these requests were then assigned to bi-modal (shuttle-train-shuttle) or uni-modal (shuttles only) transportation. However, the reality is far more intricate, as user adoption of public transportation systems exhibits significant variability. In the present paper, we study the effects of such adoption variability on the holistic performance of bi-modal transportation systems. We explore two distinct scenarios: one where $x = 1\%$ of the total population utilizes public transportation and another where the adoption rate increases to $x = 10\%$ of the total population. For both scenarios, we assume that the rest of the people use private cars or MIVs to commute. Our study unveils the dynamics between user adoption patterns and the overall performance of bi-modal transportation systems, offering insights essential for optimizing their design and operation.

By studying bi-modal transportation in real cities, we aim to provide valuable insights into how effective bi-modal transportation can be when operated with the existing infrastructure of the rail network.

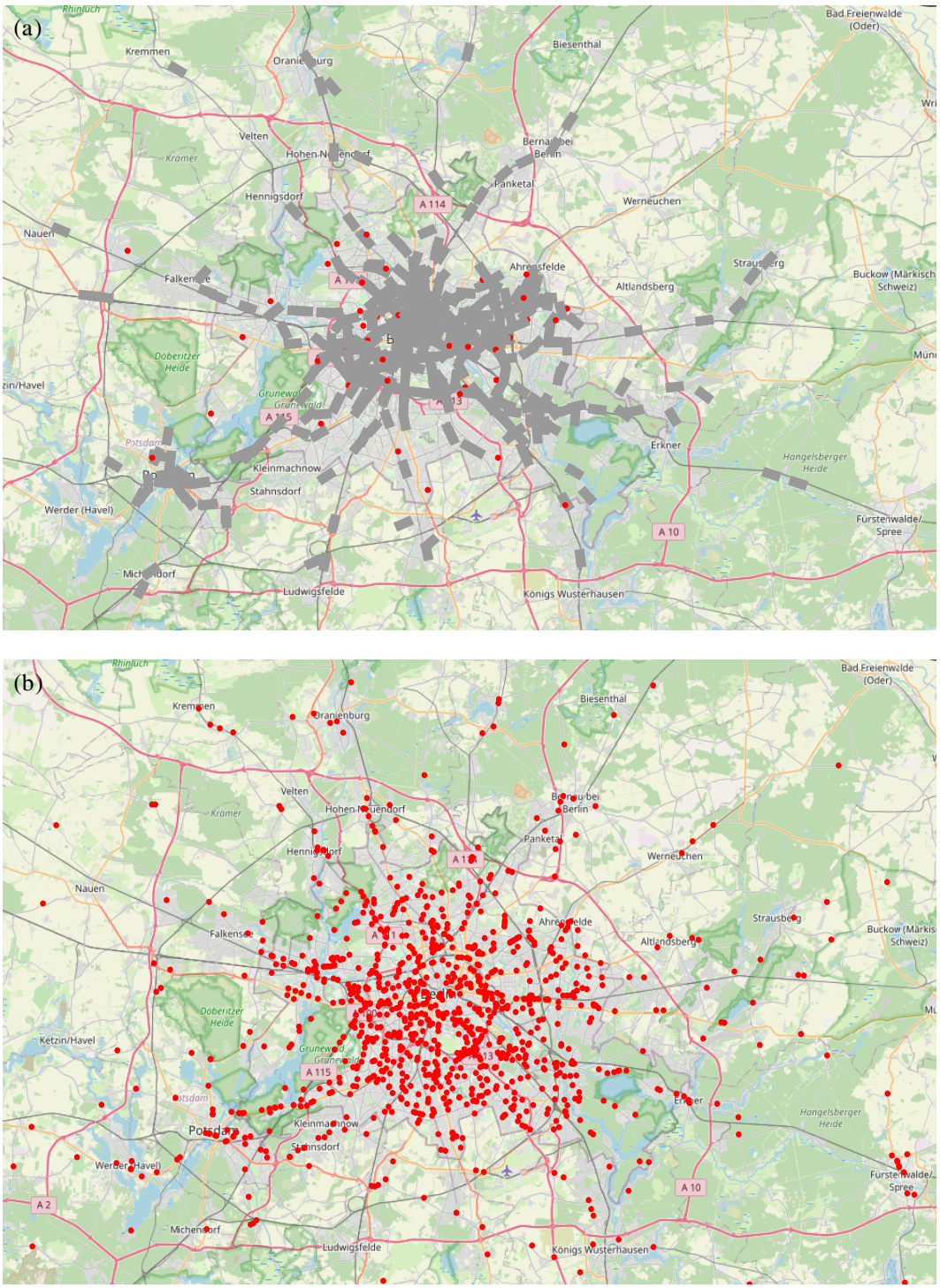

FIG. 1: **Bi-modal transport network in Berlin and Brandenburg** A snapshot of simulations for 1% user-adoption fraction ($x = 0.01$). **(a)** A bi-modal scenario where grey rectangles represent trains and red dots represent the shuttles. **(b)** MIV scenario where people use private cars to commute. Red dots represent private cars. The number of required shuttles in a bi-modal system (a) is much lower than the number of MIVS required in (b). See Subsec. III C 0 a for quantitative analysis.

II. METHODS

A. Definition of the system

For simulating a system of bi-modal transport, with on-demand shuttles and trains operating on lines, we deploy the open-source, multi-agent transport simulation framework MATSim [24]. We used the map from [25]. We used the passenger travel patterns that were artificially generated using the census data [26]. The data is provided by the Transport Systems Planning and Transport Telematics group of Technische Universität Berlin. We used an openly available General Transit Feed Specification (GTFS) dataset for the Berlin-Brandenburg region [27] to generate MATSim public transport schedule and vehicle files and to add public transport links to the network. The dataset provides schedules and vehicles for various transport modes available, however, we only use rail-bound line services as a means of public transport. Each link on the transportation network has an associated speed for the vehicles.

a. Bi-modal transit system The trains operating in the study area serve as the primary mode of transportation similar to what has been proposed in the previous study [22]. These trains run according to the schedule described above.

The transit system is further characterized by a number of shuttles, $\mathcal{S}$, in the plane. For the sake of conciseness and simplicity, we assume that the number of shuttles $\mathcal{S}$ is just sufficient to serve all user requests emanating in the system in a day. Shuttles require energy e_{shuttle} per unit distance of travel. User requests served by DRRP/shuttles are subject to the constraint that the maximum accepted detour (traveled distance / direct distance) is $\delta_m = 3$, the maximum waiting time is $\tau_{w,\,\max} = 5\,\text{min} = 0.5 \cdot t_0$ and the maximum travel time is $\alpha \cdot t_{\text{direct}} + \gamma$, where $\alpha = 3$, $\gamma = 10\,\text{min}$ are simulation parameters and t_{direct} is the direct travel time. Note that we consider trains and shuttles a part of the public transit system.

1. Parameters and objectives of operation

a. Choosing the type of transport service A single user that adopts public transit in the model system may either be transported by uni-modal service, i.e., by shuttle (DRRP) only, or by bi-modal service, i.e., be brought from $\mathcal{P} = (x_p, y_p)$ to the nearest train station by means of a shuttle, followed by a train journey, which is again followed by a shuttle journey to $\mathcal{D} = (x_d, y_d)$. It is the task of the dispatcher system to decide, for each individual request $(\mathcal{P}, \mathcal{D})$, whether the desired door-to-door service should be completed by uni-modal transportation (shuttles only) or bi-modal transportation (shuttle-train(s)-shuttle). [22] showed that the requested travel distance, $d = |\overline{\mathcal{P}\mathcal{D}}|$, irrespective of the direction of travel, may serve as a reasonable discriminating parameter. Therefore, in order to choose the mode of transportation for an individual user request, we adhere to the previous policy [22] of assigning user requests with travel distance $d > \boldsymbol{d}_{\text{c}}$ to bi-modal transportation (shuttle-train(s)-shuttle). Shorter trips, i.e., user requests with travel distance $d \leq \boldsymbol{d}_{\text{c}}$, are assigned to uni-modal transportation (shuttle only). The cut-off distance, $\boldsymbol{d}_{\text{c}}$, is the control parameter we will use to optimize the performance of the system. It is in one-to-one correspondence to the fraction of bi-modal transportation $F(\boldsymbol{d}_{\text{c}}) = \int_{\boldsymbol{d}_{\text{c}}}^{\infty} p(y)\,dy$, out of the fraction of people, x, that adopt the public transit system, with $p(\cdot)$ the probability density of requested distances.

b. Service quality For the two 10% and 1% population scenarios, we define the service quality as the ratio between the average travel times by MIV and bi-modal transit, respectively, for the corresponding population fraction,

$$\mathcal{Q} = \frac{t_0}{(1-F)\cdot t_{\text{uni}} + F \cdot t_{\text{bi}}}\,, \tag{1}$$

where $F = F(\boldsymbol{d}_{\text{c}})$ is the fraction of requests served by bi-modal transportation.

To compute the average travel time by MIV for a simulated scenario, we perform independent simulations where the MIV is the only allowed mode of transportation. If t_i^{MIV} represents the travel time for user i, then t_0 can be obtained by averaging over all users in the system, i.e., $t_0 = 1/\mathcal{N}\sum t_i^{\text{MIV}}$. Similarly, we compute the denominator in Eq. 1, from simulations by averaging over all users in the system.

In a mean-field approach, with square-grid geometry, [22] derived an analytical expression for $\mathcal{Q}$ as

$$\mathcal{Q}^{-1} = (1-F)\cdot \underbrace{\left(\tilde{\tau}_w + \delta\langle\tilde{d}\rangle_{\tilde{d}<\tilde{\boldsymbol{d}}_{\text{c}}}\right)}_{\tilde{t}_{\text{uni}}} + F\cdot \underbrace{\left(2\tilde{\tau}_w + 2\beta\tilde{\ell}\delta + \frac{1}{\tilde{\mu}} + \frac{4}{\pi}\frac{\langle\tilde{d}\rangle_{\tilde{d}>\tilde{\boldsymbol{d}}_{\text{c}}}}{\tilde{v}_{\text{train}}}\right)}_{\tilde{t}_{\text{bi}}}\,. \tag{2}$$

The $\tilde{}$ indicates quantities non-dimensionalized via division by the respective unit (D, t_0, and v_0 as units for length, time, and velocity, respectively). $\langle\tilde{d}\rangle_{\tilde{d}>\tilde{\boldsymbol{d}}_{\text{c}}}$ is the mean of requested distances larger than $\boldsymbol{d}_{\text{c}}$ and δ is the average detour

incurred by a user during the DRRP trip, $\tilde{\tau}_w$ is the average waiting time for shuttles and $\tilde{\mu}$ the train frequency, $\tilde{\ell}$ is grid constant or distance between two nearest train stations. $\beta = \frac{1}{6}(\sqrt{2} + \log(1+\sqrt{2})) \approx 0.383$ is a geometrical constant, and $4\pi^{-1}\langle\tilde{d}\rangle_{\tilde{d}>\tilde{\boldsymbol{d}}_c}$ is the average distance traveled on trains.

c. Energy consumption We assess the overall energy consumption by transportation in the two use cases discussed above. To assess the overall energy consumption by the transportation system, we define the dimensionless energy consumption $\mathcal{E}$ as the ratio of total energy consumed when 10% and 1% population uses the bi-modal transportation and the total population using fleet of MIV, mathematically, $\mathcal{E}$ can be written as

$$\mathcal{E} \equiv \frac{\Delta_{\text{shuttle}} \cdot e_{\text{shuttle}} + \Delta_{\text{train}} \cdot e_{\text{train}}}{\Delta_{\text{MIV}} \cdot e_{\text{MIV}}}\,, \tag{3}$$

where $\Delta_\cdot$ denotes the (mode-specific) total distance traveled in a unit cell of area ℓ^2 per unit time. $e_\cdot$ is the vehicle-specific energy consumption per unit distance, x is the user-adoption fraction. Note that $\mathcal{E}$ is already normalized with respect to the MIV energy consumption (denominator), as this is the door-to-door transportation system we intend to compare with. For $\mathcal{E} > 1$ (< 1), energy requirement for bi-modal transportation is larger (smaller) than for MIV serving the same requests.

[22] derived an analytical expression for a mean-field approach in a square grid geometry as follows. Both, uni-modal (shuttle only) and bi-modal trips, contribute to the total distance driven by shuttles per unit time due to requests from a unit cell of area ℓ^2, hence

$$\Delta_{\text{shuttle}} = \frac{\nu E \ell^2}{\eta}\left(\underbrace{\langle d\rangle_{d<\boldsymbol{d}_c}(1-F)}_{\text{shuttle only}} + \underbrace{2\beta\ell F}_{\text{two shuttle trips}}\right)\,, \tag{4}$$

where η is the DRRP pooling efficiency, which is the ratio of direct distance requested by the users and the distance actually driven by the shuttles (for MIV, $\eta = 1$). [28] has observed that η scales with demand Λ roughly in an algebraic manner, $\eta(\Lambda) \approx \Lambda^\gamma$, with $\gamma \approx 0.12$. In a bi-modal system, however, some of the demand Λ is directed towards trains. Therefore, we need to compute an adjusted demand, $\Lambda_{\text{shuttle}} \equiv (E\nu_{\text{shuttle}} D^3_{\text{shuttle}})/v_0$, considering shuttle trips only. ν_{shuttle} is the effective request frequency for shuttle trips and D_{shuttle} is the average distance of a shuttle trip. One can show that [22]

$$\Lambda_{\text{shuttle}} = \Lambda\,(1+F)^{-2}((1-F)\langle\tilde{d}\rangle_{\tilde{d}<\tilde{\boldsymbol{d}}_c} + 2\beta\tilde{\ell}F)^3\,. \tag{5}$$

We compute the theoretical pooling efficiency, η, according to the power law mentioned above

$$\eta \equiv \Lambda^{0.12}_{\text{shuttle}}\,. \tag{6}$$

The distance travelled per unit cell by line service, Δ_{train}, remains constant throughout our study because trains operate at a constant frequency μ, mathematically,

$$\Delta_{\text{train}} = 4 \cdot \mu \cdot \ell\,. \tag{7}$$

Δ_{MIV} is the total distance requested by users per unit time,

$$\Delta_{\text{MIV}} = \nu E \ell^2 D\,. \tag{8}$$

Analytically, Eq. 3 can then be written as

$$\mathcal{E} = \underbrace{\eta^{-1}\left(\langle\tilde{d}\rangle_{\tilde{d}<\tilde{\boldsymbol{d}}_c}(1-F) + 2\beta\tilde{\ell}F\right)\cdot\frac{e_{\text{shuttle}}}{e_{\text{MIV}}}}_{\text{shuttles}} + \underbrace{\frac{4\tilde{\mu}}{\Lambda\tilde{\ell}}\cdot\frac{e_{\text{train}}}{e_{\text{MIV}}}}_{\text{train}}\,. \tag{9}$$

We consider electric light rails with a maximum seating-capacity $k = 100$ and $e_{\text{train}} = 9.72\,\text{kN}$ [29] for the line service. For MIV we consider Diesel cars with $e_{\text{MIV}} = 2.47\,\text{kN}$ [30]. For the shuttles we choose Mercedes Sprinter (8.8 liters of Diesel per 100 km [31]), resulting in $e_{\text{shuttle}} = 3.28\,\text{kN}$.

In order to compute the ratio above in Eq. 3 for a simulated scenario, we perform independent simulations for MIV and bi-modal transit with identical user requests. The denominator in Eq. 3 is obtained from MIV simulations by multiplying the total driven distance by e_{MIV}. The numerator in Eq. 3 is obtained from bi-modal simulations by multiplying mode-specific total driven distance with the respective vehicle-specific energy consumption per unit distance.

d. Traffic Road traffic is a source of local noise and air pollution and occupies significant shares of urban space. Bi-modal transit aims at the reduction of road traffic by utilizing line services for trips over larger distances.

To obtain a quantitative estimate, we define as traffic volume for the two used cases, $\tilde{\Delta}$, cumulative distance driven by shuttles, Δ_{shuttle} normalized with respect to the equivalent of total MIV distance requested, Δ_{MIV} (Eq. 8), or, equivalently, the relative number of driving shuttles as compared to MIV.

$$\tilde{\Delta} \equiv \frac{\Delta_{\text{shuttle}}}{\Delta_{\text{MIV}}} = \eta^{-1} \cdot (1+F)\, \tilde{D}_{\text{shuttle}}\,, \tag{10}$$

with pooling efficiency, η, bimodal fraction, F, and average requested distance for trips by shuttles involved in bi-modal transit, $\tilde{D}_{\text{shuttle}}$.

III. RESULTS

Below in Subsec. III A, we first present how DRRP performs with a bi-modal system when the bi-modal transit system is used by 10%, and 1% population. Then in Subsecs. III B , and III C, we describe the overall performance of the bi-modal transit system for the two used cases above. We conclude the results section with an analysis of the potential reduction in traffic volume.

A. DRRP performance

a. Occupancy In Fig. 2a, we show the mean DRRP occupancy, b, averaged over non-empty driving vehicles against the bi-modal fraction, F, for 10% and 1% use case. We observe that the shuttles have a higher mean occupancy for larger use case, i.e., larger demand because of the greater possibility of pooling. Mean occupancy decreases with the involvement of trains (increasing F). This is because shuttle trips are shortened causing passengers to spend less time in shuttles during their transit. The black symbols represent mean occupancy for a uni-modal (shuttles only) scenario. We observe that the mean occupancy is larger for uni-modal scenarios.

b. Detours In Fig. 2b, we observe that higher use case, i.e., 10% population has larger detours. Detour δ and b trend observed above shows a well-known trade-off between detour and pooling for DRRP, i.e., desirable pooling necessitates undesirable detours for passengers [19]. We observe that the detours decrease with the involvement of line services, this can be attributed to the 'common stop effect', a phenomenon observed in the previous study [23]. With greater involvement of line services, more passengers are picked up and dropped of at the same train station, thereby reducing detours.

c. Pooling efficiency The pooling efficiency which is defined as the ratio between mean occupancy and mean detour is shown in Fig. 2c. We observe that the pooling efficiency, η, is higher for larger demand, i.e., 10% use case as also reported in previous studies [23, 28]. This suggests that the larger use of shuttles or bi-modal service will be favorable for pooling efficiency. We observe that the involvement of line service reduces DRRP pooling efficiency because user requests are diverted toward the line which shortens the average distance a passenger travels on the shuttle during the entire journey.

d. Waiting time In Fig. 2d, we study the mean waiting time for shuttle-borne trips. We plot the mean waiting time normalized with the average trip duration, t_0, against the bi-modal fraction, F. We observe that larger demand, that is, the use case of ten percent has larger waiting times because shuttles are busier. We also observe that the involvement of line services decreases the waiting time for shuttle trips because of the 'common stop effect' and a lower share of distance traveled in shuttles.

The main messages from Fig. 2 are: 1) Shuttles become more efficient with demand, while user experience suffers due to larger detours and waiting times, as also found in the previous study [23]. 2) The involvement of line services makes the shuttle trips more convenient for users by reducing the waiting time and detours.

B. Overall energy consumption and service quality of bi-modal transit

Now, we will analyze the overall objectives, i.e., energy consumption (Eq. 9) and service quality (Eq. 2) of the transportation system for the two use cases.

a. Energy consumption In Fig. 3a, relative energy consumption, $\mathcal{E}$, is plotted as a function of bi-modal fraction, F, for the two use cases discussed above. We observe a general trend of decreasing energy consumption with the involvement of line services. This is because $\tilde{\Delta}_{\text{shuttle}}$ decreases with the involvement of line services (see Fig. 5a) while

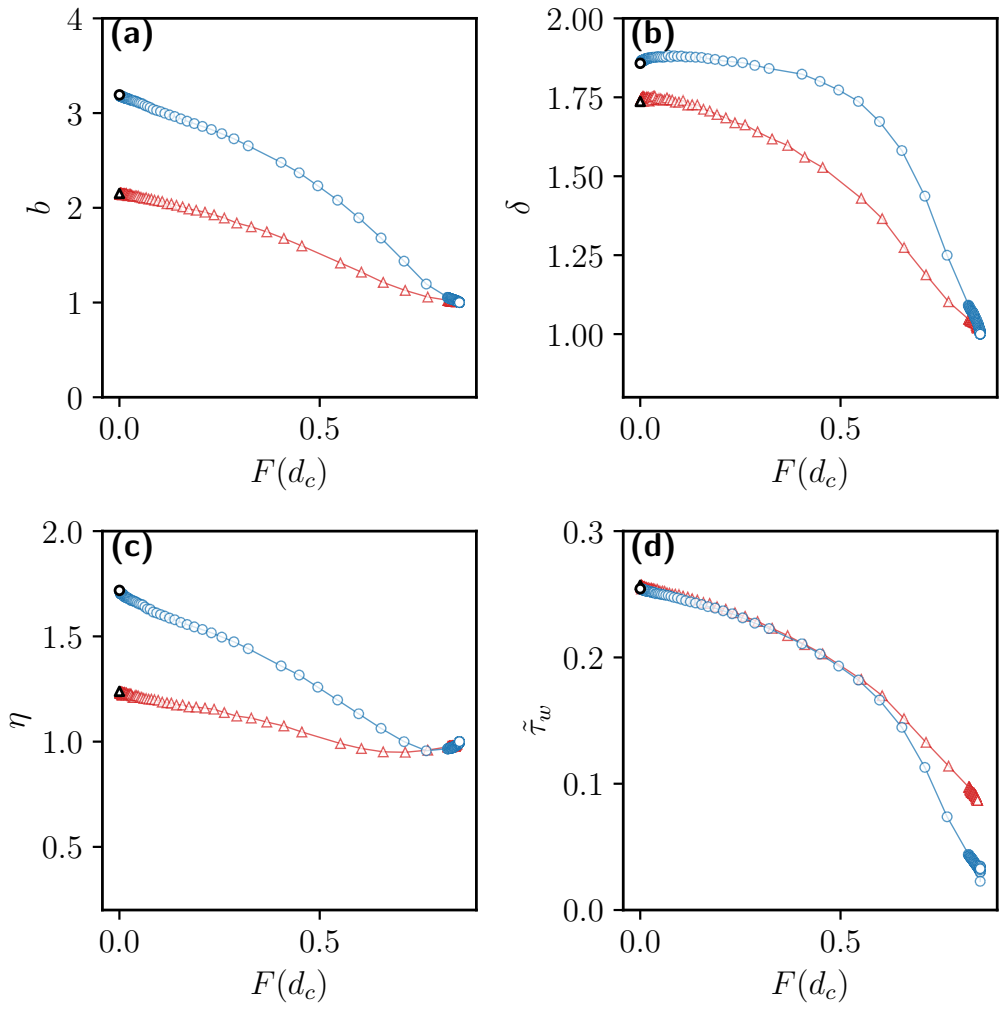

FIG. 2: **DRRP performance statistics:** DRRP/Shuttle performance parameters are plotted against bi-modal fraction F. Blue circles and red triangles represent 10%, and 1% population of Greater Berlin, respectively. Black circle, and triangle represent uni-modal transport (shuttles only) **(a)** Mean DRRP occupancy for non-standing vehicles, b. **(b)** Mean detour, δ, for shuttle users. **(c)** Mean DRRP pooling efficiency $\eta \equiv b/\delta$. **(d)** Mean waiting time, $\tilde{\tau}_w$, for shuttles normalized with t_0.

$\tilde{\Delta}_{\text{train}}$ is constant due to a fixed schedule of trains in the simulations, thus reducing the total energy consumption by the bi-modal transportation system. We also observe that energy consumption is reduced with increasing demand, i.e., for a higher used case. This is evident from Eq. 9. Note that the emission curves for bi-modal transportation start above the emissions for uni-modal scenarios (black symbols). This is because in our bi-modal simulations, trains are always running at fixed schedules. For low bi-modal fraction, F, trains are underutilized because they operate at low occupancies (see Fig. 4b). We observe that for 10% use case, the energy consumption can easily drop below 20%, however, for a 1% use case, it's not advisable to use bi-modal transportation, suggesting that a larger adoption of bi-modal transportation can significantly reduce the energy consumption.

b. Quality In Fig. 3b, the overall quality of the system is plotted against the bi-modal fraction, F, for the two use cases. We observe that the demand doesn't significantly impact the overall service quality and service quality decreases with the involvement of the line services. Large waiting times (see Fig. 4a) contribute to degrading quality with the bi-modal fraction, F. This suggests that user quality can be improved by increasing the train frequency and adapting the train capacity, k, depending on the demand. We see in Fig. 4b that trains are barely full.

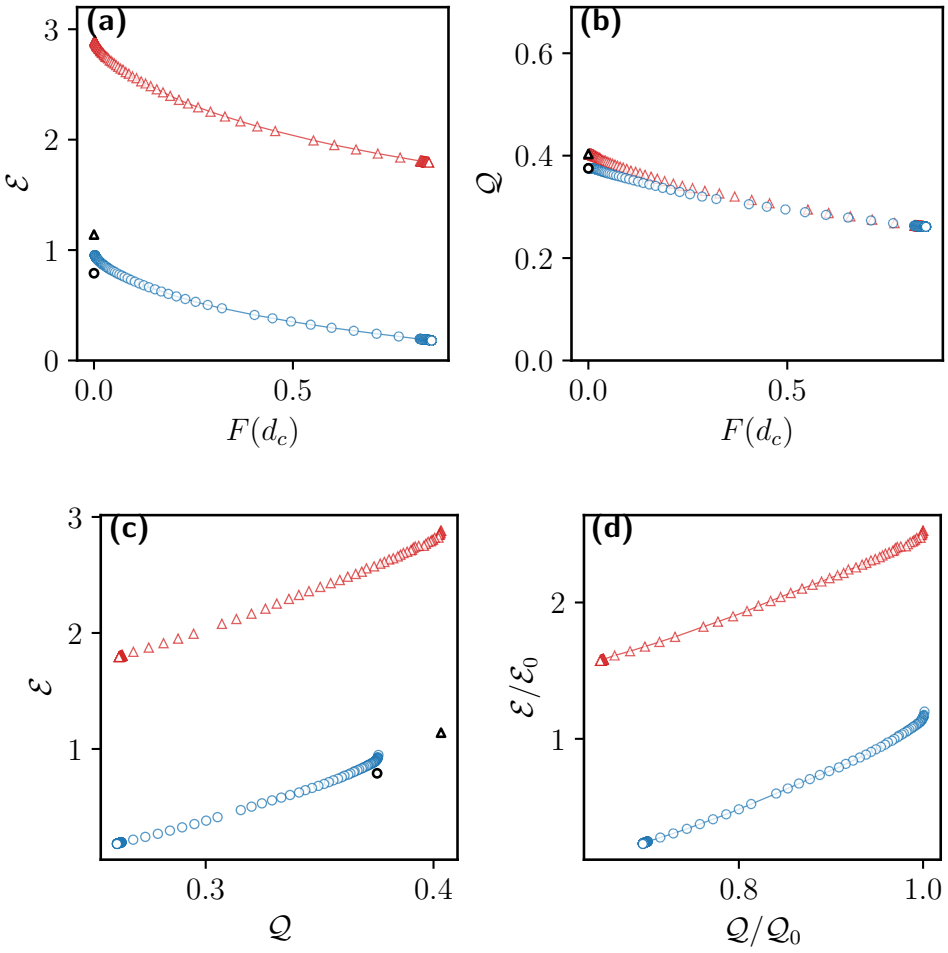

FIG. 3: **Overall performance of bi-modal transit:** Blue circles and red triangles represent data for 10%, and 1% greater Berlin population respectively. **(b)** Quality, $\mathcal{Q}$, as a function of F. **(c)** Pareto fronts of energy consumption, $\mathcal{E}$, vs. service quality, $\mathcal{Q}$ determined from the data shown in (a), (b). Data not part of Pareto fronts is not shown. The black circle and triangle represent uni-modal transport (shuttles-only) data for 10%, and 1% greater Berlin population respectively. **(d)** Pareto fronts as in (c), but normalized with respect to the performance, $(\mathcal{Q}_0, \mathcal{E}_0)$, of the uni-modal system (shuttles only).

C. Pareto optimization

A tuple of parameter values, in our case $(\mathcal{E}, \mathcal{Q})$, is called Pareto-optimal if none of the parameters (or objectives) can be further optimized without compromising on at least one of the others. The set of all such tuples of parameters is called the Pareto front [32–34]. We now apply this concept to our results, keeping in mind that we aim at maximum service quality at minimum energy consumption. Hence, in diagrams spanned by $\mathcal{Q}$ as the abscissa and $\mathcal{E}$ as the ordinate, system operation as far as possible to the lower right is desirable.

In order to study the overall performance of bi-modal transportation in real scenarios and the impact of user adoption, we explore two distinct scenarios: one where 1% of the total population utilizes bi-modal transportation, and another where the adoption rate increases to 10% of the total population. In each case, we vary $\boldsymbol{d}_c$ to obtain the Pareto fronts.

In Fig. 3c, we show the Pareto fronts obtained for data in Figs. 3a,b. We observe that the energy consumption can go below 20% for a service quality of around 0.25 for the 10% use case. The black circle represents the uni-modal data for the 10% use case. We observe that bi-modal transportation can significantly reduce emissions as compared to uni-modal (shuttles only) case with some compromise on service quality. This is clear from Fig. 3d, where we plot the Pareto-optimal $\mathcal{E}$ and $\mathcal{Q}$ normalized with uni-modal $\mathcal{E}_0$ and $\mathcal{Q}_0$ respectively.

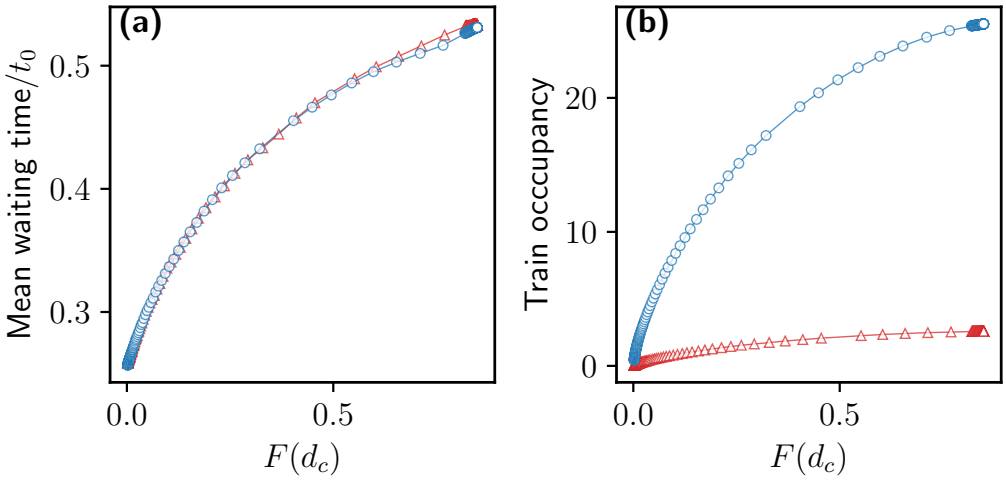

FIG. 4: **Mean waiting time and Train occupancy:** Blue circles and red triangles represent 10% and 1% population of Greater Berlin, respectively. **(a)** Mean waiting times normalized with t_0. **(b)** Mean train occupancy.

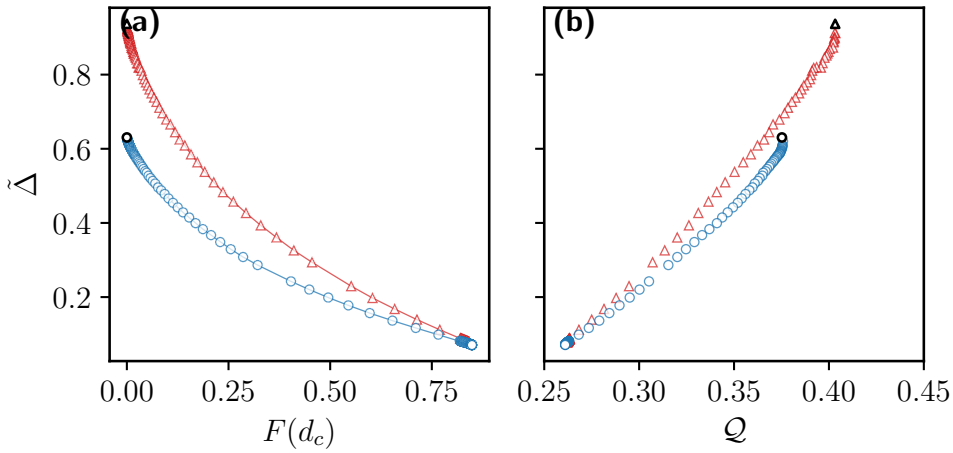

FIG. 5: **Traffic volume.** Blue circles and red triangles represent 10%, and 1% greater Berlin population respectively. **(a)**Relative bi-modal traffic in simulations, $\tilde{\Gamma}$, as defined in Eq. 10, as a function of the bi-modal fraction, F. Black circle and triangle represent uni-modal transport (shuttles-only) data for 10%, and 1% greater Berlin population respectively. **(b)** Relative bi-modal traffic in simulations, $\tilde{\Gamma}$, determined along the Pareto fronts in Fig. 3, against corresponding service quality $\mathcal{Q}$.

For the 1% use case, it is not advisable to deploy bi-modal transportation at all because requests are better served by uni-modal transportation (black triangle) both in terms of energy consumption and service quality.

a. Traffic volume In Fig. 5a, we plot the total relative traffic volume, $\tilde{\Delta}$, described above in subsec II A 1 d on the vertical axis as a function of bi-modal fraction, F, for the two used cases. We observe a trend of decreasing bi-modal traffic with the involvement of line services, i.e., with increasing F. Also, $\tilde{\Delta}$ decreases when the user adoption goes from 1% to 10% because the shuttles become more efficient due to the possibility of larger pooling (see also Fig. 2c).

In Fig. 5b, we plot the total relative traffic volume, $\tilde{\Delta}$, for simulations, determined along the Pareto fronts in Fig. 3c, against corresponding service quality, $\mathcal{Q}$. The traffic volume for uni-modal (shuttles-only) scenarios is plotted with black symbols. We observe that the relative traffic volume for uni-modal scenarios decreases with demand due to increased pooling efficiency, η (see Fig. 2c). The relative traffic volume for uni-modal (shuttles only) scenario for 1% use case is not significantly less than that of MIV because of low pooling efficiency, η (see Fig. 2c). The uni-modal

traffic volume for the 10% use case is around 60% of MIV traffic. This suggests that the relative uni-modal traffic volume can be further reduced if more people adopt ride pooling.

Bi-modal public transportation allows for further reduction in relative traffic volume Below the uni-modal scenario, albeit, at a lower service quality. The bi-modal traffic can go as low as 15% for 10% user adoption.

D. Discussion

Our investigation had two primary goals. First to study the feasibility of bi-modal demand-responsive public transportation in Berlin and Brandenburg with the existing rail network. Second, to study the impact of user adoption of public transit on the overall performance of bi-modal demand-responsive public transportation in Berlin and Brandenburg.

Our study suggests that bi-modal demand-responsive transportation can be deployed in Berlin and Brandenburg with the existing rail network of public transportation. We find that the overall performance of bi-modal transportation improves with higher user adoption. While 10% user adoption can significantly reduce emissions and vehicular traffic, it is not advisable to deploy bi-modal transit with existing rail network and train schedules if the user adoption is 1%. This suggests that the overall performance of the bi-modal transit can be further improved by devising strategies to attract users towards bi-modal transportation.

[1] Y. V. Fan, S. Perry, J. J. Klemeš, C. T. Lee, A review on air emissions assessment: Transportation, Journal of Cleaner Production 194 (2018) 673–684. URL: https://www.sciencedirect.com/science/article/pii/S0959652618314914. doi:doi:https://doi.org/10.1016/j.jclepro.2018.05.151.

[2] D. MacKenzie, S. Zoepf, J. Heywood, Determinants of US passenger car weight, Int. J. Veh. Des 65 (2014) 73–93.

[3] R. Tachet, O. Sagarra, P. Santi, G. Resta, M. Szell, S. H. Strogatz, C. Ratti, Scaling law of urban ride sharing, Scientific Reports 7 (2017) 1–6.

[4] Y. V. Fan, S. Perry, J. J. Klemeš, C. T. Lee, A review on air emissions assessment: Transportation, Journal of Cleaner Production 194 (2018) 673–684. URL: https://www.sciencedirect.com/science/article/pii/S0959652618314914. doi:doi:https://doi.org/10.1016/j.jclepro.2018.05.151.

[5] C. A. Kontovas, H. N. Psaraftis, Transportation Emissions: Some Basics, Springer International Publishing, Cham, 2016. URL: https://doi.org/10.1007/978-3-319-17175-3_2. doi:doi:10.1007/978-3-319-17175-3_2.

[6] European Environment Agency, Air quality in europe — 2020 report, https://www.eea.europa.eu/publications/air-quality-in-europe-2020-report, 2020. Accessed: 2022-05-18.

[7] F. Caiazzo, A. Ashok, I. A. Waitz, S. H. Yim, S. R. Barrett, Air pollution and early deaths in the united states. part i: Quantifying the impact of major sectors in 2005, Atmospheric Environment 79 (2013) 198–208. URL: https://www.sciencedirect.com/science/article/pii/S1352231013004548. doi:doi:https://doi.org/10.1016/j.atmosenv.2013.05.081.

[8] A. T. Chin, Containing air pollution and traffic congestion: Transport policy and the environment in singapore, Atmospheric Environment 30 (1996) 787–801. URL: https://www.sciencedirect.com/science/article/pii/1352231095001735. doi:doi:https://doi.org/10.1016/1352-2310(95)00173-5, supercities: Environment Quality and Sustainable Development.

[9] Koźlak, Aleksandra, Wach, Dagmara, Causes of traffic congestion in urban areas. case of poland, SHS Web Conf. 57 (2018) 01019. URL: https://doi.org/10.1051/shsconf/20185701019. doi:doi:10.1051/shsconf/20185701019.

[10] R. Arnott, K. Small, The economics of traffic congestion, American Scientist 82 (1994) 446–455. URL: http://www.jstor.org/stable/29775281.

[11] M. Barth, K. Boriboonsomsin, Traffic congestion and greenhouse gases, Access Magazine 1 (2009) 2–9.

[12] K. Pietrzak, O. & Pietrzak, The role of railway in handling transport services of cities and agglomerations., Transportation Research Procedia 39 (2019) 405–416.

[13] R. D. Ferbrache, F. & Knowles, City boosterism and place-making with light rail transit: A critical review of light rail impacts on city image and quality., Geoforum 80 (2017) 103–113.

[14] H. Kato, Y. Kaneko Y. & Soyama, Economic benefits of urban rail projects that improve travel-time reliability: Evidence from tokyo, japan., Transport Policy 35 (2014) 202–210.

[15] Eurostat, Passenger mobility statistics, https://ec.europa.eu/eurostat/statistics-explained/index.php?title=Passenger_mobility_statistics#Urban_trips, 2022. Accessed: 2022-09-29.

[16] D. Fiorello, A. Martino, L. Zani, P. Christidis, E. Navajas-Cawood, Mobility data across the eu 28 member states: Results from an extensive cawi survey, Transportation research procedia 14 (2016) 1104–1113.

[17] J. Kent, Secured by automobility: why does the private car continue to dominate transport practices?, Ph.D. thesis, UNSW Sydney, 2013.

[18] J. Alonso-Mora, S. Samaranayake, A. Wallar, E. Frazzoli, D. Rus, On-demand high-capacity ride-sharing via dynamic trip-vehicle assignment, Proceedings of the National Academy of Sciences 114 (2017) 462–467.

[19] S. Herminghaus, Mean field theory of demand responsive ride pooling systems, Transportation Research Part A: Policy and Practice 119 (2019) 15–28.
[20] I. Lobel, S. Martin, Detours in shared rides, Available at SSRN 3711072 (2020).
[21] F. Zwick, N. Kuehnel, R. Moeckel, K. W. Axhausen, Agent-based simulation of city-wide autonomous ride-pooling and the impact on traffic noise, Transportation Research Part D: Transport and Environment 90 (2021) 102673.
[22] P. Sharma, K. M. Heidemann, H. Heuer, S. Mühle, S. Herminghaus, Sustainable and convenient: Bi-modal public transit systems outperforming the private car, Multimodal Transportation 2 (2023) 100083. URL: https://www.sciencedirect.com/science/article/pii/S2772586323000151. doi:doi:https://doi.org/10.1016/j.multra.2023.100083.
[23] P. Sharma, K. M. Heidemann, S. Herminghaus, under review: Impact of the density of line service stations on overall performance in bi-modal public transport settings, 2023.
[24] A. Horni, K. Nagel, K. Axhausen (Eds.), Multi-Agent Transport Simulation MATSim, Ubiquity Press, London, 2016. doi:doi:10.5334/baw.
[25] OpenStreetMaps, Open street map, https://www.openstreetmap.org/, 2023. Last accessed on 2023-09-22.
[26] D. Ziemke, I. Kaddoura, K. Nagel, The matsim open berlin scenario: A multimodal agent-based transport simulation scenario based on synthetic demand modeling and open data, Procedia Computer Science 151 (2019) 870–877. URL: https://www.sciencedirect.com/science/article/pii/S1877050919305848. doi:doi:https://doi.org/10.1016/j.procs.2019.04.120, the 10th International Conference on Ambient Systems, Networks and Technologies (ANT 2019) / The 2nd International Conference on Emerging Data and Industry 4.0 (EDI40 2019) / Affiliated Workshops.
[27] V.-F. via GTFS, Verkehrsverbund berlin-brandenburg., https://www.vbb.de/unsere-themen/vbbdigital/api-entwicklerinfos/datensaetze, 2017. Accessed: April,2017.
[28] S. Mühle, An analytical framework for modeling ride pooling efficiency and minimum fleet size, Multimodal Transportation 2 (2023) 100080. URL: https://www.sciencedirect.com/science/article/pii/S2772586323000126. doi:doi:https://doi.org/10.1016/j.multra.2023.100080.
[29] W. Knörr, C. Heidt, S. Gores, F. Bergk, Aktualisierung „Daten- und Rechenmodell: Energieverbrauch und Schadstoffemissionen des motorisierten Verkehrs in Deutschland 1960-2035“ (TREMOD) für die Emissionsberichterstattung 2016 (Berichtsperiode 1990-2014) Anhang, Technical Report, 2016.
[30] BMDV, Verkehr in Zahlen 2021/2022, Technical Report, Bundesministerium für Verkehr und digitale Infrastruktur, 2022.
[31] Mercedes-Benz, Mercedez-Benz Configurator, https://voc.mercedes-benz.com/voc/de_de?_ga=2.230012379.695886780.1664812666-1473138929.1664499805, 2022. Accessed:2022-10-03.
[32] G. Debreu, Valuation equilibrium and pareto optimum, Proceedings of the National Academy of Sciences 40 (1959) 588–592.
[33] B. Greenwald, J. E. Stiglitz, Externalities in economies with imperfect information and incomplete markets, Quarterly Journal of Economics 40 (1959) 229–264.
[34] M. Magill, M. Quinzii, Theory of incomplete markets, MIT Press, 2002.

Bibliography

[1] Damian J Kulash. "Transportation and society". In: *Transportation Planning Handbook, Institute of Trasnportation Engineers, Washington, DC* (1999).

[2] Davide Fiorello et al. "Mobility Data across the EU 28 Member States: Results from an Extensive CAWI Survey". In: *Transportation research procedia* 14 (2016), pp. 1104–1113.

[3] Davide Fiorello et al. "Mobility Data across the EU 28 Member States: Results from an Extensive CAWI Survey". In: *Transportation Research Procedia* 14 (2016). Transport Research Arena TRA2016, pp. 1104–1113. ISSN: 2352-1465. DOI: https://doi.org/10.1016/j.trpro.2016.05.181. URL: https://www.sciencedirect.com/science/article/pii/S2352146516301831.

[4] Will Steffen et al. "The Anthropocene: From global change to planetary stewardship". In: *Ambio* 40 (2011), pp. 739–761.

[5] Paul J Crutzen. "Geology of mankind". In: *Paul J. Crutzen: A pioneer on atmospheric chemistry and climate change in the Anthropocene* (2016), pp. 211–215.

[6] Johan Rockström et al. "A safe operating space for humanity". In: *Nature* 461.7263 (2009), pp. 472–475.

[7] Leah H. Martinez. "Post Industrial Revolution human activity and climate change: Why the United States must implement mandatory limits on industrial greenhouse gas emissions". In: *Journal of Land Use Environmental Law* 20.2 (2005), pp. 403–421. ISSN: 08924880. URL: http://www.jstor.org/stable/42842978 (visited on 09/28/2023).

[8] Charles D. Keeling Ralph F; Keeling. *In Scripps CO2 Program Data. UC San Diego Library Digital Collections.* https://doi.org/10.6075/J08W3BHW. Atmospheric Monthly In Situ CO2 Data - Mauna Loa Observatory, Hawaii.

[9] William W Kellogg. "The World Climate Conference: A Conference of Experts on Climate and Mankind, held in Geneva, Switzerland, during 12–23 February 1979". In: *Environmental Conservation* 6.2 (1979), pp. 162–162.

[10] Rebecca Lindsey and LuAnn Dahlman. "Climate change: Global temperature". In: *Available online: climate. gov (accessed on 22 March 2021)* (2020).

[11] Peter Wadhams, Nick Hughes, and João Rodrigues. "Arctic sea ice thickness characteristics in winter 2004 and 2007 from submarine sonar transects". In: *Journal of Geophysical Research: Oceans* 116.C8 (2011). DOI: https://doi.org/10.1029/2011JC006982. eprint: https://agupubs.onlinelibrary.wiley.com/doi/pdf/10.1029/2011JC006982. URL: https://agupubs.onlinelibrary.wiley.com/doi/abs/10.1029/2011JC006982.

[12] Abiy S Kebede et al. "Impacts of climate change and sea-level rise: a preliminary case study of Mombasa, Kenya". In: *Journal of Coastal Research* 28.1A (2012), pp. 8–19.

[13] Mohammed Fazlul Karim and Nobuo Mimura. "Impacts of climate change and sea-level rise on cyclonic storm surge floods in Bangladesh". In: *Global environmental change* 18.3 (2008), pp. 490–500.

[14] Yee Van Fan et al. "A review on air emissions assessment: Transportation". In: *Journal of Cleaner Production* 194 (2018), pp. 673–684. ISSN: 0959-6526. DOI: https://doi.org/10.1016/j.jclepro.2018.05.151. URL: https://www.sciencedirect.com/science/article/pii/S0959652618314914.

[15] Rene Diekstra and Martin Kroon. "Cars and behaviour: Psychological barriers to car restraint and sustainable urban transport". In: *Sustainable Transport* (Aug. 2003), pp. 252–264. DOI: 10.1016/B978-1-85573-614-6.50025-2.

[16] Donald MacKenzie, Stephen Zoepf, and John Heywood. "Determinants of US passenger car weight". In: *Int. J. Veh. Des* 65.1 (2014), pp. 73–93.

[17] Remi Tachet et al. "Scaling law of urban ride sharing". In: *Scientific Reports* 7.1 (2017), pp. 1–6.

[18] European Environment Agency. *Air quality in Europe — 2020 report*. https://www.eea.europa.eu/publications/air-quality-in-europe-2020-report. Accessed: 2022-05-18. 2020.

[19] Fabio Caiazzo et al. "Air pollution and early deaths in the United States. Part I: Quantifying the impact of major sectors in 2005". In: *Atmospheric Environment* 79 (2013), pp. 198–208. ISSN: 1352-2310. DOI: https://doi.org/10.1016/j.atmosenv.2013.05.081. URL: https://www.sciencedirect.com/science/article/pii/S1352231013004548.

[20] *European Environment Agency: Are we moving in the right direction? Indicators on transport and environmental integration in the EU*. https://www.eea.europa.eu/ds_resolveuid/0c1c4a6acf289ffdefa1876ea5d60f07. Accessed: 2022-07-14. 2020.

[21] Jeffrey A Joireman, Paul AM Van Lange, and Mark Van Vugt. "Who cares about the environmental impact of cars? Those with an eye toward the future". In: *Environment and behavior* 36.2 (2004), pp. 187–206.

[22] Anthony T.H. Chin. "Containing air pollution and traffic congestion: Transport policy and the environment in Singapore". In: *Atmospheric Environment* 30.5 (1996). Supercities: Environment Quality and Sustainable Development, pp. 787–801. ISSN: 1352-2310. DOI: https://doi.org/10.1016/1352-2310(95)00173-5. URL: https://www.sciencedirect.com/science/article/pii/1352231095001735.

[23] Koźlak, Aleksandra and Wach, Dagmara. "Causes of traffic congestion in urban areas. Case of Poland". In: *SHS Web Conf.* 57 (2018), p. 01019. DOI: 10.1051/shsconf/20185701019. URL: https://doi.org/10.1051/shsconf/20185701019.

[24] Richard Arnott and Kenneth Small. "The Economics of Traffic Congestion". In: *American Scientist* 82.5 (1994), pp. 446–455. ISSN: 00030996. URL: http://www.jstor.org/stable/29775281 (visited on 09/29/2022).

[25] Matthew Barth and Kanok Boriboonsomsin. "Traffic congestion and greenhouse gases". In: *Access Magazine* 1.35 (2009), pp. 2–9.

[26] Jennifer Kent. "Secured by automobility: why does the private car continue to dominate transport practices?" PhD thesis. UNSW Sydney, 2013.

[27] Han Hao, Yong Geng, and Joseph Sarkis. "Carbon footprint of global passenger cars: Scenarios through 2050". In: *Energy* 101 (2016), pp. 121–131. ISSN: 0360-5442. DOI: https://doi.org/10.1016/j.energy.2016.01.089. URL: https://www.sciencedirect.com/science/article/pii/S0360544216300263.

[28] K. Pietrzak. "Analysis of the Possibilities of Using "Light Freight Railway" for the Freight Transport Implementation in Agglomeration Areas (Example of West Pomerania Province)." In: *Transportation Research Procedia* 16 (2016), 464–472.

[29] K. Pietrzak O. & Pietrzak. "The role of railway in handling transport services of cities and agglomerations." In: *Transportation Research Procedia* 39 (2019), 405–416.

[30] R. D. Ferbrache F. & Knowles. "City boosterism and place-making with light rail transit: A critical review of light rail impacts on city image and quality." In: *Geoforum* 80 (2017), 103–113.

[31] H. Kato and Y. Kaneko Y. & Soyama. "Economic benefits of urban rail projects that improve travel-time reliability: Evidence from Tokyo, Japan." In: *Transport Policy* 35 (2014), 202–210.

[32] Bhuiyan Monwar Alam, Hilary Nixon, and Qiong Zhang. "Investigating the Determining Factors for Transit Travel Demand by Bus Mode in US Metropolitan Statistical Areas". In: 2015.

[33] Stephan Herminghaus. "Mean field theory of demand responsive ride pooling systems". In: *Transportation Research Part A: Policy and Practice* 119 (2019), pp. 15–28.

[34] Javier Alonso-Mora et al. "On-demand high-capacity ride-sharing via dynamic trip-vehicle assignment". In: *Proceedings of the National Academy of Sciences* 114.3 (2017), pp. 462–467.

[35] Ilan Lobel and Sebastien Martin. "Detours in shared rides". In: *Available at SSRN 3711072* (2020).

[36] Carlos F Daganzo, Yanfeng Ouyang, and Haolin Yang. "Analysis of ride-sharing with service time and detour guarantees". In: *Transportation Research Part B: Methodological* 140 (2020), pp. 130–150.

[37] Felix Zwick et al. "Ride-Pooling Efficiency in Large, Medium-Sized and Small Towns -Simulation Assessment in the Munich Metropolitan Region". In: *Procedia Computer Science* 184 (2021). The 12th International Conference on Ambient Systems, Networks and Technologies (ANT) / The 4th International Conference on Emerging Data and Industry 4.0 (EDI40) / Affiliated Workshops, pp. 662–667. ISSN: 1877-0509. DOI: https://doi.org/10.1016/j.procs.2021.03.083. URL: https://www.sciencedirect.com/science/article/pii/S1877050921007195.

[38] Steffen Mühle. "An analytical framework for modeling ride pooling efficiency and minimum fleet size". In: *Multimodal Transportation* 2.2 (2023), p. 100080. ISSN: 2772-5863. DOI: https://doi.org/10.1016/j.multra.2023.100080. URL: https://www.sciencedirect.com/science/article/pii/S2772586323000126.

[39] Puneet Sharma et al. "Sustainable and convenient: Bi-modal public transit systems outperforming the private car". In: *Multimodal Transportation* 2.3 (2023), p. 100083. ISSN: 2772-5863. DOI: https://doi.org/10.1016/j.multra.2023.100083. URL: https://www.sciencedirect.com/science/article/pii/S2772586323000151.

[40] https://voc.mercedes-benz.com/voc/de_de?_ga=2.47468067.508157909.1664499805-1473138929.1664499805. Accessed: 2022-09-30.

[41] *Wikipedia*. https://en.wikipedia.org/wiki/New_York_City_Subway. Accessed: 26-10-2022. 2022.

[42] *Wikipedia*. https://en.wikipedia.org/wiki/Berlin_U-Bahn. Accessed: 26-10-2022. 2022.

[43] Wolfram Knörr et al. *Aktualisierung Daten- und Rechenmodell: Energieverbrauch und Schadstoffemissionen des motorisierten Verkehrs in Deutschland 1960-2035" (TREMOD) für die Emissionsberichterstattung 2016 (Berichtsperiode 1990-2014) Anhang*. Tech. rep. 2016, p. 141.

[44] Gerard Debreu. "Valuation equilibrium and Pareto optimum". In: *Proceedings of the National Academy of Sciences* 40 (1959), pp. 588–592.

[45] B. Greenwald and J. E. Stiglitz. "Externalities in economies with imperfect information and incomplete markets". In: *Quarterly Journal of Economics* 40 (1959), pp. 229–264.

[46] M. Magill and M. Quinzii. *Theory of incomplete markets*. MIT Press, 2002.

[47] Maria Salonen and Tuuli Toivonen. "Modelling travel time in urban networks: comparable measures for private car and public transport". In: *Journal of Transport Geography* 31 (2013), pp. 143–153. ISSN: 0966-6923. DOI: https://doi.org/10.1016/j.jtrangeo.2013.06.011. URL: https://www.sciencedirect.com/science/article/pii/S096669231300121X.

[48] Yuan Liao et al. "Disparities in travel times between car and transit: Spatiotemporal patterns in cities". In: *Scientific Reports* 10.1 (2020), pp. 1–12.

[49] Nir Fulman and Itzhak Benenson. "Approximation method for estimating search times for on-street parking". In: *Transportation Science* 55.5 (2021), pp. 1046–1069.

[50] Emmanouil Chaniotakis and Adam J. Pel. "Drivers' parking location choice under uncertain parking availability and search times: A stated preference experiment". In: *Transportation Research Part A: Policy and Practice* 82 (2015), pp. 228–239. ISSN: 0965-8564. DOI: https://doi.org/10.1016/j.tra.2015.10.004. URL: https://www.sciencedirect.com/science/article/pii/S0965856415002542.

[51] Andreas Horni, Kai Nagel, and Kay Axhausen, eds. *Multi-Agent Transport Simulation MATSim*. London: Ubiquity Press, 2016, p. 618. ISBN: 978-1-909188-75-4, 978-1-909188-76-1, 978-1-909188-77-8, 978-1-909188-78-5. DOI: 10.5334/baw.

[52] *Berlin Underground Network*. https://commons.wikimedia.org/wiki/File:Berlin_U-bahn_und_S-bahn.svg.

[53] MTA. *New York City Subway*. https://new.mta.info/map/5256.

[54] Peter E. Hart, Nils J. Nilsson, and Bertram Raphael. "A Formal Basis for the Heuristic Determination of Minimum Cost Paths". In: *IEEE Transactions on Systems Science and Cybernetics* 4.2 (1968), pp. 100–107. DOI: 10.1109/TSSC.1968.300136.

[55] New York City Department of Transportation. *New York City Mobility Report*. https://www1.nyc.gov/html/dot/html/about/mobilityreport.shtml. Accessed: 2022-10-05. 2018.

[56] T. Salonen M. & Toivonen. "Modelling travel time in urban networks: comparable measures for private car and public transport." In: *Journal of Transport Geography* 31 (2013), 143–153.

[57] Giuliano Mingardo, Susan Vermeulen, and Anna Bornioli. "Parking pricing strategies and behaviour: Evidence from the Netherlands". In: *Transportation Research*

Part A: Policy and Practice 157 (2022), pp. 185–197. ISSN: 0965-8564. DOI: https://doi.org/10.1016/j.tra.2022.01.005. URL: https://www.sciencedirect.com/science/article/pii/S0965856422000052.

[58] Michael Manville and Donald Shoup. "Parking, people, and cities". In: *Journal of urban planning and development* 131.4 (2005), pp. 233–245.

[59] Dominik Ziemke, Ihab Kaddoura, and Kai Nagel. "The MATSim Open Berlin Scenario: A multimodal agent-based transport simulation scenario based on synthetic demand modeling and open data". In: *Procedia Computer Science* 151 (2019). The 10th International Conference on Ambient Systems, Networks and Technologies (ANT 2019) / The 2nd International Conference on Emerging Data and Industry 4.0 (EDI40 2019) / Affiliated Workshops, pp. 870–877. ISSN: 1877-0509. DOI: https://doi.org/10.1016/j.procs.2019.04.120. URL: https://www.sciencedirect.com/science/article/pii/S1877050919305848.

[60] OpenStreetMaps. *Open Street Map*. https://www.openstreetmap.org/. last accessed on 2023-09-22. 2023.

[61] VBB-Fahrplandaten via GTFS. *Verkehrsverbund Berlin-Brandenburg*. https://www.vbb.de/unsere-themen/vbbdigital/api-entwicklerinfos/datensaetze. Accessed: April,2017.

[62] Puneet Sharma, Knut M. Heidemann, and Stephan Herminghaus. *under review: Impact of the density of line service stations on overall performance in bi-modal public transport settings*. 2023.

[63] Niklas Avermann and Jan Schlüter. "Determinants of customer satisfaction with a true door-to-door DRT service in rural Germany". In: *Research in Transportation Business & Management* 32 (2019), p. 100420.

[64] Andreas Nyga, Aljoscha Minnich, and Jan Schlüter. "The effects of susceptibility, eco-friendliness and dependence on the consumer's willingness to pay for a door-to-door DRT system". In: *Transportation Research A* 132 (2020), pp. 540–558.

[65] Leif Sörensen et al. "How much flexibility does rural public transport need? - Implications from a fully flexible DRT system". In: *Transport Policy* 100 (2021), pp. 5–20.